

Kristine Stray

High-density sEMG electrode array and data acquisition

Master's thesis in Cybernetics and Robotics

Supervisor: Prof. Øyvind Stavadahl

July 2022

NTNU
Norwegian University of Science and Technology
Faculty of Information Technology and Electrical Engineering
Department of Engineering Cybernetics



Norwegian University of
Science and Technology

Kristine Stray

High-density sEMG electrode array and data acquisition

Master's thesis in Cybernetics and Robotics
Supervisor: Prof. Øyvind Stavdahl
July 2022

Norwegian University of Science and Technology
Faculty of Information Technology and Electrical Engineering
Department of Engineering Cybernetics



MSc Assignment

Student's name: Kristine Stray
Field: Engineering Cybernetics
Title (Norwegian): Høy-tetthets SEMG-elektrodematrise og datainsamling
Title (English): High-density SEMG electrode array and data acquisition

Description:

In upper-limb prosthesis control, a central challenge is to estimate the motor intent of the user. The most popular source of motor intent information is the surface myoelectric (SEMG) signal, usually acquired through a set of discrete electrodes placed on the skin surface of the residual limb. One trend in prosthesis control research has been to include increasing numbers of electrodes in order to get a more complete picture of the muscle activity in the residual limb and thus gain robustness against such problems as electrode shift and changes in the limb position. In the extreme, the surface of the residual limb is covered by a dense grid of electrodes.

In this assignment you will produce a prototype of such an electrode grid and an associated data acquisition module for high-fidelity SEMG signal acquisition in a geometrically dense pattern. The system will be used in future research and student activities at the department's Neuromotor Laboratory.

The assignment will include the following:

1. Discuss the specific challenges associated with dense electrode grids in the current application and identify critical parameters for proper function.
2. Establish a functional specification for the electrode grid and the data acquisition module.
3. Design and implement a prototype system.
4. To the extent allowed by the time available, carry out a rudimentary characterization of the system.

Trondheim, 13. January 2022

Øyvind Stavadahl
Supervisor

Preface

This thesis marks the end of my M.Sc. in Cybernetics and Robotics at the Norwegian University of Science and Technology (NTNU). The thesis is written as part of my specialization in biomedical cybernetics, and the project was carried out during the spring semester of 2022 under the supervision of Prof. Øyvind Stavdahl at the Department of Engineering Cybernetics, NTNU.

The project involves the development of a prototype for a high-density electrode grid and associated data acquisition module for use at the Department of Engineering Cybernetics' Neuromotor Laboratory.

This thesis partly builds on theory from my preliminary specialization project, which was carried out during the autumn semester 2021. Below follows a complete list of the material included from or based on the specialization project. The sections belong exclusively to Chapter 2, and each section states whether all or parts of it and its subsections are based on the specialization project.

- Section 2.1
- Section 2.2
- Section 2.3
- Section 2.5

The reader is expected to be familiar with basic concepts related to digital signal processing and electronic circuits, as well as understand the workings of common electronic components such as analog amplifiers and the analog-to-digital converter. It is advantageous for the reader to be familiar with electromyography and its usage for control of prosthetic devices, however, the theory presented in this thesis gives a thorough introduction to the most important topics.

During my work, I have been provided access to the Neuromotor Laboratory at the Department of Engineering Cybernetics, NTNU. In addition, I have received help with creating the mechanical parts of the electrode grid. Specifically, Glenn Angell and Daniel Bogen at NTNU's Department of Engineering Cybernetics have produced the electrodes, electrode connectors and cables, as well as designed and produced the closing mechanism of the sleeve. Assembling the mechanical parts to create a functioning electrode grid has been my own work.

The Arduino driver and Python client driver used to interface the ADS1299 has been developed by Adam Feuer of Starcat LLC. Parts of the drivers have been adapted to better suit this project, including the addition of undefined registers, adding

a check for detecting active channels, overcoming timing issues when sending commands and altering the exception handling when reading responses from the ADS1299. Python scripts regarding configurations of and communications with the ADS1299, sampling sEMG data from a subject, as well as scripts for processing and plotting the acquired signals, have been developed entirely during this work.

Trondheim, July 2022

Kristine Stray

Acknowledgements

I want to thank my supervisor, Prof. Øyvind Stavdahl, for his guidance and enlightening discussions on everything from muscle anatomy to electrode design. I am grateful for being allowed the freedom to take this project in the direction of my choosing while receiving support and technical input from you.

A special thanks to Glenn Angell and Daniel Bogen at NTNU's Department of Engineering Cybernetics for their help with creating the mechanical components for the grid, not to mention the clever design and production of the closing mechanism of the sleeve. Without you there would be no electrode grid.

Thanks to my future colleagues, Harald Sabro, Tor A. Olsen and Ines Hafizovic, for allowing me to pick your brains on everything from noise reduction in analog signals and digital signal processing to characterization of prototype devices.

My family and friends also deserve a big thanks for their unlimited support and comfort. Thank you, Mom, for asking all the stupid questions that I myself did not dare to ask.

Last, but definitely not least, a major thank you to my partner, Håvard Mellbye, for encouraging me when I most need it, for joining my discussions despite your lack of interest in electromyography, for providing valuable input and for helping me through the emotional roller coaster that it is to write a M.Sc. thesis. Thank you for everything.

Abstract

This work revolves around the implementation of a prototype for a dense electrode grid and accompanying data acquisition module for high-density surface EMG signal acquisition for the upper limb. Traditional acquisition systems are usually based on sparsely spaced surface electrodes, however a trend in clinical research has been to include an increasing number of electrode channels configured in dense geometrical patterns. Dense electrode grids have shown promise when used for multichannel prosthesis control, as they better capture the intention of the user's movements and gestures compared to single- or two-channel approaches. The prototype consists of an 8-channel dense electrode grid with dry stainless steel surface electrodes embedded in a rubber sleeve that is placed on the ventral side of the forearm above the muscles responsible for flexing the wrist. The data acquisition module builds on an Arduino shield with the ADS1299, which is an analog front end with integrated programmable gain amplifier and ADC, at its core. The prototype is used to record surface EMG signals and allows for distinguishing between weak, medium and strong muscle contractions when utilizing a differential electrode configuration. The acquired signals are not redundant across all channels, mostly due to an imbalance in electrode-skin interface impedance and the challenge of finding an accurate electrode placement. Future efforts should be put into a more deliberate electrode design, or alternatively consider commercial electrodes, in order to ensure good signal quality across all channels, as well as extend the data acquisition module to include even more electrode channels to increase redundancy and robustness of the prototype.

Sammendrag

Dette arbeidet omhandler implementeringen av en prototype for en høy-tetthets elektrodematrise og tilhørende datainnsamlingsmodul for overflate EMG-signaler fra den øvre lem. Tradisjonelle innsamlingsystemer er vanligvis basert på mer spredte overflateelektroder, men en trend i klinisk forskning har vært å inkludere et økende antall elektrodekanaler konfigurert i tette geometriske mønstre. Høy-tetthets elektrodematiser har vist seg å være lovende når de brukes til flerkanales protesekontroll, ettersom disse bedre fanger opp intensjonen bak brukerens bevegelser sammenlignet med en- eller to-kanals tilnærminger. Prototypen i dette arbeidet består av en 8-kanals tett elektrodematrise bestående av tørre overflateelektroder i rustfritt stål innebygd i et gummi-erme som er plassert på den ventrale siden av underarmen over musklene som er ansvarlige for å bøye håndleddet. Datainnsamlingsmodulen bygger på et Arduino-shield med ADS1299, som er en analog frontend med integrert programmerbar differensialforsterker og ADC, i senter. Prototypen brukes til å registrere overflate-EMG-signaler og kan skille mellom svake, middels og sterke muskelsammentrekninger ved bruk av en differensiell elektrodekonfigurasjon. De innhentede signalene er ikke redundante på tvers av alle kanaler, hovedsakelig på grunn av en ubalanse i impedansen til elektrode-hud-grensesnittet, samt at det er utfordrende å finne en nøyaktig elektrodeplassering. Fremtidig innsats bør fokusere på et mer tilsiktet elektrodedesign, eller alternativt vurdere kommersielle elektroder, for å sikre god signalkvalitet på tvers av alle kanaler, samt utvide datainnsamlingsmodulen til å inkludere enda flere elektrodekanaler for å øke redundansen og robustheten til prototypen.

Contents

Preface	v
Acknowledgements	vii
Abstract	ix
Sammendrag	xi
Contents	xiii
Figures	xvii
Tables	xxi
1 Introduction	1
1.1 Background and motivation	1
1.2 Interpretation of project task and scope	2
1.3 Contributions	3
1.4 Outline	3
2 Theory	5
2.1 Anatomical planes and directional terms	5
2.2 The nervous system	6
2.2.1 Electrical signals of neurons	8
2.2.2 Motor functions and neural circuits	9
2.3 The musculoskeletal system	10
2.3.1 Anatomy and physiology of skeletal muscle	12
2.3.2 Muscle contraction	14
2.4 Electromyography	16
2.4.1 Acquiring the myoelectric signal	17
2.4.2 The electrode-skin interface	20
2.5 Myoelectric prosthetic systems	22
3 Dense electrode grids for prosthesis control	25
3.1 Introduction to dense electrode grids	25
3.1.1 Limitations of single-channel myoelectric control	25
3.1.2 High-density surface EMG	26
3.2 Previous work	28
3.2.1 Real-time gesture classifier using HD-sEMG and deep learning	29
3.2.2 HD-sEMG E-Textile systems for control of active prostheses	30
3.2.3 HD-sEMG after targeted muscle reinnervation	32
3.2.4 Gesture recognition by instantaneous surface EMG images	32
3.2.5 Surface electromyography in clinical gait analysis	34

3.3	Challenges and advantages with dense electrode grids	35
3.3.1	Available space and muscle on the residual limb	36
3.3.2	Spatial and temporal sampling	36
3.3.3	The effect of electrode shifts	37
3.3.4	The limb position effect	37
3.3.5	Crosstalk from nearby muscles	37
3.3.6	Increased complexity	38
3.3.7	Critical parameters for proper function	39
4	Requirements analysis	41
4.1	Electrode-skin interface	41
4.1.1	Effect of electrode-skin contact area	41
4.1.2	Skin preparation	42
4.1.3	Balancing contact impedances	42
4.2	Electrode grid	42
4.2.1	Type of surface electrode	43
4.2.2	Effect of electrode shape and size	43
4.2.3	Inter-electrode distance	44
4.2.4	Number of channels	45
4.2.5	Biocompatible materials	45
4.2.6	Fixation	46
4.3	Data acquisition module	46
4.3.1	Analog front end	46
4.3.2	Electrical safety	50
4.3.3	Digital signal processing	50
4.4	Functional specification	50
5	Design and implementation	53
5.1	General design considerations	53
5.1.1	Electrical safety	53
5.1.2	Materials	53
5.1.3	Fixation method	54
5.1.4	Skin preparation	55
5.2	Electrode grid design	55
5.2.1	Electrodes and electrode connectors	56
5.2.2	Inter-electrode distance	58
5.3	Choosing an analog front end	58
5.4	Digital signal processing	61
5.4.1	Bandpass filter	61
5.4.2	Comb filter	62
5.4.3	Spectral gating	62
6	Characterization of prototype	65
6.1	Application note: Intro to ADS1299	65
6.1.1	Channel configurations	68
6.1.2	Operational mode	69
6.1.3	Bias drive	70

6.1.4	Channel offset	71
6.2	Basic data acquisition	72
6.3	SNR	78
6.4	Technical specification	78
6.4.1	Data acquisition module	79
6.4.2	Physical	79
7	Discussion	83
7.1	Requirements evaluation	83
7.2	Locating the noise source	86
7.3	HD-sEMG recordings with the prototype	87
7.3.1	Electrode-skin contact	87
7.3.2	Differential mode	89
7.3.3	Single-ended mode	89
7.4	Prototype improvements	90
8	Concluding remarks	91
8.1	Conclusion	91
8.2	Future work	91
	Bibliography	93
A	Commercially available electrodes and prosthetic systems	99
A.1	Coapt Complete Control System Gen2	99
A.2	Coapt Dome Electrodes	100
A.3	Steeper TruSignal AC Electrodes	101
A.4	TMSi HD-EMG electrode grids	101
B	Schematics for HackEEG Arduino shield	105

Figures

2.1	The anatomical planes and directional terms. Adapted from [8]. . .	6
2.2	Structure of a large neuron in the brain connected to second-order neurons in the spinal cord. From [9].	7
2.3	(a) A typical action potential across the cell membrane of a neuron, and (b) simultaneous firing of many synapses will raise the summed potential to the threshold of excitation and cause a superimposed action potential. From [9].	8
2.4	Propagation of action potentials in both directions along a conductive fiber. From [9].	9
2.5	A simple reflex circuit – the knee-jerk response – illustrating the functional organization of neural circuits. From [10].	10
2.6	The three types of joints – (a) fibrous, (b) cartilaginous and (c) synovial – that connect the bones of the skeletal system. From [7]. .	11
2.7	The major bones of the forearm, 1) radius and 2) ulna. Figure A shows the bones' position during supination of the forearm, while B shows the bones' position during pronation. From [12].	12
2.8	The superficial muscles of the ventral side of the forearm. Muscles important for prosthesis control are given in bold writing. Adapted from [12].	13
2.9	The superficial muscles of the dorsal side of the forearm. Muscles important for prosthesis control are given in bold writing. Adapted from [12].	13
2.10	Illustration of the anatomy and organization of skeletal muscle. The structures labeled <i>F</i> , <i>G</i> , <i>H</i> and <i>I</i> represent cross sections at different levels of the sarcomere. From [9].	15
2.11	“Walk-along” mechanism for contraction of the muscle. From [9]. .	16
2.12	Illustration of the volume conductor, which is the conductive tissues between the surface electrode and the muscle source.	17
2.13	Experimental surface recording of myoelectric signals during low-level contraction. From [2].	18
2.14	Illustration of the capacitive coupling between the body of a subject and the environment. From [2].	19
2.15	Illustration of two different electrode configurations. Based on [3].	20

2.16	Switchable single-ended/differential front-end amplifier for detection of sEMG signals. Based on [3].	21
2.17	A simple physical model of an electrode contact (or of a pair of electrodes) is indicated with the inclusion of the half- (or full-) cell potential V_b and of the equivalent noise generator V_n of the interface. Z_e represents the electrode-skin impedance. Based on [3]. . .	22
2.18	Block diagram illustrating how a myoelectric control system differs from the “control system” of a healthy person. Based on [14].	23
3.1	Threshold-based control using a single sEMG channel to open and close a prosthetic hand, as well as stop the hand motion. Adapted from [15].	26
3.2	Examples of different HD-sEMG arrays. (a) Flexible electrode array made by separable modules. (b) Arrays placed on soleus and gastrocnemius muscles (the main flexors of the ankle joint). (c) Electrode array mounted inside a flexible sleeve, connected to a portable amplifier. (d) Flexible electrode array with double adhesive foam whose cavities are filled with conductive gel. From [3]. . .	27
3.3	EMG maps corresponding to the extension of each finger. The maps are generated from monopolar signals using an array of 128 electrodes. From [3].	28
3.4	Concept illustration of the proposed myoelectric prosthesis system. From [5].	29
3.5	Electrode configuration with shared reference electrodes. From [5].	29
3.6	Examples of HD-sEMG muscle activation maps where each pixel correspond to one channel of the high-density electrode grid. From [5].	30
3.7	Textile electrode sleeve for recording of HD-sEMG signals. From [16].	30
3.8	Recorded sEMG signals from three representative electrode channels during the performance of the 9 contraction tasks. From [16].	31
3.9	Illustration of signal pick-up for prosthetic control after targeted muscle reinnervation. From [4].	32
3.10	Contour plots of HD-sEMG recordings during four different movements. From [17].	33
3.11	Classification of hand gestures based on sEMG images sampled from a high-density electrode grid. From [18].	34
3.12	WEAR system architecture. From [19].	35
3.13	Electrode grid configuration. From [20].	35
3.14	Illustration of how sEMG electrodes can pick up crosstalk from nearby muscles. From [25].	38
3.15	Experimental set-up of electrodes A, B and C in a double differential configuration. Adapter from [24].	39
4.1	Impedance of electrode-gel-skin interface against electrode surface area. Adapted from [21].	42

4.2	Overview of the number of channels commonly used in different applications of sEMG acquisition systems. From [30].	45
4.3	Illustration of a one-channel sEMG detection chain. Based on [3].	46
4.4	Variation of sEMG signal with contraction level. From [2].	48
4.5	Commonly used ADC resolutions for different sEMG applications. From [30].	49
4.6	Concept illustration of the overall function of the HD-sEMG system.	51
5.1	Adjustable attachment mechanism of the sleeve consisting of aluminium braces and velcro straps.	55
5.2	M2x8mm pan head machine screw. From [35].	56
5.3	Final shape of the electrodes used for the prototype.	57
5.4	Assembly of electrodes and electrode connectors embedded in sleeve.	57
5.5	The grid template used to make holes in the sleeve. The grid is 4x8 and has a distance between holes of 5.5mm.	58
5.6	Arduino shield from HackEEG connected on top of an Arduino Due.	61
5.7	Prototype consisting of dense electrode grid embedded in a rubber sleeve and connected to the Arduino shield with the ADS1299 at its core. The Arduino shield is stacked on top of an Arduino Due, which is connected to a battery-powered laptop (not shown in figure).	62
5.8	Power spectrum of the noise floor before and after applying a comb filter with notch frequency = 50Hz.	63
5.9	Frequency response of a comb filter with notch frequency = 50Hz and quality factor = 10.0.	63
6.1	Functional block diagram for the ADS1299. From [36].	66
6.2	Schematic of the ADS1299 and connected electrodes configured in differential mode. From [36].	69
6.3	Schematic of the ADS1299 and connected electrodes configured in single-ended mode. From [36].	70
6.4	Channel offset for electrodes shorted externally to analog ground.	71
6.5	Setup of the recording includes placing the electrode grid on the ventral side of the forearm above the muscles responsible for flexing the wrist. The reference electrode is placed on the elbow above an area consisting of mostly bone, while the bias electrode is attached to an arbitrary point on the skin, both using adhesive tape.	72
6.6	Acquired sEMG signal from channel 3 recorded in differential mode. Shaded areas indicate when the subject is told to contract and with what contraction level.	73
6.7	Recorded sEMG signals in differential mode.	74
6.8	Recorded sEMG signals in differential mode with BIAS_SENS enabled.	75
6.9	Recorded sEMG signals in single-ended mode.	76
6.10	Recorded sEMG signals in single-ended mode with BIAS_SENS enabled.	77

6.11	Noise and signal power obtained from the respective shaded areas of the sEMG signal from channel 3 recorded in differential mode. .	79
7.1	Power spectrum obtained when (a) electrodes are internally shorted, (b) electrodes are externally shorted to the bias electrode, and (c) electrodes are configured as normal electrode inputs and arm is at rest.	86
7.2	Recorded sEMG signals from channel 4, 5 and 6 in differential mode.	88
A.1	Contents of the Complete Control System Gen2 kit. From [48]. . . .	100
A.2	(a) Cross section of electrode connection and assembly in prosthetic socket, and (b) Coapt Dome Electrodes mounted in socket for prosthetic device. From [34].	101
A.3	Component specification for the Coapt Stainless Steel Dome Electrode. From [34].	102
A.4	Steeper TruSignal AC Electrodes. From [49].	103
A.5	TMSi HD-EMG electrode grids. From [50].	103

Tables

4.1	Overview of the functional specification for the HD-sEMG prototype system.	52
5.1	Feature comparison of different analog front ends.	60
6.1	Overview of ADS1299 command definitions. Adapted from [36]. . .	67
6.2	Characteristics of the data acquisition module of the HD-sEMG prototype system.	80
6.3	Overview of the physical components of the HD-sEMG prototype system.	81
6.4	Dimensions of the physical components and modules of the HD-sEMG prototype system. All dimensions are given in millimeters. . .	81
6.5	Materials of the physical components of the HD-sEMG prototype system.	81
6.6	Connectors between the modules of the HD-sEMG prototype system.	82
7.1	Evaluation of the requirements from the functional specification for the HD-sEMG prototype system.	84

Chapter 1

Introduction

1.1 Background and motivation

As defined by Kilby *et al.* (2016), electromyography (EMG) is “the study of electrical signals that are obtained from muscle activity by means of sensory electrodes”. The word “electromyography” comes from three Greek words; “electron” is associated with electricity, “myos” is a prefix used in biology to denote that it is something to do with muscle, and “graph” which means “to write” or “writing”. Putting the three words and their meanings together, electromyography is essentially “a method of recording and analysing electrical signals, when generated by the muscles performing muscular activities”[1]. Electrical signals sourced from biological organisms are usually called “bioelectrical signals”, “biopotential signals” or just “biosignals”[1]. More specifically, electrical signals sourced from muscle are often referred to as “myoelectric signals”[2].

In surface electromyography (sEMG), myoelectric signals are measured by surface electrodes that are placed on the skin above the muscle of interest[1]. EMG electrodes can measure the electrical activity produced when contracting a muscle, and applications of sEMG ranges from research on neurological disorders and analysis of muscle fatigue to human-machine interfaces and prosthesis control[3, p. 149], the latter being the focus of this thesis. Usually, signals sampled from surface electrodes are used as input to the control system of prosthetic devices. This method is referred to as “myoelectric control”, and the goal of using myoelectric signals as input to prosthetic systems is to capture the user’s intention. The signal detected during muscle contraction is mapped to analogous movement of the prosthetic device. For instance, when the user contracts the muscles responsible for closing the hand, the hand of the prosthetic device should also close[4, p. 127, 148].

While many different control schemes exist for controlling prosthetic devices, even the most advanced prosthetic systems struggle to realize easy and intuitive control[5]. Traditionally, myoelectric signals from one or a few pairs of sparsely spaced electrodes are used as input to the control system of prosthetic devices. In recent years, a technique called “high-density surface EMG” (HD-sEMG) has been

employed in various clinical settings. HD-sEMG involves placing a grid of densely spaced surface electrodes above the muscle of interest, and the detected myoelectric signals provide a so-called sEMG map or image[3, p. 149]. This technique can be used for improved control of prosthetic devices, as the sEMG map captured by a densely spaced electrode grid better reflects the user's intention compared to the myoelectric signal detected by a single electrode pair[5].

The goal of this project is to develop a prototype for a high-density surface EMG electrode grid, together with an accompanying data acquisition module, for use at NTNU's Neuromotor Laboratory. The prototype is to be used for future research and student activities, and the hope is that it can serve as a contribution towards more intuitive prosthesis control in the future.

1.2 Interpretation of project task and scope

The project description clearly outlines four assignments, including:

1. Discuss the specific challenges associated with dense electrode grids in the current application and identify critical parameters for proper function.
2. Establish a functional specification for the electrode grid and the data acquisition module.
3. Design and implement a prototype system.
4. To the extent allowed by the time available, carry out a rudimentary characterization of the system.

For the first assignment, it is assumed that "the current application" refers to prosthesis control. The discussion should make use of the available literature on dense electrode grids for prosthesis control and supply with additional literature from relevant applications where necessary. In this context, a "critical parameter for proper function" is interpreted as referring to *a variable or criterion of a dense electrode grid that is considered essential for the prosthetic system's correct operation*. In addition to discussing challenges and identifying critical parameters, it is also of interest to explore the advantages with using dense electrode grids for prosthesis control.

For the second assignment, no requirements have been issued by the end user. A functional specification should therefore be established based on a requirements analysis of relevant multichannel sEMG acquisition systems. This includes highlighting requirements for the prototype system to allow for effective design and implementation of the prototype in assignment three.

The prototype is to be used in future research and student activities at the department's Neuromotor Laboratory, and it is assumed that the prototype will initially be used by healthy subjects that have their limbs intact. Nevertheless, the discussion on challenges with dense electrode grids will not make this assumption, as available space on the residual limb is one of the major challenges. To avoid any conflicting design requirements, however, this thesis will assume that the users of the prototype system are non-amputees.

Finally, the last assignment involves carrying out a rudimentary characterization of the system. Since the prototype is to be used as research equipment at a laboratory, the characterization should include suggested usage and technical specifications so that it can be easily applied in future projects. Additionally, the prototype should be evaluated in light of the requirements from the requirements analysis.

In order to limit the scope of the project, this thesis will mainly focus on upper-limb prosthetics and the reader can assume that all mentions of amputation refer to below-elbow amputation.

1.3 Contributions

The supervisor, Prof. Øyvind Stavdahl, has provided guidance and feedback throughout the project, while the responsibility of making decisions and completing each assignment according to the author's interpretation of the project description has remained with the author.

Parts of the theory in Chapter 2 are based on the theory presented by the author's preliminary specialization project, and each section states whether this is the case. The reader is not expected to be familiar with the contents of the specialization project, as it relates to a different topic of prosthesis control.

Some of the illustrations and figures included in the thesis are created by the author herself using Adobe Illustrator. Of these, some are inspired by or based on figures from the literature, and in these cases the original sources are referenced in the figure text. Some figures are adaptations or reproductions. The figure text will state whether this is the case and reference the original source of the figure in question. If not otherwise stated, the reader can assume a figure to be the author's own creation.

1.4 Outline

Following this introduction is Chapter 2, which presents the reader with theory related to three main topics; anatomy and physiology of the human body, electromyography and prosthetic systems. Next, Chapter 3 introduces dense electrode grids and its applications, and discusses the challenges and advantages of dense electrode grids used for prosthesis control. Chapter 4 contains a requirements analysis of relevant multichannel sEMG acquisition systems that are summarized as a functional specification. The functional specification for the electrode grid and data acquisition module lays the foundation for the design and implementation of the prototype, which is described in Chapter 5. Chapter 6 presents a characterization and technical specification of the prototype, and an application note for future users is also included here. The prototype is further evaluated in light of the requirements from the functional specification in Chapter 7, which also discusses the results, uncertainties and future improvements. Finally, Chapter 8

presents concluding remarks and summarizes what should be done in terms of future work.

Chapter 2

Theory

Several of the sections in this chapter are based on or inspired by the theory presented in the author's preliminary specialization project, Stray (2021) [6]. Though the objective of the specialization project is not the same as for this thesis, most of the theory remains highly relevant. Each section states whether it is based on the preliminary specialization project.

2.1 Anatomical planes and directional terms

This section is in its entirety based on Stray (2021).

“Anatomy refers to the internal and external structures of the body and their physical relationships, while physiology refers to the study of the functions of those structures” [7, p. 74].

In order to refer to and describe the human body, it is handy to define some anatomical planes and terms that are used to describe the position of a body part. As reference, the **anatomical position** is used. When standing in the anatomical position, the body is facing forward and the arms are hanging to the sides with palms facing forward. This position, labeled with the anatomical planes and directional terms, is shown in Figure 2.1. The figure shows the ventral (or anterior) side of the body. The directions **proximal**, **distal**, **medial**, **lateral**, **ventral** and **dorsal** are used to describe the relative position of a body part. Often, the attached end of a limb is used as a reference point to define whether a body part is proximal or distal to the end of the limb. For instance, the elbow is proximal to the shoulder since it is closer to the shoulder, while the hand is distal to the shoulder, since it is further away from the shoulder. If a body part is located close to the midline of the body, it is said to be medial. On the other hand, a body part far from the midline is said to be lateral. Finally, ventral implies that something is in front of or on the front side of the body, while dorsal means behind the body [7, p. 74-75]. Some additional directional terms exist, but only those relevant for this thesis are included here.

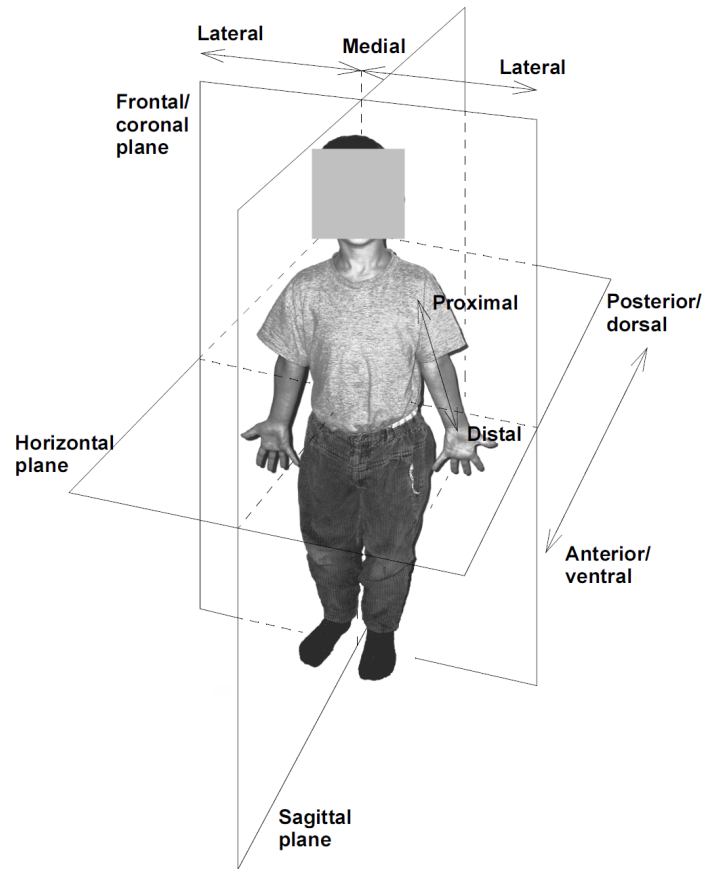


Figure 2.1: The anatomical planes and directional terms. Adapted from [8].

2.2 The nervous system

This section is in parts based on Stray (2021), while additional theory on the structure of neurons, signaling and motor functions has been added to better prepare the reader for the sections that follow.

The nervous system can be divided into the central nervous system (CNS) and the peripheral nervous system (PNS). The CNS consists of all nervous tissue that is enclosed by bone – i.e. the brain and the spinal cord. The PNS entails “all the rest” – i.e. the nervous tissue that is not encased by bone [7, p. 107]. The CNS contains more than 1 billion nerve cells, which are the basic functional units of the nervous system. A nerve cell, often called **neuron**, generally consists of a cell body, dendrites, an axon and synapses. The structure of a typical neuron in the brain is shown in Figure 2.2. The region connecting the axon to the cell body of the neuron is called the **axon hillock**. Input signals enter the neuron through synapses from a preceding neuron connected to the dendrites, and the signal propagates along the neuron’s axon. The axon has many separate branches that are connected to subsequent neurons through synaptic terminals, thus connecting a neuron

in the brain to other parts of the nervous system or peripheral body[9, p. 543]. Section 2.2.1 further explains how signals are transmitted throughout the nervous system.

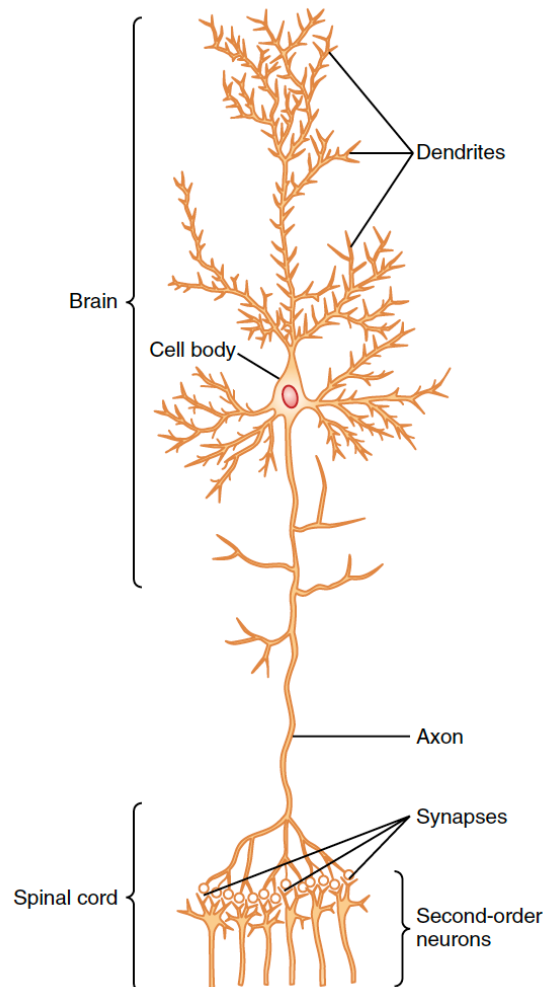


Figure 2.2: Structure of a large neuron in the brain connected to second-order neurons in the spinal cord. From [9].

Nerve cells that carry information from the periphery *toward* the CNS are called **afferent** neurons. Nerve cells that carry information *away* from the CNS – or away from the circuit in question – are called **efferent** neurons[10, p. 10]¹. Afferent neurons often transmit sensory information from peripheral nerves, for instance from sensory receptors in the fingertips, whereas efferent neurons are particularly important for motor functions and the contraction of muscle[9, p.

¹One can think of afferent neurons as “neurons affecting the CNS”, while efferent neurons are “neurons having an effect on whatever body part is receiving the nerve signals”.

543]. Before looking at how nerve signals trigger motor functions, as explained in Section 2.2.2, it is important to understand the signalling process itself.

2.2.1 Electrical signals of neurons

Generally, all cells of the human body have electrical potentials across their cell membranes. Some cells, such as nerve cells, are able to generate electrochemical impulses at their membranes. When at rest, the neuron has a negative voltage potential across its cell membrane. This membrane potential comes from a difference in concentration of certain ions – sodium and potassium ions – inside and outside the cell membrane[9, p. 57].

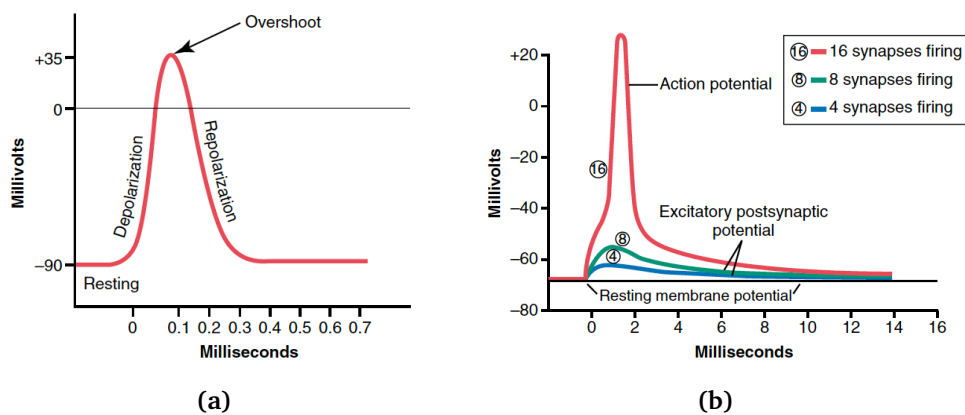


Figure 2.3: (a) A typical action potential across the cell membrane of a neuron, and (b) simultaneous firing of many synapses will raise the summed potential to the threshold of excitation and cause a superimposed action potential. From [9].

Neurons transmit information throughout the nervous system by what is called **action potentials**, illustrated in Figure 2.3a. An action potential is triggered when the membrane potential is increased (depolarized) and reaches a certain threshold potential. During the depolarization stage, the membrane’s permeability changes to allow sodium ions into the cell. Being positively charged, the sodium ions further increase the potential across the cell membrane. Repolarization of the membrane occurs as a result of diffusion of potassium ions out of the cell. This re-establishes the normal negative resting potential of the membrane. The action potential propagates along the nerve fiber’s axon until it reaches the end, which is connected to another nerve cell, thus triggering another action potential[10, p. 33-35][9, p. 60-61].

An action potential follows the “all-or-nothing principle”, meaning that “once an action potential has been elicited at any point on the membrane of a normal fiber, the depolarization process travels over the entire membrane if conditions are right, or it does not travel at all if conditions are not right”. This is because the depolarization of the cell membrane must be above a certain threshold for

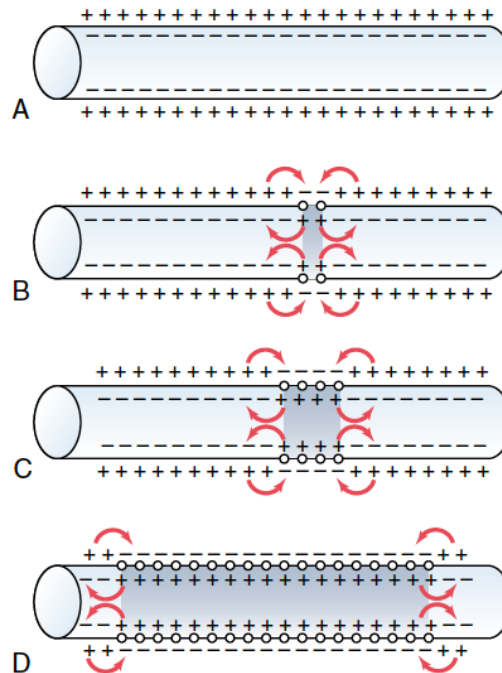


Figure 2.4: Propagation of action potentials in both directions along a conductive fiber. From [9].

an action potential to be generated and for further propagation of action potentials along the membrane[9, p. 65]. Figure 2.4 illustrates how an action potential propagates along a conductive fiber. Note that while propagation generally occurs in all directions away from the stimulus, the direction of propagation for action potentials in neurons is along the axon toward the post-synaptic terminals. The reason for this is that the action potential begins in the axon hillock – the initial segment of the axon – because this region contains a greater concentration of sodium channels than the cell body. In other words, less is required to overcome the threshold of excitation and generating an action potential[9, p. 554].

2.2.2 Motor functions and neural circuits

Controlling bodily activities and functions is one of the many important roles of the nervous system. Among other things, this includes controlling the contraction of appropriate skeletal muscles throughout the body, and such activities are called **motor functions** of the nervous system. Recall that neurons carrying information from the CNS to a body part is termed efferent neurons – the muscles receiving nerve signals are often called **effectors** because “they are the actual anatomical structures that perform the functions dictated by the nerve signals”[9, p. 543]. Neurons that are connected to muscle are called **motor neurons**. While their cell bodies are located in the spinal cord, motor neurons have a long axon

that branches out into synaptic terminals connected to the muscle fiber. These connections make out what are called **neuromuscular junctions** – also called “end-plates” – and the region comprising these neuromuscular junctions are called **innervation zone**[11, p. 95-96].

Carrying and processing information is not a one-man (or rather, one-nerve) job. Neurons never function in isolation, but are instead organized in **neural circuits**, as illustrated in Figure 2.5. The figure shows how the afferent and efferent neurons are connected in a simple reflex circuit called the myotatic reflex – more commonly known as the knee-jerk response. Sensory receptors in the extensor muscle sense a stretch when the small hammer hits the tendon below the knee. This triggers an action potential in the sensory afferent neurons and a signal is sent to interneurons (local circuit neurons) in the spinal cord. An inhibitory signal is forwarded to motor neurons connected to the flexor muscle, which tells the muscle to relax. At the same time, an excitatory signal is sent to motor neurons connected to the extensor muscle, telling it to contract. Since the extensor muscle is attached to tendons, that are again attached to the bones in the foot, the foot is lifted – or jerked – forwards[10, p. 10-11]. Though just a simple example of a neural reflex circuit, the myotatic reflex illustrates how afferent and efferent neurons are connected and what role they play in the many kinds of motor functions of the human body.

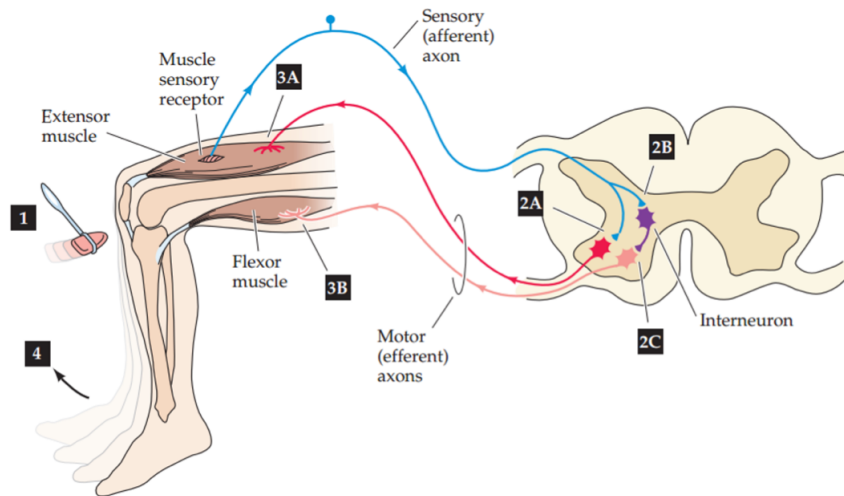


Figure 2.5: A simple reflex circuit – the knee-jerk response – illustrating the functional organization of neural circuits. From [10].

2.3 The musculoskeletal system

The first part of this section is based on Stray (2021). Section 2.3.1 and Section 2.3.2 has been added to better prepare the reader for the theory presented

in Section 2.4.

The musculoskeletal system consists of the skeletal system and the muscular system. Very briefly, the skeletal system is made up of rigid bones that form the major supporting and protecting elements of the body. The bones are attached to each other at three different types of joints, shown in Figure 2.6, namely fibrous, cartilaginous and synovial joints. Bones connected by fibrous joints are bound tightly and are relatively immovable, like the joints in the skull. Cartilaginous joints, like the joints that attach the ribs to the spine, allow some movement. The knee and elbow are examples of synovial joints, which consist of cavities that are filled with fluid, as well as connective tissue that holds the bones together[7, p. 111-113].

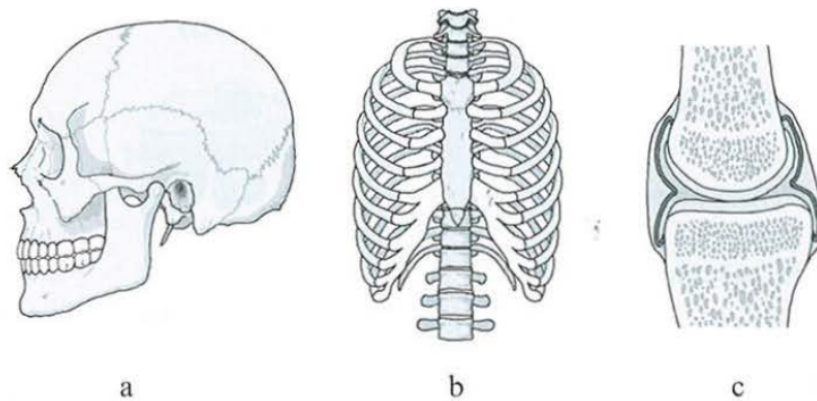


Figure 2.6: The three types of joints – (a) fibrous, (b) cartilaginous and (c) synovial – that connect the bones of the skeletal system. From [7].

Detailed knowledge about the skeletal system is not required for understanding the concepts presented in this thesis. However, the reader should be familiar with the two major bones of the forearm – radius and ulna – as shown in Figure 2.7. Radius and ulna are attached to the elbow joint and can engage in two different types of movements. The first kind of movement is flexion and extension of the elbow joint and the other is supination and pronation, the latter being illustrated in Figure 2.7. During supination and pronation, radius is rotated about an axis along the forearm[12, p. 382]. These movements engage some of the superficial muscles of the forearm and is therefore often used for prosthesis control[2].

The muscular system consists of three types of muscle tissue; skeletal, cardiac and smooth muscle tissue. The heart is the only place where one can find cardiac muscle tissue, while smooth muscle encapsulates tissue in almost all organs. Skeletal muscle, which consists of skeletal muscle tissue and connective tissue, as well as blood vessels and nervous tissue, is attached to bone, skin or other muscle tissue. Skeletal muscle is under voluntary control and allows for moving the bones and joints of the body, as well as the skin of the face[7, p. 113-116].

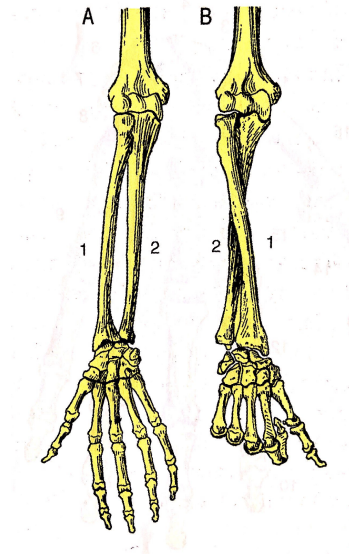


Figure 2.7: The major bones of the forearm, 1) radius and 2) ulna. Figure **A** shows the bones' position during supination of the forearm, while **B** shows the bones' position during pronation. From [12].

2.3.1 Anatomy and physiology of skeletal muscle

Detailed knowledge about the anatomy and physiology of skeletal muscle is not necessary for understanding the concepts presented in this thesis.

The muscles that are of most importance to prosthesis control are the superficial muscles of the forearm engaged during flexion and extension of the wrist joint, as well as those engaged during supination and pronation. More specifically, the flexor carpi ulnaris, flexor carpi radialis, palmaris longus and flexor digitorum superficialis, located on the ventral side of the forearm as shown in Figure 2.8, are activated when flexing the wrist, while the extensor carpi ulnaris, extensor carpi radialis longus, extensor carpi radialis brevis and extensor digitorum, located on the dorsal side of the forearm as shown in Figure 2.9, are activated when extending the wrist[12, p. 410-418]. The reader can find comfort in that remembering the muscles' Latin names is not as important as knowing their approximate locations and functionality².

It is also important to understand how muscle contractions work, as muscle contractions are what produce the signals that can be used to control prosthetic

²Though hard to remember, the Latin name of a muscle provides useful information about the muscle's functionality and location, given that one is familiar with the major bones of the human body. Take the flexor carpi ulnaris as an example. From "flexor", one can gather that the muscle's functionality is to flex *something*. That *something* is described by the following words "carpi" and "ulnaris". The word "carpus" means "wrist", while "ulnaris" refers to the ulna – one of the bones of the forearm. Hence, the flexor carpi ulnaris' function is to flex the wrist and it is located along the ulna[12, p. 413].

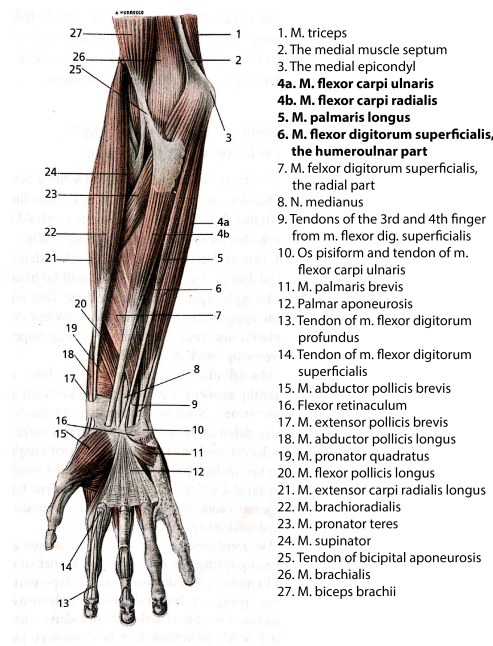


Figure 2.8: The superficial muscles of the ventral side of the forearm. Muscles important for prosthesis control are given in bold writing. Adapted from [12].

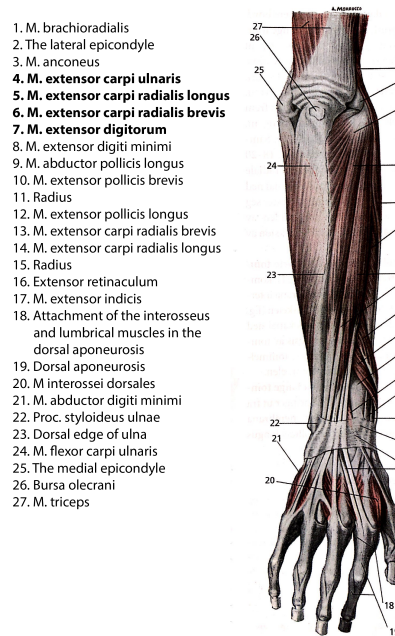


Figure 2.9: The superficial muscles of the dorsal side of the forearm. Muscles important for prosthesis control are given in bold writing. Adapted from [12].

devices. In order to understand the concept of muscle contraction, it is useful to take a closer look at the organization and anatomy of skeletal muscle, as well as the contractile units responsible for producing muscle contractions.

As illustrated in Figure 2.10, skeletal muscle consists of what is called **fascicles** – labelled **B** in the figure. Each fascicle is made up of numerous muscle fibers – labelled **C** in the figure – ranging from 10 to 80 micrometers in diameter. Each fiber consists of hundreds to thousands of smaller sub-units called **myofibrils**. Diving even deeper into the anatomy of skeletal muscle reveals that a myofibril consists of consecutive parts called **Z disks** – due to its “zigzag” pattern – and the portion between two consecutive Z disks is what is termed a **sarcomere**. The sarcomere is the smallest contractile unit of skeletal muscle, and it is within this unit that muscle contraction takes place. Muscle contraction is further explained in Section 2.3.2. Part **D** of Figure 2.10 shows a longitudinal view of the myofibril, including the Z disks as well as the so-called **A bands**, **I bands** and **H bands**. Attached to the Z disks are what are called **actin filaments** – labelled **K** in the figure – which extend in both directions to interdigitate with **myosin filaments** – the part labelled **L**. It is the actin and myosin filaments that are responsible for the actual contraction[9, p. 71-71].

2.3.2 Muscle contraction

As an illustrative example, imagine someone doing a bicep curl. When the person lifts their arm to flex the muscles of the bicep, an action potential travels along the corresponding motor neuron to the neuromuscular junctions on the muscle fibers. At the neuromuscular junction, a neurotransmitter is released, which opens multiple ion channels. This locally depolarizes the muscle fiber membrane and initiates an action potential at the membrane. The action potential travels along the muscle fiber membrane to further depolarize the membrane. This triggers the release of calcium ions, which initiates “attractive forces between the actin and myosin filaments, causing them to slide alongside each other”, thus contracting the sarcomeres[9, p. 73-74]. Figure 2.11 shows how hinges of the myosin filaments bind to active sites on the actin filaments to produce muscle contractions. As the muscles of the bicep contract, the muscle fibers shorten. Since the muscles are attached to the bones of the elbow, the arm is lifted, and the person has performed a bicep curl.

When an action potential travels along the motor neuron and initiates muscle contraction, the muscle is said to be **innervated** or, in other words, active³. Each motor neuron innervates multiple muscle fibers, depending on the type of muscle. The collection of all the muscle fibers innervated by a single motor neuron, including the motor neuron itself, is called a **motor unit**[2, p. 22]. The muscle fibers of a motor unit are generally spread throughout the muscle, which means that stimulating a single motor unit initiates a weak contraction of the entire muscle. As all

³The terms “innervated” and “active” are used interchangeably when referring to contracting muscles.

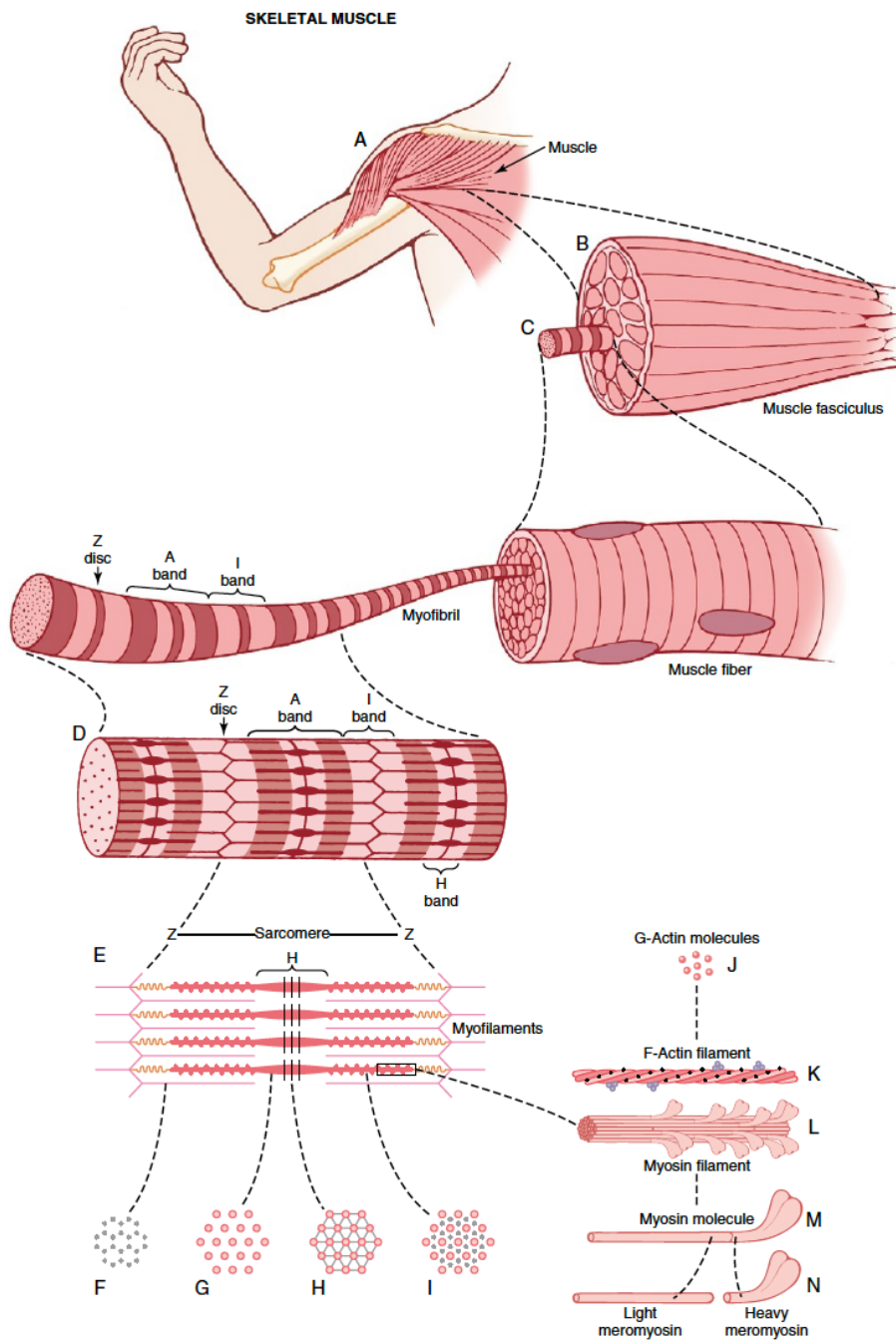


Figure 2.10: Illustration of the anatomy and organization of skeletal muscle. The structures labeled *F*, *G*, *H* and *I* represent cross sections at different levels of the sarcomere. From [9].

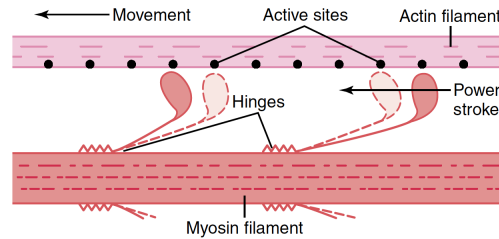


Figure 2.11: “Walk-along” mechanism for contraction of the muscle. From [9].

the fibers of a motor unit are innervated by the same motor neuron, they depolarize synchronously, and the corresponding externally observed signal is called a **motor unit action potential**, which is a summation of the activity from all the muscle fibers of that motor neuron[2, p. 28-29]. The force generated during muscle contraction depends on the rate at which the muscle fibers are firing and how many are innervated. The velocity at which the action potential propagates is referred to as the conduction velocity[3, p. 33].

2.4 Electromyography

Electromyography (EMG) includes the detection, analysis and utilization of electrical signals from muscle. These signals are often termed **myoelectric signals**, and can be defined as “the electrical activity produced by a contracting muscle”[2, p. 17]. Recall that in order for a muscle to contract, the outer muscle fiber membrane must be depolarized. The depolarization generates an electric potential field, which can be detected and measured using either intramuscular electrodes placed on the muscle fiber membrane itself or surface electrodes placed on the skin above the muscle of interest. To distinguish between EMG signals detected using intramuscular electrodes and surface electrodes, the detected signals are usually termed EMG signals and surface EMG (sEMG) signals, respectively[3, p. 30].

The muscle fibers that are active during muscle contraction are usually termed **sources**, and the tissue that separates the recording electrodes from the sources acts as a so-called **volume conductor**. For instance, the volume conductor can include the skin, fatty layers, inactive muscles and other biological tissue that separates the surface electrode from the innervated muscle source, as illustrated in Figure 2.12. Biological tissue has conductive properties, so the myoelectric signal from the source travels through the conductor volume and is detected by the surface electrode. The features of the detected myoelectric signal are largely affected by the properties of the volume conductor because the tissue acts as a spatial and temporal low-pass filter on the distribution of the electric potential. The effect of the volume conductor is relatively small for intramuscular recordings as the electrodes are rather close to the sources. For surface electrodes on the other hand,

the volume conductor accounts for a significant deforming effect on the detected sEMG signal[3, p. 30-31].

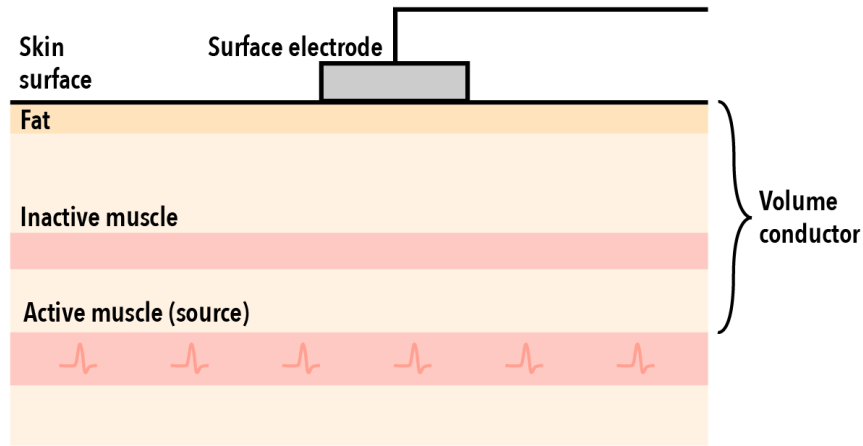


Figure 2.12: Illustration of the volume conductor, which is the conductive tissues between the surface electrode and the muscle source.

Figure 2.13 shows the myoelectric signal from a low-level contraction recorded using surface electrodes. Three motor units – labeled 1, 2 and 3 – can be distinguished from the signal, and although the electrical activity of all motor units is the same, the volume conductor heavily influences the appearance of the myoelectric signal. By comparing the amplitudes of the three motor units in Figure 2.13, one can conclude that motor unit 1 is quite superficial, meaning it is located closer to the surface of the skin so that the recording electrode detects a “stronger” signal. Motor unit 3 is, on the contrary, heavily attenuated as it is located deeper in the tissue. It is also possible to make a rough estimate of the firing rate of the distinct motor units based on the frequency of the peaks. For instance, the peaks of motor unit 2 are roughly 0.2 seconds apart, which means that it has a firing rate of about 5Hz[2, p. 30-31].

Usually, the raw sEMG signal is processed to extract information regarding its amplitude and power spectrum. The amplitude provides information about the muscle contraction “strength”, whereas the power spectrum is used to obtain the frequency content of the signal. In certain conditions, muscle contraction strength and frequency are manifestations of muscle fatigue[3, p. 91].

2.4.1 Acquiring the myoelectric signal

When a muscle contracts, ionic currents are generated deep within the muscle structure and these currents can be detected using electrodes. Using intramuscular electrodes is a rather invasive form of measurement, as it involves injecting microneedles beneath the skin to get closer to the source of the signal. However, this increases the magnitude of the signal. The signal obtainable from surface

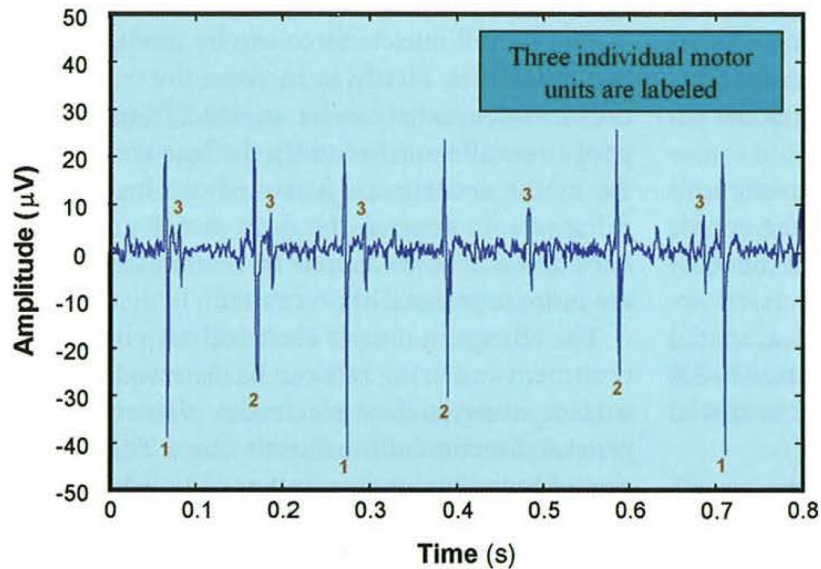


Figure 2.13: Experimental surface recording of myoelectric signals during low-level contraction. From [2].

electrodes, on the other hand, generally has an amplitude in the range $10\mu\text{V} - 10\text{mV}$. Depending on how deep the microneedles are injected, one can obtain larger amplitudes with intramuscular electrodes compared to surface electrodes. The amplitude and appearance of the myoelectric signal obtained by an electrode is a function of, among other things, the strength of the contraction, the overlying tissue, the depth at which the muscle is located, as well as the size, location and orientation of the electrode [2, p. 17-18, 37-38].

Since the level of the signal obtained by surface electrodes is so small, the first step in any myoelectric acquisition system should be signal amplification. According to Lovely (2004), any biomedical instrumentation system that involves a subject is affected by capacitive coupling between the subject and the environment. The capacitive coupling is a result of a difference in electric potential between the subject and the environment – mainly due to the electric field generated by domestic voltage cables and overhead lights in the environment. The domestic supply is usually at a higher potential than the subject, which causes a small current to flow from the domestic supply through the capacitive coupling of the subject, as illustrated in Figure 2.14. Since the current is only a few microamperes in magnitude, it is below the subject's **threshold of perception**, meaning the current goes undetected by the subject. Although small, the current results in a rather large voltage being developed on the body of the subject. The voltage is in the range 5 - 15V, which is much larger than that of the sEMG signals detected by electrodes on the subject. This voltage is called the **common-mode voltage** since it is common to all electrodes placed on the body of the subject

when measuring myoelectric activity[2, p. 37-39].

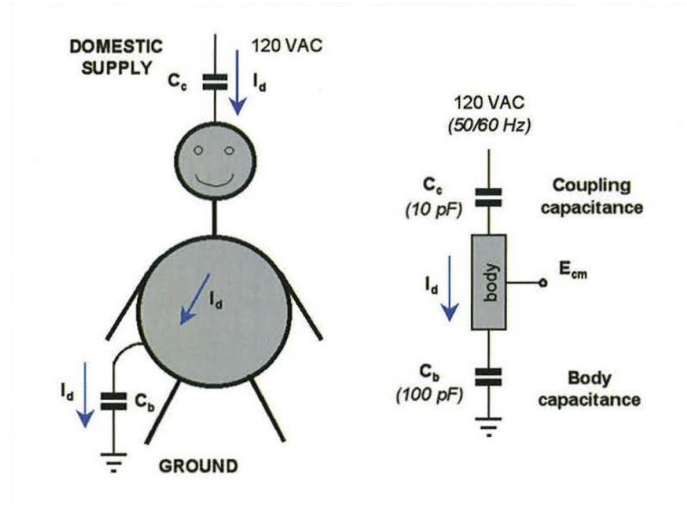


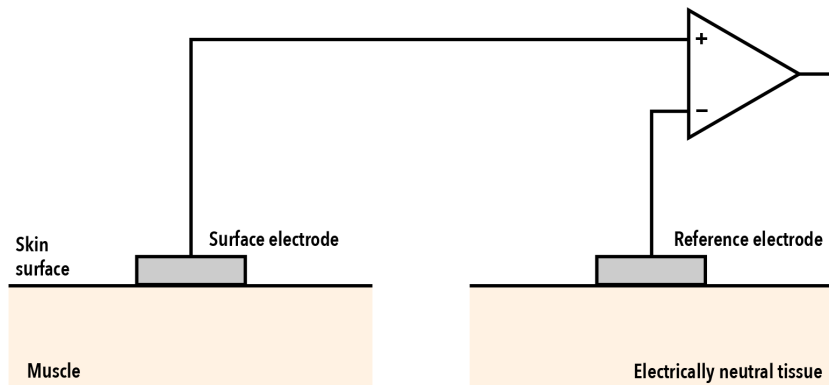
Figure 2.14: Illustration of the capacitive coupling between the body of a subject and the environment. From [2].

Being a result of power line interference from the domestic power supply, the common-mode voltage is at the line frequency of 50Hz or 60Hz (depending on country or region), which overlaps with the frequency bandwidth of the myoelectric signal. Consequently, simple filtering is not possible without distorting the myoelectric signal itself, and therefore a differential amplifier is used[2, p. 37-39]. Differential amplifiers are used in different configurations or montages to extract sEMG signals. Only the most common configurations are presented here.

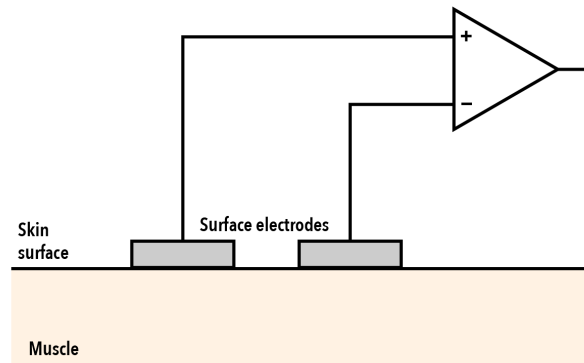
Electrode configurations

The most common electrode configurations for detecting sEMG signals are the **single-ended** and **differential** configurations. Single-ended detection involves detecting the signal of each single electrode with respect to a common reference electrode, as shown in Figure 2.15a. Conversely, the differential configuration detects EMG signals between two adjacent electrodes connected to each input on a differential amplifier, as shown in Figure 2.15b. Note that, since the individual electrode voltages are measured with respect to a common reference electrode, the single-ended configuration is differential in nature.

Multiple surface electrodes can be placed on the surface of the skin, as in Figure 2.16, and this is often referred to as **multichannel** sEMG. Note that the switches S_i in Figure 2.16 are only used to easily illustrate the difference between single-ended and differential configuration; when the switches S_i are in position 1, the acquisition system is configured for differential detection, while position 2 is used for single-ended configuration. Also note that the signal from the electrodes E_i can be used as input to more than one differential amplifier, however,



(a) Single-ended electrode configuration



(b) Differential electrode configuration

Figure 2.15: Illustration of two different electrode configurations. Based on [3].

the electrodes must then be placed along the muscle fiber to detect the propagation of the action potential. The impedances Z_i represent the impedance at the electrode-skin interface[3, p. 58-63].

2.4.2 The electrode-skin interface

The contact area between a surface electrode and the skin is called the **electrode-skin interface**, and this is where charge is carried from the surface of the skin to the recording electrodes. In electrolytes – such as biological tissues – charge is carried by ions, while in metals – like in electrodes – charge is carried by electrons. The exchange of carriers at the boundary generates noise in some form or another[3, p. 56].

The electrode-skin contact can be either wet or dry – either the electrodes are gelled or not. Wet electrodes have an outer layer of conductive gel or paste

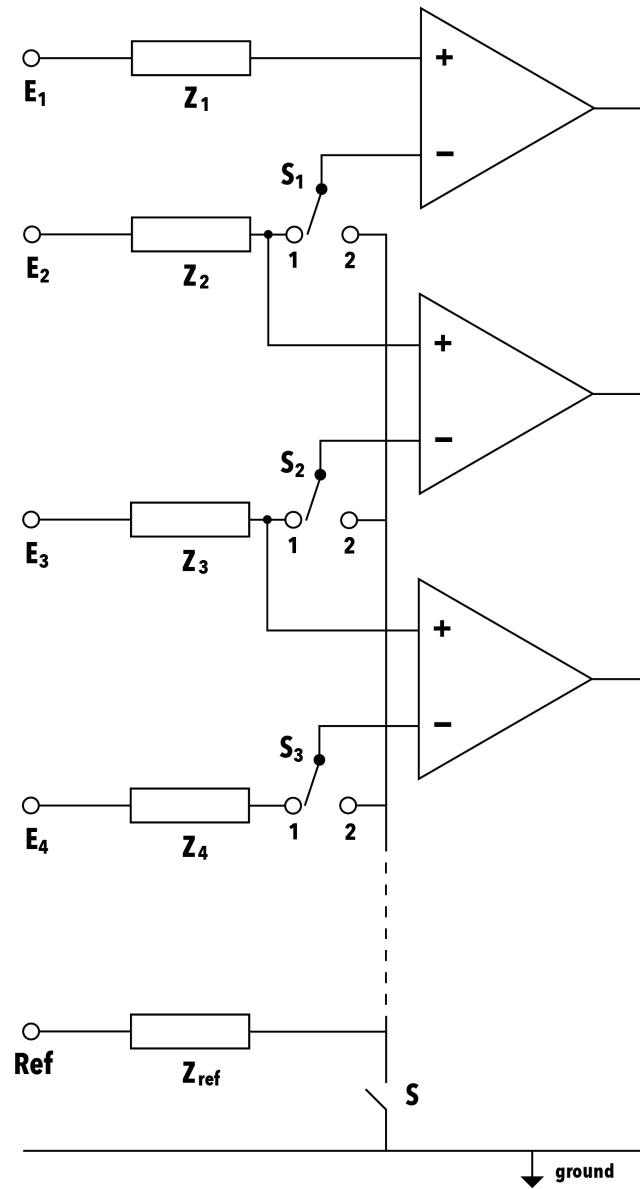


Figure 2.16: Switchable single-ended/differential front-end amplifier for detection of sEMG signals. Based on [3].

to reduce the impedance of the interface and thus achieve increased signal-to-noise ratio (SNR). Dry electrodes are placed directly on the skin without applying any conductive gel or paste. Whether gelled or not, the electrode-skin interface is intrinsically noisy, and the impedance of the interface depends on the type of metal of the electrode and the electrode size, as well as the conductive gel (if used) and the condition of the skin⁴[3, p. 55].

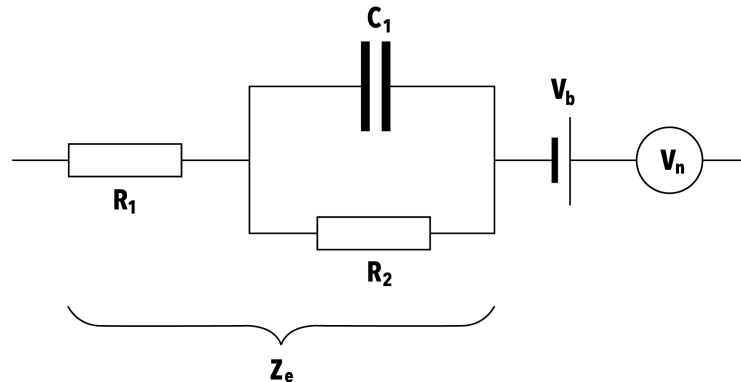


Figure 2.17: A simple physical model of an electrode contact (or of a pair of electrodes) is indicated with the inclusion of the half- (or full-) cell potential V_b and of the equivalent noise generator V_n of the interface. Z_e represents the electrode-skin impedance. Based on [3].

At the metal-skin (or metal-gel and gel-skin) interface, charge layers that contribute to the imaginary (capacitive) component of the interface impedance are created. Merletti and Farina (2016) suggest what they claim to be a rather realistic, although simple, model of the electrode-skin interface for a single electrode channel, shown in Figure 2.17.

2.5 Myoelectric prosthetic systems

Parts of this section are based on Stray (2021).

A brief introduction to myoelectric prosthetic systems is given here. Being its own field of research, control of prosthetic devices is not covered in great detail. Emphasis is put on how myoelectric signals are measured and used to control prosthetic devices, and only the topics necessary to understand the workings of simple myoelectric prosthetic systems are presented here. For simplicity's sake, only electrically powered prosthetic devices are regarded, although it should be mentioned that other types – body-powered prostheses – exist.

⁴Here, “condition” refers to any factor that might influence the electrode-skin contact. Such factors can include dry, clammy or moist skin, for instance. Hairy skin can also affect the electrode-skin contact negatively.

After a transradial (below the elbow) amputation, the lost motor functions can, to a certain degree, be restored by using an electrically powered hand prosthesis. Typically, electrically powered hand prostheses are controlled by myoelectric signals and are then usually referred to as **myoelectric prostheses**[4, p. 127]. EMG electrodes measure the electrical activity produced when a muscle is contracted, and the signal is used as input to the control system of the prosthetic device[13]. Figure 2.18 shows how a myoelectric control system, consisting of EMG electrodes, control system and prosthesis, can provide an alternative means of motor control for amputees[14, p. 453-454]. In healthy humans, feedback about limb position is provided by the somatosensory system, which includes the somatic sensations of touch, pressure, vibration, limb position (also known as proprioception), pain and temperature, among others[9, p. 559]. These sensations are detected by different types of receptors in the skin, muscles, tendons and joints, and are transmitted to the CNS where the information is processed[10, p. 181].

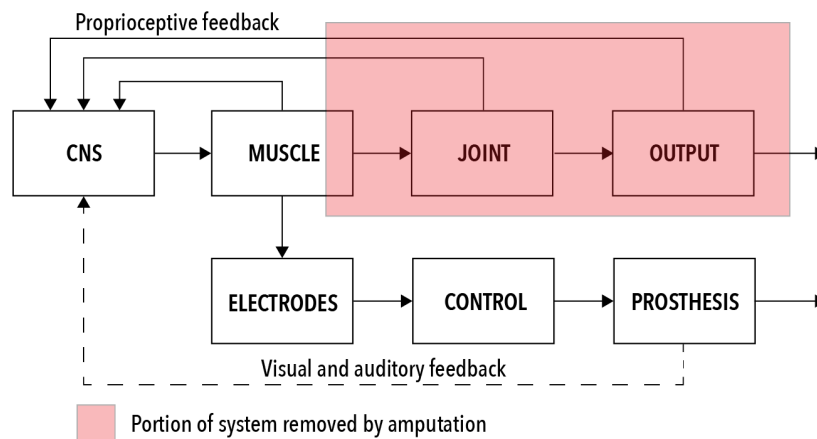


Figure 2.18: Block diagram illustrating how a myoelectric control system differs from the “control system” of a healthy person. Based on [14].

Following amputation, the source of the control signals is the remaining muscle of the residual limb. A muscle control channel can be established by placing a pair of surface electrodes on the skin above the residual muscle. Very simply put, having a closely spaced electrode pair allows for sampling myoelectric signals from a specific muscle, given that the muscle is superficial and that the electrodes are carefully placed above said muscle with a very small distance between them. Electrode pairs placed further apart will collect myoelectric signals from a muscle group, and the signal is a sum of all the motor unit action potentials from the muscle group[14, p. 455]. Myoelectric prostheses are controlled by “commands” translated from the electrical activity of the user’s muscles. For upper-limb pros-

theses, the sEMG electrodes usually target the flexor and extensor muscles of the forearm. These are the muscles that, before amputation, typically were used to move the hand. In myoelectric hand prostheses, the activation of these muscles is mapped to analogous functions – such as opening and closing the hand – in the prosthetic device, making the control relatively intuitive[4, p. 148].

The optimal control scheme for a prosthetic user has to be chosen based on the user's individual abilities and needs[4, p. 200]. Many different kinds of control schemes for prosthetic systems exist, the simplest being the single-channel approach, which only involves a single pair of electrodes, while more complex approaches can involve multiple channels and are often based on machine learning and classification[4, p. 128-130]. Most importantly is that the prosthetic system is able to capture the user's intention. From a control information point of view, it is advantageous with multiple electrode channels, since the signals collected from a muscle group reflects the intention of the muscle contraction – be that opening the hand or rotating the wrist – as the sum of motor unit action potentials from a muscle group is a function of the intended limb movement[14, p. 455]. Chapter 3 further discusses how dense electrode grids consisting of multiple channels are able to capture the user's intention.

Chapter 3

Dense electrode grids for prosthesis control

This chapter gives an introduction to dense electrode grids, how they are used for different applications and discusses the most important challenges associated with dense electrode grids for prosthesis control.

3.1 Introduction to dense electrode grids

According to the authors of *Surface Electromyography: Physiology, Engineering, and Applications*, it is well known that sEMG signals are strongly affected by the distance between electrodes, as well as electrode size and placement. Despite this, the traditional modality used in clinical applications is still mostly based on placing a single or few pairs of individual electrodes on the skin in the region above the muscle of interest. Before going into what dense electrode grids are and how they are used for prosthesis control, it is important to understand why having a single myoelectric channel is not enough.

3.1.1 Limitations of single-channel myoelectric control

Though control schemes for prosthetic systems is not the topic of this thesis, a brief introduction to single-channel approaches – more specifically threshold-based control – is given here as it is essential for understanding the problems related to single-channel myoelectric control.

For single-channel approaches in general, only one EMG channel is used to control both directions of a single degree of freedom (DOF) – for instance opening and closing the hand. Threshold-based control involves using a single sEMG channel to control different states with different levels of contraction or thresholds. For instance, a slight contraction can be used to open the hand, while a strong contraction is used to close the hand. No contraction usually stops the movement. Figure 3.1 illustrates how different thresholds are used to control three states – open hand, close hand and stop – using a single sEMG channel[15].

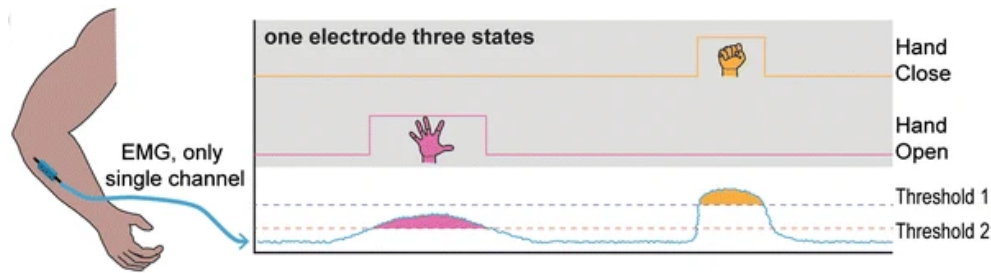


Figure 3.1: Threshold-based control using a single sEMG channel to open and close a prosthetic hand, as well as stop the hand motion. Adapted from [15].

Given the low intensity of sEMG signals, high overall threshold values are needed to distinguish the sEMG signals from background noise and other artifacts, meaning it is harder for the user of the prosthetic system to perform contractions at the different levels[4, p. 138]. Another problem is that the activation of the higher-level state also triggers the lower-level state. This is usually resolved by adding a slight time delay in the control scheme to allow the user to pass through the lower-level contraction without activating its state. In other words, in order to trigger the prosthetic hand to close, the user must perform a higher-level contraction for a slightly longer time. Although reducing the occurrence of error, this results in slow response time of the prosthetic device[2, p. 45]. Slow response time negatively affects the reliability and overall performance of prosthetic devices, which increases frustration and device abandonment rates among users[4, p. 138].

Another challenge with single-channel systems concerns the question of where to place the electrode pair. Generally, finding the best possible electrode placement requires the specialized skills of a trained therapist, and the optimal electrode sites are selected based on where there is muscle activity in the residual limb and what is most intuitive for the prosthesis user. Additionally, prosthetic socket design also affects electrode placement[4, p. 200]. With a single myoelectric channel, electrode placement becomes very crucial for intuitive prosthesis control.

3.1.2 High-density surface EMG

In more recent research, techniques involving multichannel detection by means of 1D or 2D electrode arrays have been adopted. Such arrays can, among other things, provide a spatially sampled image or map of the features of the sEMG signal, which in turn can be used for improved control of prosthetic devices[3, p. 126].

Recall that muscle fibers generate electrical activity during contraction and the myoelectric signals appear on the surface of the body as distributions of electric potentials. By using a grid of electrodes, the detected electric potentials result in **EMG maps** or **images**. When the electrodes in the grid are densely spaced, this technique is referred to as **high-density surface EMG (HD-sEMG)** or sometimes

simply **EMG imaging**. The term **inter-electrode distance** is used to describe the center-to-center distance between electrodes in a grid, and for HD-sEMG arrays, the inter-electrode distance is rarely more than 10mm[3, p. 126]. Figure 3.2 shows a few examples of HD-sEMG arrays.

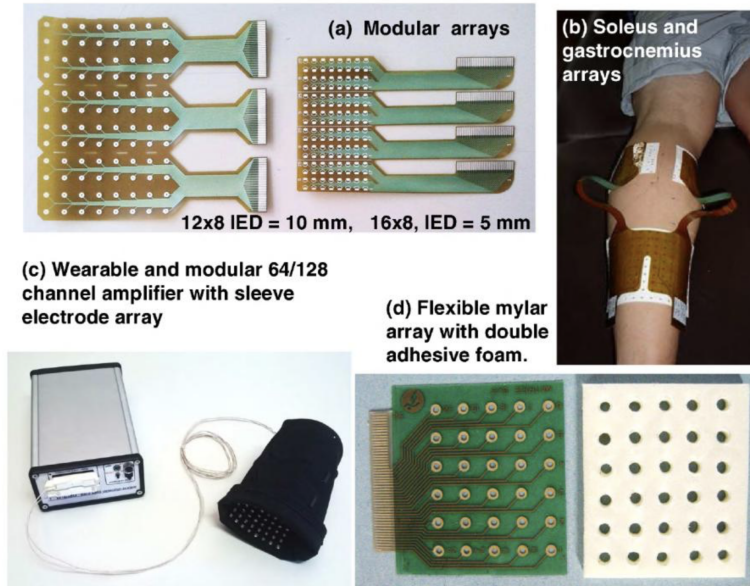


Figure 3.2: Examples of different HD-sEMG arrays. (a) Flexible electrode array made by separable modules. (b) Arrays placed on soleus and gastrocnemius muscles (the main flexors of the ankle joint). (c) Electrode array mounted inside a flexible sleeve, connected to a portable amplifier. (d) Flexible electrode array with double adhesive foam whose cavities are filled with conductive gel. From [3].

The perhaps most basic application of EMG maps is the study of where the different muscles are located in a body part. Figure 3.3 shows five EMG maps generated from monopolar signals using an array consisting of 128 electrodes covering the dorsal side of the forearm. Each map corresponds to the extension of one finger. The maps demonstrate relatively abrupt spatial changes, which makes classification of the activation of individual muscles possible[3, p. 136-137]. Such maps can for instance be used as input to pattern recognition-based control systems for improved prosthetic control, as Section 3.2.1 and Section 3.2.4 are examples of.

TMSi is one of the few actors that has developed a commercial high-density grid for clinical research of HD-sEMG applications, however, to the author's knowledge, there are no commercially available high-density electrode grids specifically made for prosthesis control at the time of writing. The HD-sEMG grids from TMSi are further described in Appendix A.4.

Most prosthetic systems on the market employ control systems based on single or dual contraction patterns, which means that the same contraction pattern is

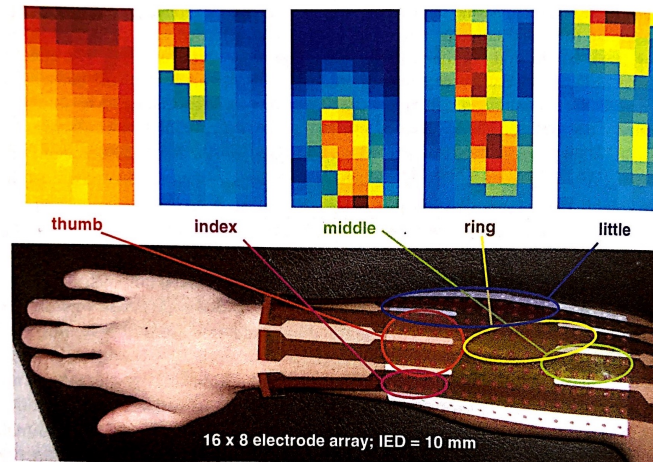


Figure 3.3: EMG maps corresponding to the extension of each finger. The maps are generated from monopolar signals using an array of 128 electrodes. From [3].

used to control different gestures or grips of the prosthetic device. Pattern recognition has become more and more common in prosthetic systems as it allows more flexible control. It is based on the classification of motion intent, which can be captured by measuring the activation of different muscles – the contraction pattern – for the motion that is to be performed[4, p. 131].

Simply put, the contraction patterns, like those in Figure 3.3, are measured by multiple surface EMG electrodes and translated into motions of the prosthetic device. Most prosthetic devices only offer control of one motion at a time, meaning the user cannot open or close the hand while also rotating the wrist, as opposed to able-bodied hand motions. Instead, the user usually has to manually switch between modes using a button, a second contraction pattern¹ or a specific sequence of contraction patterns[5]. One mode could be opening/closing the hand, whereas another could be wrist rotation. More complex systems offer different grips or gestures like pinching or giving a “thumbs up”[4, p. 208-209].

Pattern recognition relies on the precise placement of electrodes in order to target the muscles that are active during a given contraction pattern. However, the use of HD-sEMG grids makes electrode placement considerably easier, while also increasing the resolution of the obtained contraction patterns[5].

3.2 Previous work

This section goes through a few select works related to HD-sEMG systems. These are included to give the reader a better understanding of the applications of HD-sEMG systems, however details are not of great importance.

¹Often, co-contractions are used to switch between modes[4, p. 131].

3.2.1 Real-time gesture classifier using HD-sEMG and deep learning

Tam *et al.* (2020) aims to improve the state-of-the-art and commercially available myoelectric prosthetic systems by providing a control scheme based on HD-sEMG and deep learning. Figure 3.4 exhibits the proposed myoelectric prosthetic system. HD-sEMG data from the forearm is recorded by a dense electrode grid consisting of 32 dry electrodes.

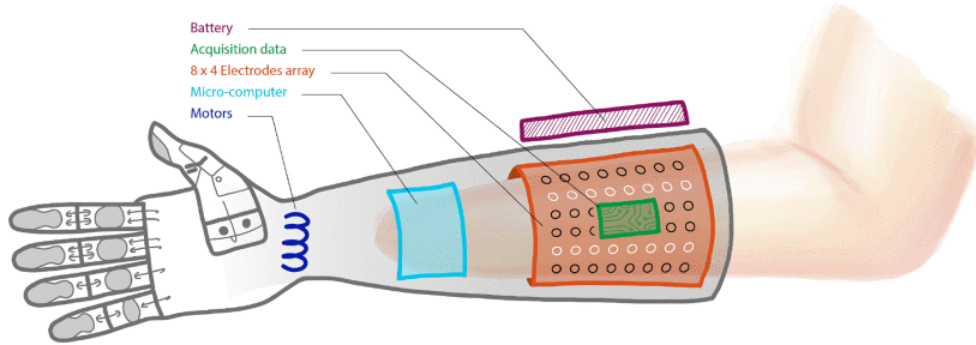


Figure 3.4: Concept illustration of the proposed myoelectric prosthesis system. From [5].

The electrode configuration features a number of shared reference electrodes, as shown in Figure 3.5, and is interfaced with the RHD2132 analog front end from Intan Technologies. A microcontroller transmits the acquired data wirelessly to a micro-computer for dataset recording, neural network training and real-time inference for gesture recognition.

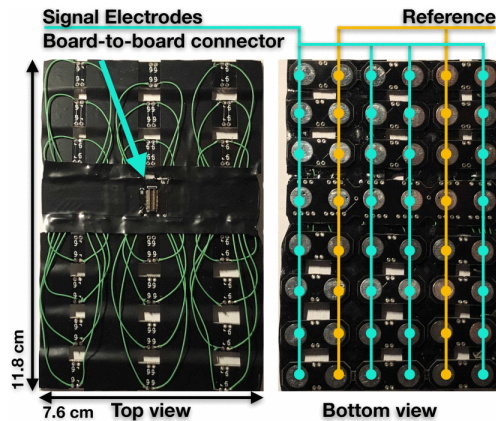


Figure 3.5: Electrode configuration with shared reference electrodes. From [5].

At each sampling instance, the electrode grid outputs a value for each of the 32 channels mapped to a 4x8 array corresponding to the spatial distribution of the electrodes. With a sampling rate of 1kHz, this means that a HD-sEMG map is produced every 1ms, and these maps provide a near-instantaneous image of

the myoelectric activity in the forearm. These images, interpreted as heat maps in Figure 3.6, form the basis of the proposed myoelectric prosthetic system's gesture recognition.

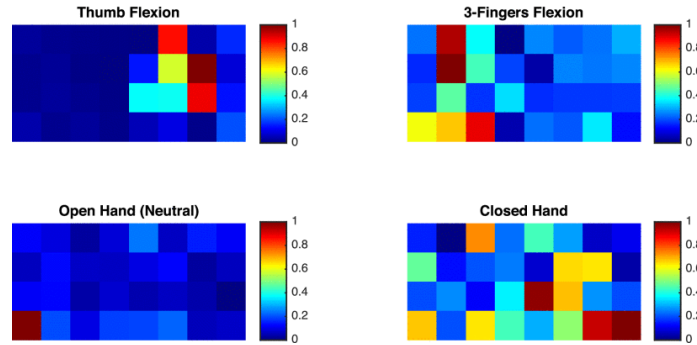


Figure 3.6: Examples of HD-sEMG muscle activation maps where each pixel correspond to one channel of the high-density electrode grid. From [5].

3.2.2 HD-sEMG E-Textile systems for control of active prostheses

As opposed to conventional electrode designs, Farina *et al.* (2010) propose the use of what they have called Smart Fabric and Interactive Textile (SFIT) systems for recording HD-sEMG signals for prosthesis control. More specifically, they propose embedding dense electrode grids in a textile sleeve for the upper limb, as shown in Figure 3.7, where the electrodes themselves are realized with stainless steel yarns. The proposed HD-sEMG system consists of 100 electrodes arranged in four 5x5 grids with an inter-electrode distance of 20mm and electrodes with 10mm diameter. Though gel-free electrodes were used, the electrodes were slightly wet before applying the sleeve to ensure good electrode-skin contact.



Figure 3.7: Textile electrode sleeve for recording of HD-sEMG signals. From [16].

The study emphasizes some of the challenges with HD-sEMG systems, including electrode preparation time and placement. When working with a large number of electrodes, as is the case for HD-sEMG systems, embedding the electrodes in a wearable sleeve that is easy to apply can drastically decrease the preparation time and simplify the process of placing the electrodes above the muscles of interest.

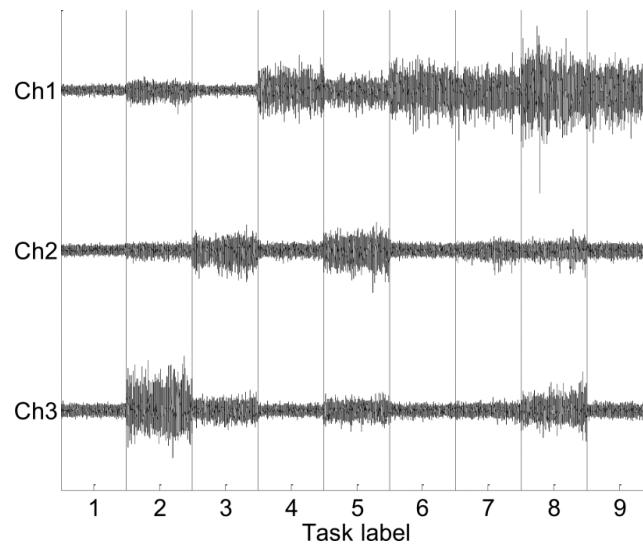


Figure 3.8: Recorded sEMG signals from three representative electrode channels during the performance of the 9 contraction tasks. From [16].

The experimental protocol consisted of performing a total of 9 static tasks commonly used as control input to prosthetic devices. Among others, the tasks included wrist flexion and extension, forearm supination and pronation, as well as opening and closing the hand. The sEMG signals were amplified and A/D converted with 12-bit resolution, recorded with a sampling frequency of 2048Hz and bandpass-filtered using an 8th order Bessel filter with bandwidth 10-750Hz. Figure 3.8 is an example of the raw sEMG signals detected from three representative channels. Each contraction was divided in non-overlapping intervals of 256ms and classified with a supervised pattern recognition approach. The average classification accuracy was approximately 89%.

The work of Farina *et al.* suggests that embedding surface electrodes in garments can be a reasonable alternative to conventional electrode grids when the need for easy application is high – as is the case for users of prosthetic devices who has to remove and re-apply electrodes daily. Further, the authors argue that textile electrodes have the potential to reduce electrode shifting between different uses – if the user removes and re-applies the sleeve in a slightly different position – since the electrodes cover most of the skin’s surface. However, the authors do not address the issue of electrode shifting while wearing the sleeve. Unless the sleeve is uncomfortably tight or embeds high-friction materials in the inner-most layer, there is a chance that electrodes can move with respect to the underlying

muscle as the user performs a muscle contraction. Such movement of electrodes causes electrode shifts and is a source of error.

3.2.3 HD-sEMG after targeted muscle reinnervation

Targeted muscle reinnervation is a surgical procedure that involves re-routing nerves that originally served a now amputated limb. For instance, after shoulder amputation, the nerves that originally were used to stimulate the muscles of the upper arm and forearm, can be re-routed to the pectoralis (chest) muscles, as illustrated in Figure 3.9. Targeted muscle reinnervation is a very complex, and sometimes painful, procedure[4, p. 93-95].

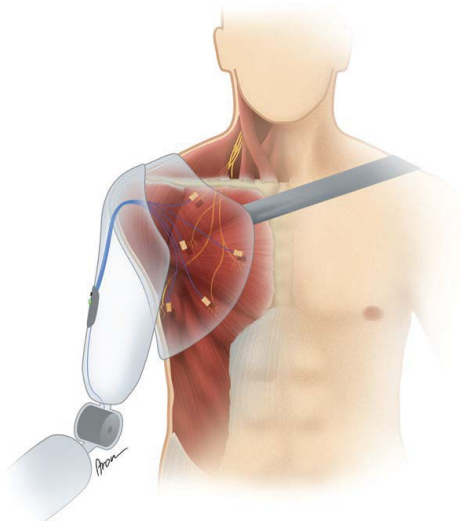


Figure 3.9: Illustration of signal pick-up for prosthetic control after targeted muscle reinnervation. From [4].

Zhou *et al.* recorded HD-sEMG signals from a patient's reinnervated muscles using an electrode grid consisting of 127 channels. Surface EMG data was recorded as the patient performed a series of 27 different movements involving the amputated limb, and the data is presented as contour plots to illustrate the spatial muscle activation patterns of the recorded sEMG signals. The sEMG maps are shown in Figure 3.10.

The authors believe that the muscle activation patterns revealed by the HD-sEMG recording have the potential to further improve myoelectric prosthesis control.

3.2.4 Gesture recognition by instantaneous surface EMG images

Observational latency can be troublesome in many medical applications, especially for applications that require almost instantaneous responses, like exoskeletons and prostheses control. Geng *et al.* (2016) investigated how gesture recog-

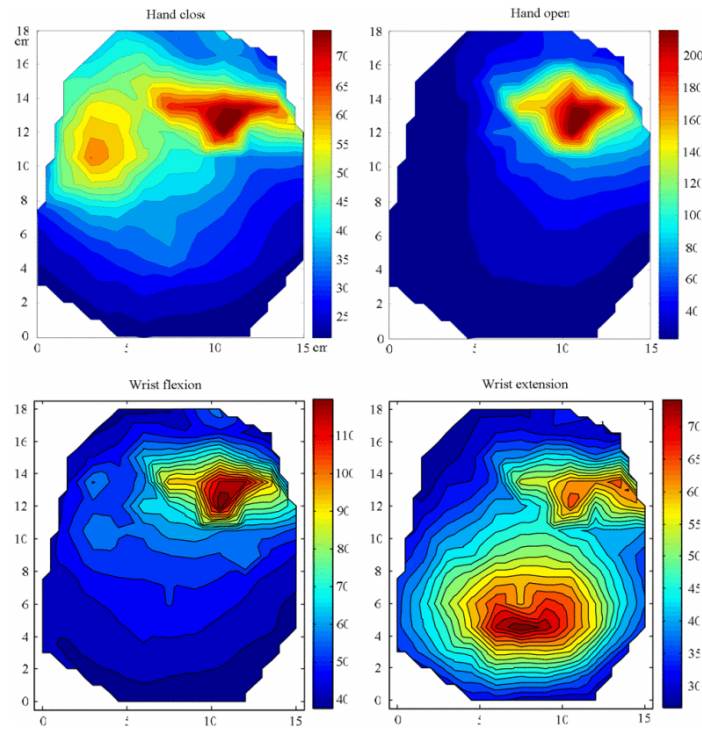


Figure 3.10: Contour plots of HD-sEMG recordings during four different movements. From [17].

nition can be performed using instantaneous high-density sEMG images. Gesture recognition approaches can broadly be divided into two categories: (1) methods based on sparse multi-channel sEMG and (2) methods based on high-density sEMG. Precise positioning of the electrodes is a key requirement for the first method, however this limits its usage in muscle-computer interfaces. High-density sEMG, on the other hand, enables the recording of both temporal and spatial changes in electrical potential since the method entails closely spaced electrodes on the skin above the muscle of interest[18].

When collecting high-density sEMG data, the sampled myoelectric signals are essentially a characterization of “the spatiotemporal distribution of myoelectric activity over the muscles that reside within the electrode pick-up area”[18]. In other words, high-density sEMG data is composed of the distribution of action potentials in time and space, and at a specific time, the instantaneous values from the high-density sEMG grid provide a global measure of the underlying muscle activity at that time. Geng *et al.* claim to have detected patterns inside these instantaneous high-density sEMG images, and that these patterns can be used to distinguish different types of hand gestures. The authors reason that different hand gestures require the contraction of different muscle groups, thus allowing the high-density sEMG grid to pick up different spatial distributions of action potentials to form an image sequence, where each image represents the instantaneous values of the

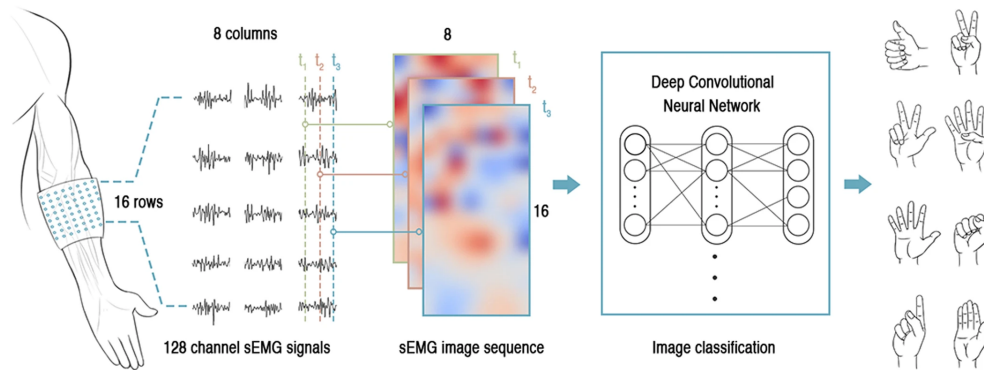


Figure 3.11: Classification of hand gestures based on sEMG images sampled from a high-density electrode grid. From [18].

myoelectric signals. The image sequence can then be fed to a deep convolutional neural network to classify hand gestures based on the myoelectric signals. Figure 3.11 illustrates the sequence of acquiring the sEMG images and performing pattern recognition to classify different hand gestures.

3.2.5 Surface electromyography in clinical gait analysis

Freed *et al.* (2011) presents a relatively new approach for performing gait analysis, which they call Wearable EMG Analysis for Rehabilitation (WEAR). Their aim is to provide an sEMG acquisition system that could overcome common barriers in the clinic at the time. Such barriers included equipment, the time it takes to find a suitable location for electrode placement and limited expertise for sEMG data acquisition. Instead of using a single electrode pair to perform sEMG acquisition, as is done in conventional approaches, the WEAR system employs an electrode grid consisting of eight electrodes integrated in a wearable sleeve. The grid is easily positioned above the muscle of interest and an optimal electrode pair can be selected automatically[19]. Although not a high-density electrode grid, the WEAR system addresses many of the same challenges and barriers of creating a sEMG acquisition system. Freed *et al.* (2012) performed a pilot study to evaluate the performance of the WEAR system with respect to signal quality[20].

As shown in Figure 3.12, the WEAR system consists of three main subsystems: physical interface, electronics and post-processing. The physical interface includes a grid of reusable dry electrodes integrated in a wearable sleeve. The grid has an inter-electrode distance of 20mm and consists of eight medium-sized dome metal electrodes from Liberating Technologies, each electrode being 14.2mm in diameter. Two columns of four electrodes are aligned in parallel with the muscle fibers, and electrodes are paired to form six data channels, as illustrated in Figure 3.13.

The electronics of the WEAR system includes an ADS1298 from Texas Instruments, which is a 24-bit analog front end, and a PIC24 from Microchip, which is

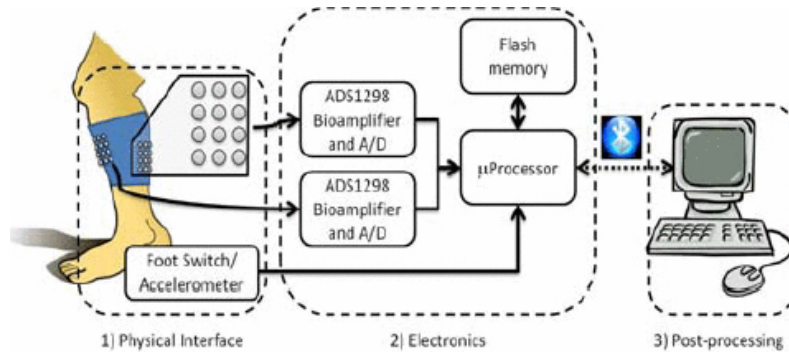


Figure 3.12: WEAR system architecture. From [19].

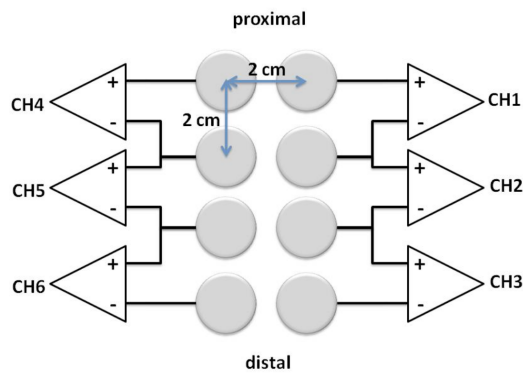


Figure 3.13: Electrode grid configuration. From [20].

a general-purpose 16-bit flash microcontroller. Additionally, the PIC24 interfaces to an SD flash memory card and a Bluetooth transceiver for wireless transfer of the stored data to the post-processing unit. Before post-processing, the sEMG signals are first amplified and then filtered to remove low frequency artifacts using a Butterworth filter.

3.3 Challenges and advantages with dense electrode grids

This section discusses some of the challenges with dense electrode grids for prosthesis control, including available space on the residual limb, the effect of inter-electrode distance on spatial and temporal sampling, as well as the increased complexity that comes with the addition of multiple channels. Few challenges on dense electrode grids are documented, as the literature mainly focuses on the advantages of using HD-sEMG for prosthesis control. Some of the advantages include how dense electrode grids can be used to reduce the effect of electrode shifts and the limb position effect, and how large HD-sEMG systems reduce the effect of crosstalk from nearby muscles.

Where applicable, critical parameters for proper function are identified. With

respect to prosthetic systems, “critical parameter for proper function” refers to a variable or criterion of a dense electrode grid that is considered essential for the prosthetic system’s correct operation.

3.3.1 Available space and muscle on the residual limb

As mentioned, the residual limb seldom has all muscles intact, larger muscles might be missing or the muscle tissue might be damaged so that there is little or no myoelectric activity for the electrodes to measure. This limits the use of pattern recognition-based control schemes – an advanced control system is useless without inputs from the electrodes. Further, a limiting factor to the size and shape of an electrode grid is the available space on the residual limb. Every amputation is different, both in terms of muscle activity and available space, which highlights the need for customized electrode placement. Consequently, dense electrode grids are limited by both the available space and the remaining active muscle tissue, hence these can be considered critical parameters for proper function of dense electrode grid systems.

3.3.2 Spatial and temporal sampling

Applying a two-dimensional array of electrodes to the skin means performing two-dimensional sampling in space. Additionally, because myoelectric signals propagate along the muscle fibers, sampling in time is also performed. 2D sampling has effects on both spatial and temporal EMG features. The spatial sampling frequency can be expressed as

$$f_{sp} = \frac{1}{e} \text{ samples/meter [Sp/m]} \quad (3.1)$$

where e is the center-to-center inter-electrode distance[21]. The signals must be sampled above the Nyquist rate, which is defined as $2f_{max}$, where f_{max} is the highest frequency of the signal, in order to avoid aliasing and, consequently, loss of information.

For an action potential propagating along the muscle fiber with conduction velocity v , the following equation holds for each signal harmonic:

$$v = \frac{\lambda}{T} = \frac{f_t}{f_s} \quad (3.2)$$

where λ is the wavelength in space, T is the period in time, $f_t = \frac{1}{T}$ is the frequency in time and $f_s = \frac{1}{\lambda}$ is the frequency in space[3, 21]. Based on the inter-electrode distance e , the required spatial and temporal sampling frequencies can be found that avoids or limits aliasing, and consequently the inter-electrode distance can be considered a critical parameter for proper function of dense electrode grids.

3.3.3 The effect of electrode shifts

When moving a limb with electrodes attached to it, the movement can cause electrodes to shift relative to the underlying muscles. Large electrode shifts – more than 1-2cm – negatively affect the sEMG recordings, as it reduces repeatability of the acquired signals[22].

Boschmann and Platzner (2012) investigated the effects of electrode shifts when using a high-density electrode grid. They found that, in combination with state-of-the-art pattern recognition algorithms, a grid of 32 sEMG electrodes is sufficient to compensate the electrode displacement effect for electrode shifts up to 1cm[22].

3.3.4 The limb position effect

Variations in limb positions can significantly decrease robustness and usability of myoelectric control systems. In their study, Boschmann and Platzner (2013) investigated whether “increasing the number of electrode channels and recording locations can improve the degraded classification accuracy caused by the limb position effect”. They performed an experiment using a high-density electrode grid consisting of 96 channels. The grid was used to distinguish 11 different hand and wrist movements that were recorded in three different limb positions. The results showed that increasing the number of channels in combination with training in multiple positions contributed to reduce the limb position effect[23].

3.3.5 Crosstalk from nearby muscles

When recording myoelectric signals with surface electrodes, the recorded potentials originate from the muscles directly under the electrodes, however other muscles further away can also contribute to the signal. This is referred to as **crosstalk**[24]. Crosstalk is mainly caused by the extinction of action potentials at the muscle tendon, and the phenomenon is present in surface recordings when the distance between the electrodes and the muscle sources of interest is the same order of magnitude as the distance to adjacent muscles[3, p. 42-43]. Two main factors influence crosstalk: 1) the inter-electrode distance and 2) the position of the electrode relative to the muscle source’s center[25]. Figure 3.14 illustrates how different sEMG electrodes can pick up signals from muscles not directly underneath them. Crosstalk is one of the most important sources of error for interpretation of sEMG signals, and is particularly relevant when studying the activation time of different muscles, for instance in gait analysis and gesture recognition[3, p. 42].

Howard (2017) recommends placing the electrodes above the muscles’ “belly” – in other words, the center of the muscle – to avoid end-of-fiber effects when an action potential reaches the muscle’s tendon. Additionally, crosstalk reduction can be achieved through the use of spatial filters. Since a dense electrode grid is a spatial filter, whose filtering effect depends on the inter-electrode distance, dense

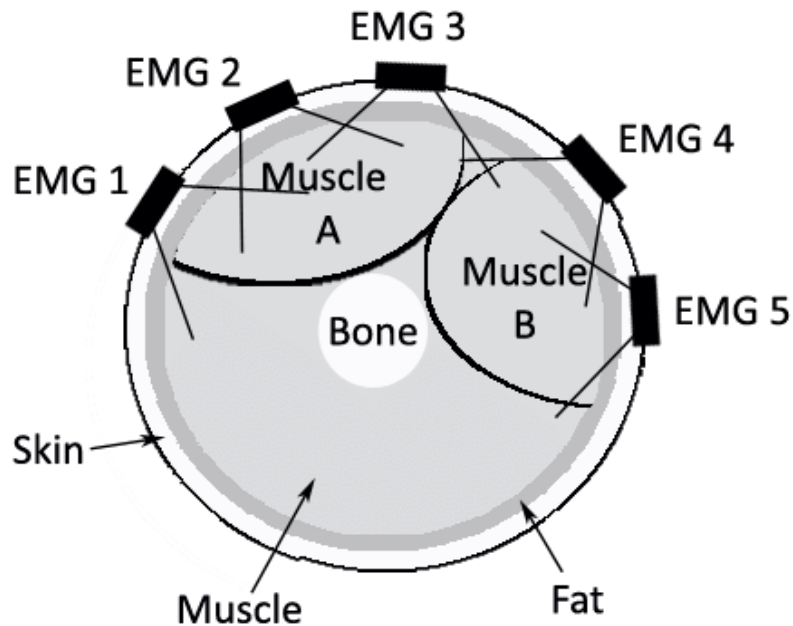


Figure 3.14: Illustration of how sEMG electrodes can pick up crosstalk from nearby muscles. From [25].

electrode grids are less prone to crosstalk compared to conventional single- or two-channel sEMG acquisition[24, 25]. That being said, the most effective method for reducing crosstalk is to use a double-differential electrode configuration, as shown in Figure 3.15.

By including a third differential amplifier, the two differential outputs are subtracted, and crosstalk is reduced because common signals present on both differential recordings of the first amplifier step is canceled by the second subtraction step[24]. Although being superior in terms of crosstalk reduction, the double differential configuration considerably increases the overall complexity of the acquisition system as three electrodes are needed to make up a channel, instead of two. Consequently, there is a trade-off between complexity and the amount of crosstalk reduction. Complexity is discussed next.

3.3.6 Increased complexity

The complexity of a prosthetic control system increases with the addition of multiple channels. Increasing the number of channels increases the computational load of the system as there is more data to be processed. Additionally, the complexity of the control algorithm is increased to account for and make use of the information from multiple inputs to support multiple degrees of freedom. The complexity of the overall design of the prosthetic system increases, not to men-

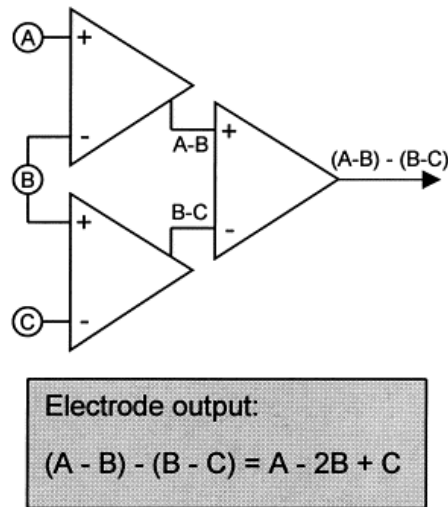


Figure 3.15: Experimental set-up of electrodes A, B and C in a double differential configuration. Adapter from [24].

tion the increase in cost, as more components are required to handle the increase in information load. Though increased complexity in itself is not considered a critical parameter for proper function, too complex systems can negatively affect the usability and intuitiveness of the prosthetic system.

3.3.7 Critical parameters for proper function

To summarize, critical parameters for proper function include the available space and remaining active muscle tissue of the residual limb, as well as the inter-electrode distance of the electrode grid. Additionally, complexity should be included as a critical parameter for *intuitive* function, rather than proper function.

Chapter 4

Requirements analysis

Seeing as no requirements were issued by the end user, a system requirements analysis is in its place. This chapter therefore analyzes relevant requirements of multichannel sEMG acquisition systems, and the goal of the chapter is to establish a functional specification for the prototype of the system. The reader is advised to look at each section individually, as this chapter is not meant to be read as a coherent text. Though not completely unrelated, each section addresses distinct topics, and the functional specification is a summary of these topics.

4.1 Electrode-skin interface

Traditionally, reducing the electrode-skin interface impedance as much as possible was necessary to ensure good signal quality of sEMG recordings. With modern times' amplifiers, having a very low interface impedance is less critical, due to most amplifiers' high input impedance[26]. Nevertheless, reducing the impedance of the electrode-skin interface is still important, since low impedance generally means less noise and, consequently, higher signal-to-noise ratio.

4.1.1 Effect of electrode-skin contact area

One way of reducing the impedance is increasing the contact area between the electrode and the skin[21]. According to Afsharipour *et al.* (2019), as well as Merletti and Farina (2016), the impedance of the electrode-skin interface decreases with increasing electrode size, as shown in Figure 4.1. However, these findings are based on measurements from only five subjects using gelled electrodes. Whether this holds for dry electrodes or not is unclear. Recall the simple model of the electrode-skin interface from Figure 2.17. When the surface area of the electrode increases, more charge can be exchanged at the electrode-skin contact, which is equivalent to decreasing the resistance of the electrode-skin interface. Impedance is the combined effect of resistance and reactance, so the impedance is in theory decreased when the resistance decreases. However, it is unclear how the reactance is affected in this scenario.

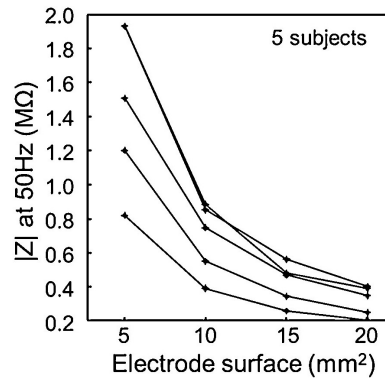


Figure 4.1: Impedance of electrode-gel-skin interface against electrode surface area. Adapted from [21].

4.1.2 Skin preparation

Another way of reducing the impedance is to perform some form of skin preparation, such as applying conductive gel to the skin or rubbing the skin's surface with abrasive paste. A conductive gel reduces the electrode-skin interface impedance by ensuring good contact between the electrode and the skin, while abrasive paste reduces impedance by removing parts of the outermost layer of skin[27].

4.1.3 Balancing contact impedances

Maybe more important than reducing the absolute level of impedance is to balance the contact impedances. A high-density array of surface electrodes applied to the skin constitutes multiple small contact areas, which will have slight differences in impedance due to small differences between each electrode, as well as differences in the skin's surface. An unbalance in impedance between contact areas can have a significant effect on the signal-to-noise ratio of the sEMG signal. Additionally, one should establish stability in impedance over time to ensure that the sEMG measurements are reliable[26]. It has been observed that the impedance stabilizes over time as a result of the human body's natural secretion of electrolytes¹[28].

4.2 Electrode grid

The requirements analysis related to the electrode grid is rather extensive and comprises types of surface electrodes, the electrode's shape and size, inter-electrode distance and number of channels, as well as suitable material choices and fixation method.

¹In other words, sweating.

4.2.1 Type of surface electrode

Silver chloride (Ag/AgCl) electrodes are commonly used for single-channel sEMG applications. Such electrodes consist of a silver plate covered with a thin layer of silver chloride[14, p. 110], which is a conductive gel. Since the electrodes are pre-gelled, they cannot be reused once taken off as the gel will be smeared, which in turn affects the electrodes' conductive properties. For high-density grids, it is common to use grid-shaped adhesive foam where the cavities are filled with conductive gel. However, due to the small spacing between cavities, the conductive gel can leak into neighbouring cavities[29]. This results in short-circuiting of the electrode channels, which means that it is no longer possible to distinguish the signals recorded by the different channels.

As opposed to gelled electrodes, dry metal electrodes can be reused. There are several advantages with using dry electrodes, including their low cost, they are easy to use and there is little risk of skin damage or allergies. Another benefit is that dry electrodes do not require adhesives for fixation, which for many increases comfort. Instead, the electrodes can be integrated with different materials for repeatable use, depending on the application. This can ensure signal quality over time. In addition, due to most metals' malleability, metal electrodes can easily be manufactured according to the application. That being said, dry electrodes are often more prone to noise as the electrode-skin interface has higher impedance for dry electrodes compared to gelled electrodes[28].

For prosthesis control, the electrodes must be suited for long-time wear, and gelled electrodes are therefore not recommended for this application[26].

4.2.2 Effect of electrode shape and size

When discussing electrode shape and size, it is the shape and size of the surface area of the electrode in contact with the skin that is being referred to.

Electrodes come in many different shapes. Circular electrodes are by far the most common, but rectangular electrodes are also used. Based on the literature, there does not seem to be any significant differences in sEMG signal quality between different electrode shapes[3, 26, 29].

As for the electrode size, an increase in electrode size will have a low-pass filtering effect, since the resulting sEMG signal will be an average of the potential detected under the surface of the electrode[21]. The low-pass filtering will decrease the high-frequency content of the sEMG signal, and thus reduce noise. However, very large surface areas can suppress too much of the high-frequency content and negatively influence the features of the sEMG signal. Evidently, there is a trade-off between electrode size and noise reduction, but it is not clear where the optimum is – if it exists.

Afsharipour *et al.* (2019) suggests using electrodes with a grooved or irregular surface area, as this will increase the total surface area that is in contact with the skin while the electrode dimensions can remain small. Alternatively, dome-shaped

electrodes can provide a large total surface area while keeping the diameter of the electrode small.

4.2.3 Inter-electrode distance

Recall that the inter-electrode distance is linked to the spatial sampling frequency with the following relationship

$$f_{sp} = \frac{1}{e} \text{ samples/meter [Sp/m]} \quad (4.1)$$

where f_{sp} is the spatial sampling frequency and e is the center-to-center inter-electrode distance[21].

The spatial sampling frequency also depends on the conduction velocity of the action potentials activating the muscles during contraction. An action potential propagating from the neuromuscular junction to the fiber-tendon junctions – the ends of the muscle fiber – travels with a conduction velocity v given by

$$v = \frac{\lambda}{T} = \frac{f_t}{f_s} \quad (4.2)$$

where λ is the wavelength in space, T is the period in time, $f_t = \frac{1}{T}$ is the frequency in time and $f_s = \frac{1}{\lambda}$ is the frequency in space[3, 21].

In order to find the required sampling frequency, one must first determine the spatial and temporal frequencies. According to Merletti and Farina (2016), the average conduction velocity of an action potential is 4m/s. There is general agreement that frequencies above 400Hz can be disregarded, as the EMG harmonics (in time) above this value are due to noise[3, 21]. This results in a maximum spatial frequency of

$$f_{s,max} = \frac{f_t}{v} = \frac{400}{4} = 100\text{Hz} \quad (4.3)$$

To avoid aliasing, the spatial sampling frequency must be at least doubled (Nyquist), resulting in $f_{sp} \geq 2f_{s,max} = 200\text{Hz}$. This means that the inter-electrode distance should be

$$e = \frac{1}{f_{sp}} \leq \frac{1}{200} = 0.005\text{m} = 5\text{mm} \quad (4.4)$$

Hence, the inter-electrode distance should be less than or equal to 5mm to avoid aliasing in space. Note that the action potential conduction velocity can vary from 3m/s to 6m/s[21], and since the inter-electrode distance of 5mm is found from an average conduction velocity, it can only serve as a theoretical pointer.

4.2.4 Number of channels

As explained in Section 2.5, the idea behind electromyography for prosthesis control is to detect myoelectric signals from the contracting muscle or muscles so that the control system can translate these “prosthesis commands” into movement of the prosthetic device as intended by the user. In other words, the goal is to capture the user’s intention. To do this requires precise placement of electrodes above the muscles of interest. Additionally, detecting several redundant signals can make it easier to translate the prosthesis commands into the intended motion, as it will be more clear which movement the user wants their prosthetic device to perform.

In general, the number of sEMG channels for HD-sEMG acquisition systems depends on the application and the muscles that are to be analyzed[30]. Commonly, 8 or more channels are used for high-density sEMG applications[3] and for prosthesis control specifically it is common to have 8-24 channels, as shown in Figure 4.2.

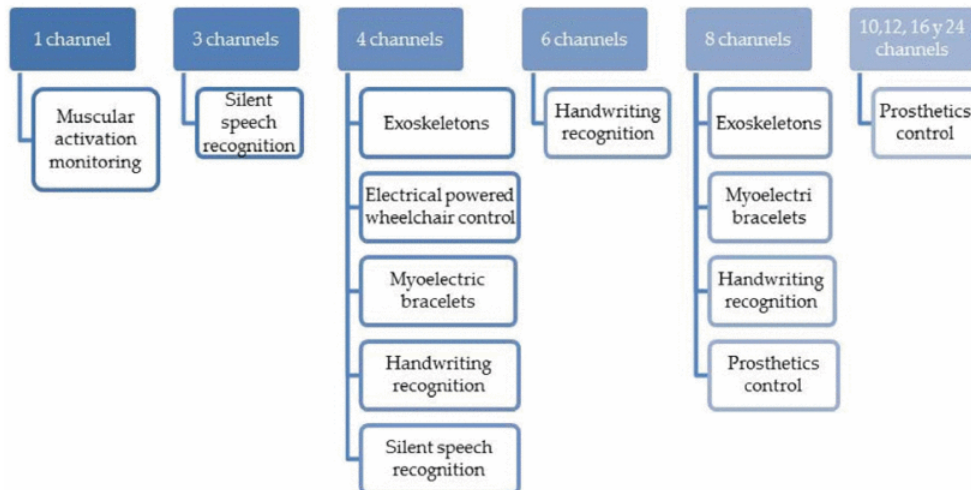


Figure 4.2: Overview of the number of channels commonly used in different applications of sEMG acquisition systems. From [30].

It should be noted that an even higher number of channels have been shown to improve prosthesis control[17, 31], as well as reduce the effects of electrode shifts and the limb position effect[22, 23], as explained in Section 3.3.3 and Section 3.3.4. However, this also affects the computational load, as the amount of information that must be processed by the data acquisition module is considerably increased[30]. The number of channels also depends on the data acquisition module’s number of analog inputs.

4.2.5 Biocompatible materials

For medical applications, it is a general requirement that all materials in contact with the skin are to be compatible with biological tissue, meaning the material

should not cause allergic reactions or any form of skin irritation. In regards to electrodes, suitable materials include copper, brass, titanium, silver, gold and platinum, as well as medical grade stainless steel – usually referred to as 316 stainless steel[26].

4.2.6 Fixation

The method or mechanism that attaches the electrodes to the skin is usually called **fixation**. Fixation is meant to facilitate good contact between the electrode and the skin, as well as limit electrode shifts and pulling of cables[26]. Common fixation methods include double-sided adhesive tape or foam, elastic bands and stickers, in addition to mounting electrodes in sockets for prosthetic devices.

4.3 Data acquisition module

The requirements analysis concerning the data acquisition module address the desirable features of multichannel analog fronts for sEMG signal acquisition and introduce important aspects related to electrical safety and digital signal processing.

4.3.1 Analog front end

Since myoelectric signals are of a very small amplitude compared to most electronic circuitry, the need for amplification is evident. The literature suggests that amplification be the first step in any data acquisition module for sEMG signals, followed by analog-to-digital conversion [2, 3, 14]. For this purpose, so-called analog front ends (AFEs) are suitable. An analog front end is a set of analog signal conditioning circuitry often consisting of analog amplifiers, analog-to-digital converters (ADCs), filters and sometimes application-specific integrated circuits. AFEs provide a configurable interface between the sensors – in this case surface electrodes – and the signal-processing circuitry[3].

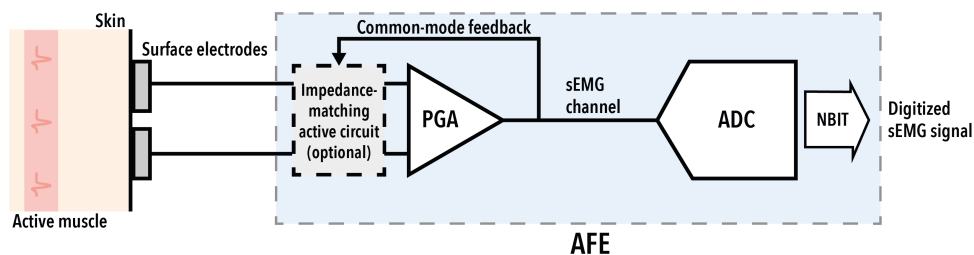


Figure 4.3: Illustration of a one-channel sEMG detection chain. Based on [3].

Figure 4.3 is an illustration of a simple sEMG detection chain consisting of three main blocks; detection using sEMG electrodes, amplification by a programmable gain amplifier (PGA) and analog-to-digital conversion (ADC). “NBIT” rep-

resents the resolution of the ADC. In Figure 4.3, the surface electrodes are configured in differential mode and serve as a positive and negative input to the PGA. If using single-ended mode, a common reference electrode is used as the negative input for all channels. An optional impedance-matching circuit, whose purpose it is to establish and remove a common interference – for instance the 50Hz electromagnetic noise from the domestic power supply – can be added before the amplification stage. An alternative to the impedance-matching circuit is to have an additional electrode that is used to drive the user's body to the same potential as the AFE. For multichannel systems, the detection chain in Figure 4.3 is simply repeated for each channel.

Merletti and Farina provides an overview of all the desirable features of a multichannel AFE for sEMG signal acquisition, and the most important features are summarized below. The following sections will go into more detail on each feature. Desirable features of a multichannel AFE for sEMG signals include[3, p. 75]:

- High input impedance
- High common-mode rejection ratio (CMRR)
- Low input-referred noise with respect to electrode-skin interface noise
- Programmable sampling frequency
- High resolution
- Simultaneous sampling of channels
- Low gain mismatch among channels
- Efficient removal of DC noise

Input impedance

As explained in Section 4.1, having high input impedance amplifiers is important to ensure good signal-to-noise ratio. To be able to measure the small voltage levels of sEMG signals accurately requires the input impedance of the amplifier to be considerably larger than the impedance of the electrode-skin interface – typically, the input impedance should be at least 10 times the impedance of the electrode-skin interface. For gelled electrodes, an input impedance of 10-100M Ω is sufficient, whereas dry electrodes require the input impedance to be in the range 1M Ω – 1G Ω , depending on the skin's condition[32].

Common-mode rejection ratio

Common-mode rejection ratio (CMRR) refers to the ability of a differential amplifier to reject signals common to both inputs of the amplifier[27]. Correlated signal components that are common to both inputs, for instance electromagnetic interference from the domestic power supply, as well as EMG signals from deep muscle sources, are attenuated. An ideal differential amplifier has infinite CMRR, however in practice a CMRR of 90dB is usually enough to reject the common-mode signal[32].

Input-referred noise

Recall that the amplitude of sEMG signals is in the range $10\mu\text{V}$ - 10mV [2, p. 38] Since the signal levels are so small, it is important to limit noise on the inputs so as not to “bury” the signal in noise.

Additionally, sEMG signals have a noisy nature – the signals lack structure and appear random. That being said, the sEMG signals vary with contraction level, as is shown in Figure 4.4 where a sEMG signal is recorded with a pair of 1 cm diameter stainless steel surface electrodes.

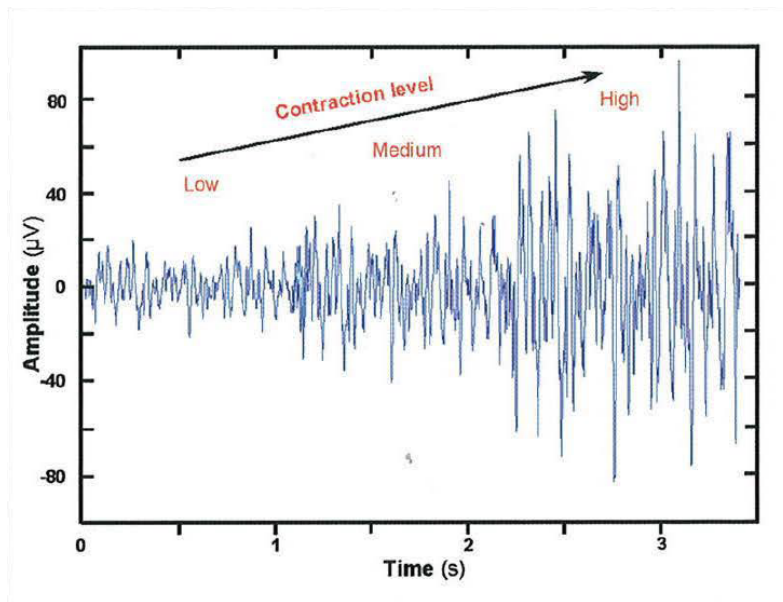


Figure 4.4: Variation of sEMG signal with contraction level. From [2].

Since sEMG signals appear noisy, distinguishing the actual signal from noise can prove challenging. Having an analog front end with as little input-referred noise as possible is therefore crucial.

Sampling frequency

As mentioned in Section 4.2.3, a frequency of 400Hz is regarded as the highest frequency of EMG signals, since frequencies above 400Hz are generally due to noise[3, 21]. To avoid aliasing in time, the sampling rate of the analog front end must be at least twice the maximum frequency of the signal (Nyquist), which in this case means that the required sampling rate must be at least 800Hz.

Resolution

When talking about ADC resolution, one usually refers to the number of bits that the ADC can convert. The range of conversion of the ADC determines the resolu-

tion of the signal. Resolution of the converted signal can be calculated from

$$V_{resolution} = \frac{V_{range}}{2^n} \quad (4.5)$$

where V_{range} is the voltage range of the ADC[27].

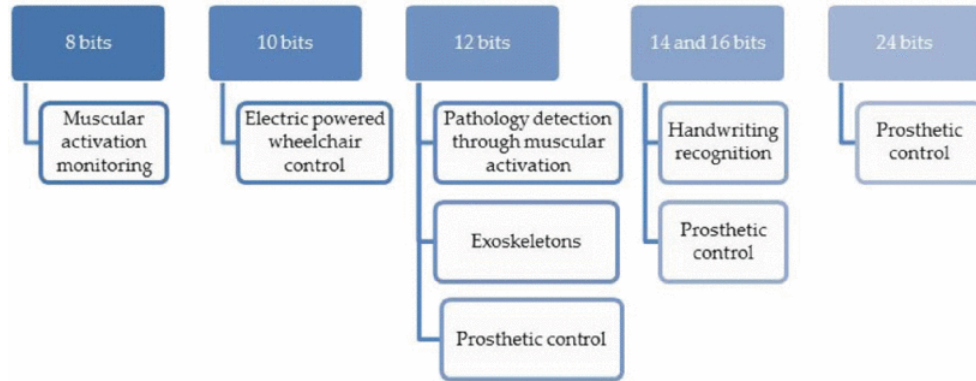


Figure 4.5: Commonly used ADC resolutions for different sEMG applications. From [30].

Figure 4.5 illustrates which ADC resolutions are commonly used for different sEMG applications. For prosthesis control, it is common to use ADC's with 12-, 14-, 16- and 24-bit resolution. Generally, applications that require simpler gesture interpretation require lower resolution, whereas more complex gesture interpretation, like that of prosthetic devices with multiple degrees of freedom, require higher resolution[30].

Assuming a bipolar voltage supply of $\pm 2.5V$, the range of the ADC would have to be 5V. If the ADC then has 16-bit resolution, the resolution of the signal would be

$$V_{resolution} = \frac{5}{2^{16}} \approx 76mV \quad (4.6)$$

which is well above the amplitude of sEMG signals and thus suitable for control of simple prosthetic devices[30].

Simultaneous sampling

For multichannel sEMG systems it is important that all channels are sampled simultaneously – otherwise, the information recorded would not make sense. Multiplexers should therefore follow a sample-and-hold circuit to allow for simultaneous digitizing of the sEMG signals across all channels[3, p. 75].

Channel gain

For prosthetic control, it is common to make use of amplifiers with programmable gain to allow for user customization and flexible configurations[30]. Maybe more

important than having programmable gain is that the channels have low gain mismatch, as small signal differences will cause errors along the line. This is especially important for prosthesis control, since channel gain mismatch can reduce the redundancy of the sEMG signals, which makes capturing the user's intention more challenging and thus reduce robustness of the prosthetic device. Generally, the channel gain error is recommended to not be larger than $\pm 1\%$ [3, p. 76]

Removal of DC-related noise

Amplifier instability can occur when there are small differences in the DC potential measured at each electrode, as such differences will be amplified and possibly saturate the amplifier. These differences in DC potential can be a result of imbalanced impedance.

4.3.2 Electrical safety

It goes without saying that the user of the sEMG acquisition system should not under any circumstances be connected to live wires. As a minimum precaution, the acquisition system should be completely separated from the domestic power distribution, and instead be battery-powered. In addition, any electrically exposed surface should be isolated. Optimally, the user should be at the same electrical potential as the acquisition system to avoid currents traveling as a result of difference in potential[33, p. 659].

4.3.3 Digital signal processing

EMG signals have a frequency range of 0-400Hz[27], however frequencies below 20Hz are generally due to DC-related noise. Consequently, sEMG signals are typically band-pass filtered with cut-off frequencies at 10 or 20Hz and 400Hz[30].

Additionally, to reduce the noise from the domestic power line interference, sEMG signals are usually notch-filtered with a notch frequency at 50Hz[30].

4.4 Functional specification

Figure 4.6 is a concept illustration of the overall design goal for the prototype of the HD-sEMG system. When contracting a muscle, action potentials travel along motor neurons to activate their respective motor units in the muscle, and the prototype is to pick up the signals from the active muscle fibers. The prototype includes a densely spaced electrode grid placed on the surface above the muscle of interest, a data acquisition module consisting of an analog front end and additional circuitry required to sample the sEMG signals and stream digitized signals to a laptop for further processing and analysis.

The design goal is formalized as a functional specification based on the requirements analysis in the previous sections of this chapter. The functional spe-

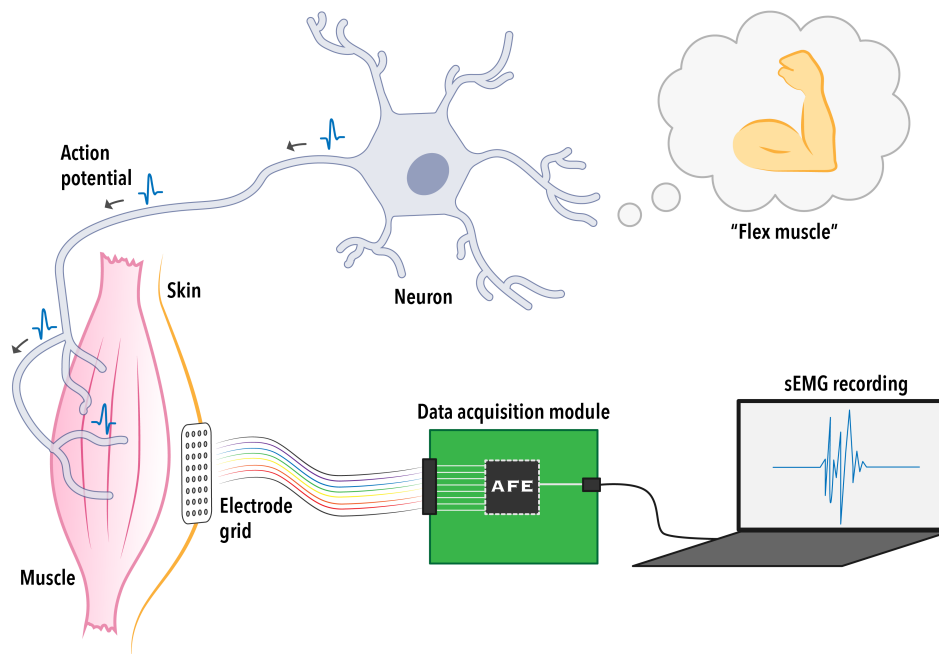


Figure 4.6: Concept illustration of the overall function of the HD-SEMG system.

cification is presented in Table 4.1. Each requirement is given an ID for easy referral throughout the rest of this thesis. Further, the requirements are labelled as either *hard* or *soft*, which describes whether a given requirement is either an *absolute* criteria or a criteria that preferably *should* be met. The requirements are cross-referenced to indicate whether certain criteria are related to or depend on each other.

Table 4.1: Overview of the functional specification for the HD-sEMG prototype system.

ID	Requirement	Type	Cross-ref.
R1	General		
R1.1	Ensure electrical safety	Hard	
R1.2	Biocompatible materials	Hard	
R1.3	Adjustable fixation to fit future users	Hard	
R2	Electrode grid		
R2.1	Balanced contact impedances	Soft	
R2.2	Dry electrodes	Hard	R1.2
R2.3	Inter-electrode distance $\leq 5\text{mm}$	Soft	
R2.4	Extendable grid	Soft	R1.3
R3	Data acquisition module		
R3.1	Input impedance $\geq 100\text{M}\Omega$	Hard	R2.2
R3.2	Simultaneous sampling of channels	Hard	
R3.3	At least 8 channels	Soft	R2.4
R3.4	Sampling frequency $> 800\text{Hz}$	Hard	
R3.5	At least 16-bit resolution	Soft	
R3.6	Programmable gain	Soft	
R3.7	CMRR $\geq 90\text{dB}$	Hard	R2.1, R2.2
R3.8	High SNR	Soft	R3.1, R3.7, R3.9
R3.9	Low input-referred noise	Soft	

Chapter 5

Design and implementation

The following discussion on design choices is based on the functional specification presented in Section 4.4.

5.1 General design considerations

As the goal of this project is to create a prototype for equipment to be used for future research and student activities at a neuromotor laboratory, the overall design should be modular and allow for easily modifying, replacing or removing different parts or components of the system. A key concern is also that the prototype be easy to use.

5.1.1 Electrical safety

Following the requirements established in Section 4.4, requirement **R1.1** says that the system should ensure electrical safety. In addition to isolating the electrical interfaces, the system should be battery-powered to avoid any connections between the user and the domestic power supply.

5.1.2 Materials

The electrodes are to be in contact with the skin for longer periods of time and must consequently be made of a material that is compatible with biological tissue and that does not cause any form of skin irritation. Many metals will satisfy requirement **R1.2**, however there are other considerations to take into account when choosing electrode material.

An important remark concerning electrode material is that it must be malleable – it must be possible to alter the shape without the material breaking. Titanium is only malleable when heated, and due to its high strength it can be hard to shape into small electrodes. Stainless steels are more malleable compared to titanium, and 316 stainless steel is commonly used for biopotential measurements

such as sEMG[34]. Appendix A.2 describes the stainless steel electrodes used by Coapt, which is a manufacturer of surface electrodes and prosthetic systems.

Another concern is cost. Noble metals, like copper, silver, gold and platinum, as well as brass – a copper alloy – are very expensive compared to stainless steel[26]. Stainless steel is also readily available and, as will be discussed in Section 5.2.1, electrodes can be manufactured out of small-sized 316 stainless steel screws or bolts to simplify the manufacturing process and minimize the risk of inconsistencies.

Taking both malleability, cost and availability, and most importantly biocompatibility, into consideration, 316 stainless steel is the most suitable choice of electrode material.

5.1.3 Fixation method

Following requirements **R1.2** and **R2.4**, the main feature of the fixation should be to ensure good electrode-skin contact, while also being easily extendable for future use with the addition of more electrodes. Good electrode-skin contact of all electrodes can help balancing the interface impedance of the electrodes. Another key concern when choosing a fixation method is avoiding electrode shifts. The forearm has a “dynamic” shape in that the shape of the forearm changes depending on what muscles are contracting. This means that fixing the electrodes to a completely stiff structure will result in small movements or shifts of the electrodes when activating the muscles of the forearm.

Section 3.3.3 discussed how dense electrode grids can reduce the effect of electrode shifts, however, it is more beneficial to avoid the problem altogether. To avoid electrode shifts, the electrodes must be mounted with a fixation method that is quite rigid so as to limit movement of the electrodes relative to the underlying muscles. However, as mentioned, the fixation method must also take into account the changing shape of the forearm, and follow the small movements of the skin as a muscle is contracted. A sleeve, like that proposed by Farina *et al.* (2010), with electrodes embedded into the sleeve material has a promising potential. As a bonus, it is easy to apply – even by the user. However, as textiles have a tendency to slide over the skin unless it is worn uncomfortably tight, an elastic band of rubber or silicone would probably be a more suitable alternative. Though the elastic itself is not rigid, the high-friction surface will keep the electrodes in place while also allowing the electrodes to follow the change in shape of the arm as muscles are contracted.

Creating a mounting that “fits all” is essential, as the prototype is to be used in future works. To allow more adjustability and comply with requirement **R1.3**, only the part of the sleeve that embeds the electrodes is made of rubber. The rubber band is held in place by an attachment mechanism¹ consisting of an aluminium brace that allows adjusting the circumference by tightening or loosening a set of

¹By the design of Glenn Angell and Daniel Bogen at the Department of Engineering Cybernetics, NTNU.

velcro straps, as shown in Figure 5.1.



Figure 5.1: Adjustable attachment mechanism of the sleeve consisting of aluminium braces and velcro straps.

5.1.4 Skin preparation

Although not a requirement, the issue of skin preparation should be addressed as it can contribute to balancing the interface impedance. Using a conductive gel or abrasive paste can reduce the electrode-skin interface impedance, however, as explained in Section 4.1, having a low absolute impedance level at the electrode-skin interface is not critical to ensure good-quality sEMG signals, as the input impedance of today's amplifiers is generally high enough. Additionally, using conductive gel or paste is not suitable for long-term use and adds a risk of causing skin irritation. While not significantly affecting impedance, the skin and electrodes should nevertheless be cleaned with gentle alcohols before applying the electrodes to remove any debris or particles that might affect the signal quality. Additionally, if the area where electrodes are to be placed is covered with hair, the area should be shaved before cleaning with alcohol.

5.2 Electrode grid design

This section discusses design choices related to the electrodes and the inter-electrode distance by addressing the requirements concerning the electrode grid in Table 4.1. The design of both the electrodes and electrode connectors are inspired by Coapt's dome electrodes, which are designed for conducting passive measurements of sEMG signals. For those interested, Coapt's dome electrodes are further described in Appendix A.2.

5.2.1 Electrodes and electrode connectors

In order to obtain balanced contact impedances, as discussed in Section 4.1.3, and satisfy requirement **R2.1**, it is very important that the electrodes are as identical as possible. Since a large number of electrodes are needed to make up a high-density grid, the electrodes should be simple to manufacture in order to minimize the risk of inconsistencies.

Based on the topics presented in Section 4.2.2, a relatively large electrode surface area is desirable to reduce the electrode-skin interface impedance, while a small electrode diameter is needed to limit the low-pass filtering effect. As suggested by Afsharipour *et al.* (2019), both can be achieved by using electrodes with a grooved surface area. However, having an irregular surface area makes the production of identical electrodes challenging. To avoid the risk of having imbalanced contact impedances at the electrode sites, a simple electrode shape is better. Seeing as dome-shaped electrodes are common among commercially available electrodes, like those of Coapt and Steeper described in Appendix A.2 and Appendix A.3, dome-shaped electrodes seems to be a good alternative.

The electrode size is to some extent limited by the inter-electrode distance. A compromise has to be made between inter-electrode distance and electrode size, as it is not possible to both have a large electrode diameter while maintaining a small inter-electrode distance. On the one hand, increasing the inter-electrode distance can introduce aliasing, while on the other hand, reducing the electrode size might result in increased impedance at the electrode-skin interface. With an inter-electrode distance of 5mm, it was found that the maximum possible diameter of the electrode contact is 4mm without short-circuiting the electrodes.

In order to simplify the manufacturing process and to reduce costs, an M2x8mm pan head machine screw is used as a starting point for manufacturing the electrodes. The M2 machine screw has a head diameter of 3.8mm, which is within the maximum diameter of the electrodes. The M2 machine screw, shown in Figure 5.2, is made of 316 stainless steel and has a thread length of 8mm.



Figure 5.2: M2x8mm pan head machine screw. From [35].

Although the electrodes preferably would be dome-shaped, it turned out to not be practically possible to manufacture with such a small electrode diameter. Additionally, the M2 machine screw has a recess which when applied to the skin will trap air. Having air trapped beneath the surface of the electrode reduces the electrode-skin contact and thus increases interface impedance. To make the electrodes as identical as possible and aim to satisfy requirement **R2.1**, it was decided that the electrode head shape should be flat. Consequently, the M2 machine screws were milled down. The final electrode shape is shown in Figure 5.3.



Figure 5.3: Final shape of the electrodes used for the prototype.

Being made of 316 stainless steel, using the modified M2 machine screw for electrodes satisfies both requirement **R1.2** and **R2.2**. Moreover, the electrodes are easy to reproduce and therefore facilitates for extending the electrode grid, as per requirement **R2.4**.

The connectors consist of a color-coded ribbon cable, separated and twisted in pairs to reduce movements of cables and cancel out parasitic capacitances, with each separate cable soldered onto a 2.87×11.76mm rectangular stainless steel plate with a hole for the electrode thread. The electrodes are secured in place by stainless steel threaded nuts.

At the time of implementation, M2 flat washers were unavailable. Instead, a second threaded nut is used first to secure the electrode to the sleeve – taking care as to avoiding the electrode head going into the material of the sleeve – followed by the connector cable and a second threaded nut to secure the connector in place. The assembly of the electrodes and connectors embedded in the sleeve is shown in Figure 5.4.

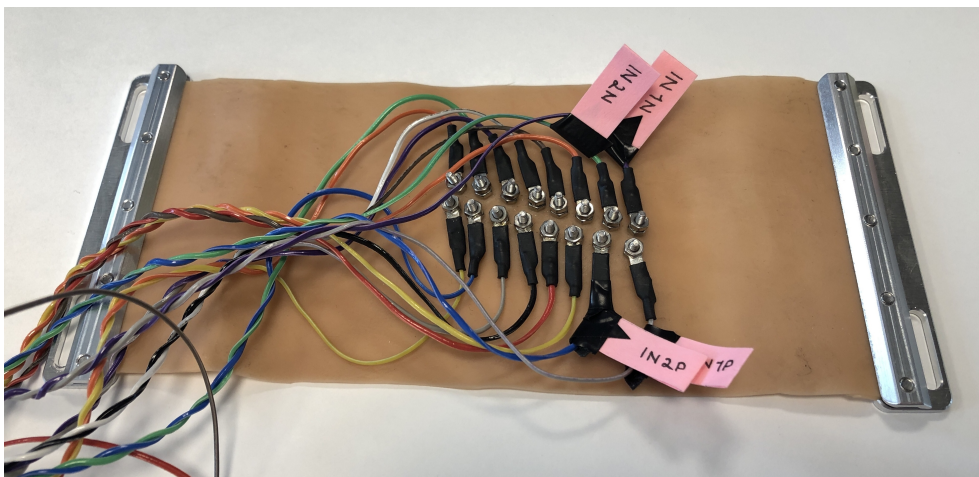


Figure 5.4: Assembly of electrodes and electrode connectors embedded in sleeve.

5.2.2 Inter-electrode distance

As discussed in Section 4.2.3 and reflected by requirement **R2.3**, an inter-electrode distance of 5mm is theoretically desirable to avoid aliasing in space. With 3.8mm electrodes, there should be no issues with having a 5mm inter-electrode distance. However, there turned out to be some space-related issues on the “backside” of the electrode grid. Due to the diameter of the threaded nuts that are used to keep the electrodes in place, the inter-electrode distance had to be increased so as to avoid short-circuiting the electrodes, which is a more severe consequence compared to aliasing². Consequently, the inter-electrode distance is increased to 5.5mm. Figure 5.5 shows the grid template that is used to make holes in the sleeve and ensure that the center of each electrode is 5.5mm apart.



Figure 5.5: The grid template used to make holes in the sleeve. The grid is 4x8 and has a distance between holes of 5.5mm.

5.3 Choosing an analog front end

Ideally, the data acquisition module design would include a custom printed circuit board (PCB) with carefully selected PGA and ADC to facilitate the requirements of the HD-sEMG prototype system. However, due to the time constraints of this thesis, as well as a lack of commercially available components, a simpler solution has to be made. This section will therefore only look at complete system-on-chips suitable as an analog front end for the HD-sEMG prototype system.

Merletti and Farina lists a number of high-performance system-on-chips suitable for EMG and sEMG systems available on the market, including the ADS119x, ADS129x and ADS1299-x families from Texas Instruments, as well as the RHA2000 series from Intan Technologies to name a few. Although many system-on-chips suitable for sEMG acquisition are commercially available, there are few analog front ends with support for more than 8 channels on the market, and only those with 8 channels or more have been considered for the prototype system.

Texas Instruments’ family of analog front ends can be daisy-chained to support up to 64 channels. The ADS119x, ADS129x and the ADS1299-x families are

²It is better to have some signal than no signal.

especially designed for synchronous measurement of biopotential signals like that of Electroencephalography (EEG), Electrocardiography (ECG) and EMG. Both the ADS129x and the ADS1299-x are 24-bit analog front ends with built-in PGAs and ADCs, but they differ in terms of noise levels. While the ADS129x family offers lower power consumption, the ADS1299-x has traded low power for low noise. The ADS119x family is very similar to both the ADS129x and ADS1299-x, however it offers lower resolution, sampling rate, CMRR and SNR[36]. All three families include 4-, 6- and 8-channel devices, however only the 8-channel versions are redeemed relevant in this case.

The RHA2000 series from Intan Technologies consists of three low-noise and low-power analog front ends for either single-ended or differential inputs. Common to all three amplifiers is that they have fixed voltage gain and a 16-to-1 or 32-to-1 analog multiplexer, depending on the number of analog inputs. The high-speed multiplexer allows all input channels to share one external ADC. The RHA2116 and RHA2132 has 16 and 32 single-ended inputs, respectively, while the RHA2216 has 16 differential inputs. Otherwise, the three AFEs are more or less identical[37].

Based on the requirements in Table 4.1, the following AFEs are found to be the most promising; the ADS1198 and ADS1299 from Texas Instruments and the RHA2216 from Intan Technologies³. Table 5.1 compares the features of the ADS1198, ADS1299 and RHA2216. The technical specification for the RHA2000 series is lacking information on sampling rate and SNR, and these are denoted by “NA” for “not available” in the table. Since the RHA2000 series does not include an on-board ADC, the resolution of the RHA2216 is not specified.

Both the ADS1198 and ADS1299 can be configured to use single-ended or differential inputs, whereas the RHA2216 only takes differential inputs. All three are designed so that no additional amplification step is required between the electrodes and the AFE[36, 37], but the RHA2216 requires an external ADC to digitize the output from the on-board analog multiplexer. While both the ADS1198 and ADS1299 have programmable gain, the RHA2216 has a fixed gain. Another drawback with the RHA2216 is that the CMRR is below the recommended value of 90dB[32] and it does therefore not satisfy requirement **R3.7**.

While originally designed for EEG applications, the literature seems to favor the ADS129x and ADS1299-x analog front ends for multichannel sEMG applications[3, 19, 20, 38]. Additionally, the ADS1299 is a key component of the Cyton Biosensing Board made by OpenBCI. The Cyton board has been used for multiple sEMG applications according to OpenBCI’s citation list with over 200 papers, including the recent works performed by Valderrama *et al.* (2021), Martin *et al.* (2018) and Zhang *et al.* (2019). Despite having higher input impedance and a

³Another alternative, the RHD2132 from Intan Technologies, was discovered at the last minute. Though not included in this evaluation, it seems like a promising analog front end as it has some of the same features as the RHA2216, but also features an integrated ADC.

⁴Can be daisy-chained for up to 64 channels[36].

⁵Not available

⁶ μV_{RMS}

Table 5.1: Feature comparison of different analog front ends.

Feature	ADS1198	ADS1299	RHA2216
Input impedance [M Ω]	1000	1000	1300
Simultaneous sampling	Yes	Yes	-
No. of channels	8 ⁴	8 ⁴	16
Sampling rate [Hz]	125-8000	250-16000	NA ⁵
Resolution	16-bit	24-bit	-
Gain	Programmable	Programmable	200
CMRR [dB]	105	110	82
SNR [dB]	97	121	NA
Input-referred noise [μ V _{pp}]	12	1	2 ⁶

higher channel count per chip, the RHA2216 loses in terms of configuration flexibility and CMRR.

Comparing the ADS1198 and ADS1299, the ADS1299 is superior in terms of sampling rate, resolution, CMRR, SNR and input-referred noise. These features make the ADS1299 an easy choice for the prototype of the HD-sEMG system.

Preferably, the ADS1299 would be embedded on a custom PCB. However, at the time of writing, the production and delivery time of the ADS1299, as well as other members of the ADS119x, ADS129x and ADS1299-x families, is approximately 23 weeks, which well extends the time span of this thesis. As an alternative, Starcat LLC offers an Arduino shield with the ADS1299 at its core. It is very similar to the Cyton Biosensing Board and is being used in clinical research and pharmaceutical companies[41]. The Arduino shield, depicted in Figure 5.6, is compatible with the Arduino Due and is licensed as an open-source project called HackEEG, according to the CERN Open Hardware Licence v.1.2[41].

With easily accessible schematics and drivers, HackEEG takes care of power supply circuitry and the ADS1299's power-up sequence, as well as communication with the microcontroller on the Arduino Due. The Arduino Due has a SAM3X8E ARM Cortex-M3 CPU[42] and communicates with the ADS1299 through SPI. With support for direct memory access (DMA), the maximum data rates of the ADS1299 can be the utilized as the CPU is released to perform other operations while waiting for input from the ADS1299. Arduino drivers provide an interface to the ADS1299's configurations and functional modes, and the HackEEG also provides a Python client for receiving data from the Arduino Due over USB. The drivers and Python client are a good starting point, but require some tweaking for optimal functioning. Easily accessible jumpers on the Arduino shield allows for

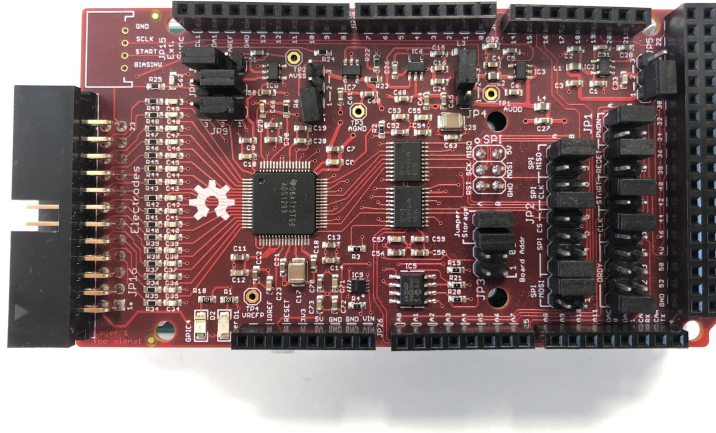


Figure 5.6: Arduino shield from HackEEG connected on top of an Arduino Due.

high configurability of the ADS1299, including options for power supply, bias input and bias drive, as well as SPI configurations for when multiple Arduino shields are daisy-chained[41]. The schematics for the Arduino shield can be found in Appendix B.

The Arduino shield is quite costly, and due to budget constraints only one can be purchased for this thesis' project. This rules out daisy-chaining the ADS1299 to include more channels. However with 8 channels, requirement **R3.3** is still satisfied, and the Arduino shield can nevertheless be used to evaluate the suitability of the ADS1299 for future use with an extended electrode grid in order to satisfy requirement **R2.4**.

The final prototype consisting of electrode grid, sleeve and acquisition module is shown in Figure 5.7.

5.4 Digital signal processing

This section describes the digital signal processing techniques applied to the signals acquired with the prototype and accompanying data acquisition module.

5.4.1 Bandpass filter

The frequency bandwidth of EMG signals is in the range 0 – 400Hz[27]. The acquired signals are bandpass-filtered with cut-off frequencies at 20Hz and 400Hz, as frequencies below 20Hz are generally due to DC-related noise and frequencies above 400Hz are disregarded as high-frequency noise.

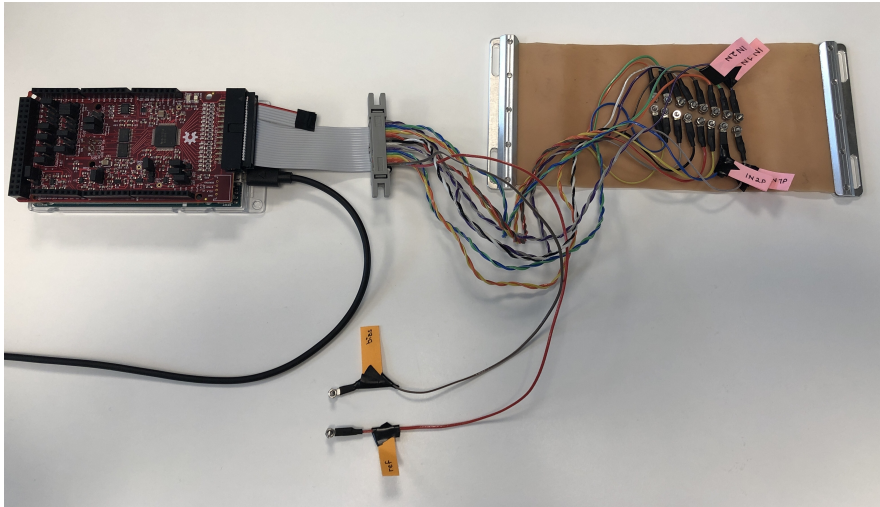


Figure 5.7: Prototype consisting of dense electrode grid embedded in a rubber sleeve and connected to the Arduino shield with the ADS1299 at its core. The Arduino shield is stacked on top of an Arduino Due, which is connected to a battery-powered laptop (not shown in figure).

5.4.2 Comb filter

Figure 5.8 shows the power spectres of the noise floor of signals acquired with the ADS1299 before and after applying a comb filter. Clearly, the signal is dominated by 50Hz and its harmonics as a result of electromagnetic interference from the domestic power supply.

Using a notch filter is not sufficient for reducing the interference from the power line harmonics. Instead, a comb filter is applied. A comb filter, in its simplest form, can be viewed as consecutive notch filters where the notches occur periodically across the frequency band, and are commonly used for suppressing power line harmonics[43, p. 341]. Figure 5.9 shows the frequency response of the applied comb filter.

The bottom plot of Figure 5.8 shows the power spectrum of the noise floor after applying a comb filter with notch frequency of 50Hz and quality factor 10.0.

5.4.3 Spectral gating

Spectral gating was attempted as a means of further reducing the 50Hz interference and its harmonics. This was done by first finding the power spectrum of the bandpass-filtered sEMG signal, removing the frequencies belonging to the 50Hz interference and its harmonics, and transforming back to the time domain by taking the inverse Fourier transform. However, this method did not perform better than the comb filter as it ended up affecting frequencies unrelated to the 50Hz harmonics, resulting in degradation of the sEMG signal. Consequently, only the bandpass and comb filters are applied to the sEMG signals.

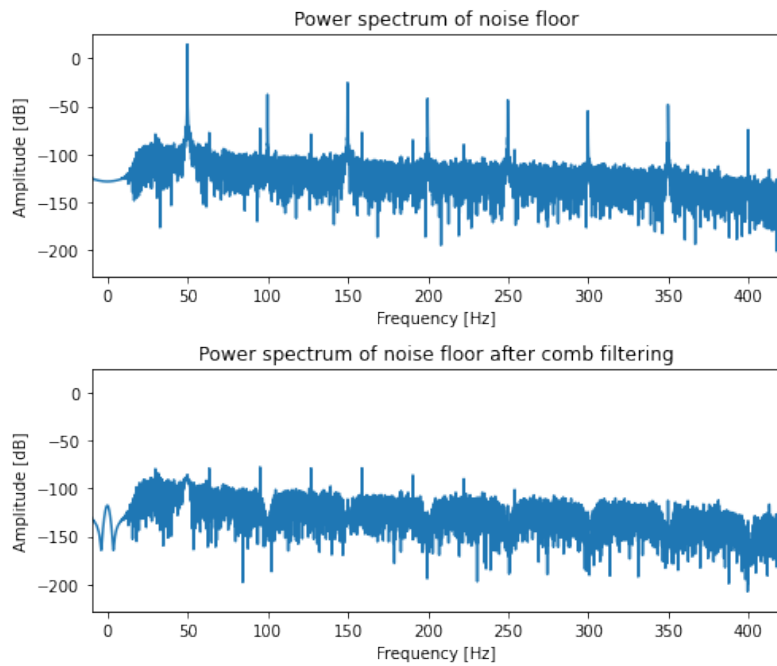


Figure 5.8: Power spectrum of the noise floor before and after applying a comb filter with notch frequency = 50Hz.

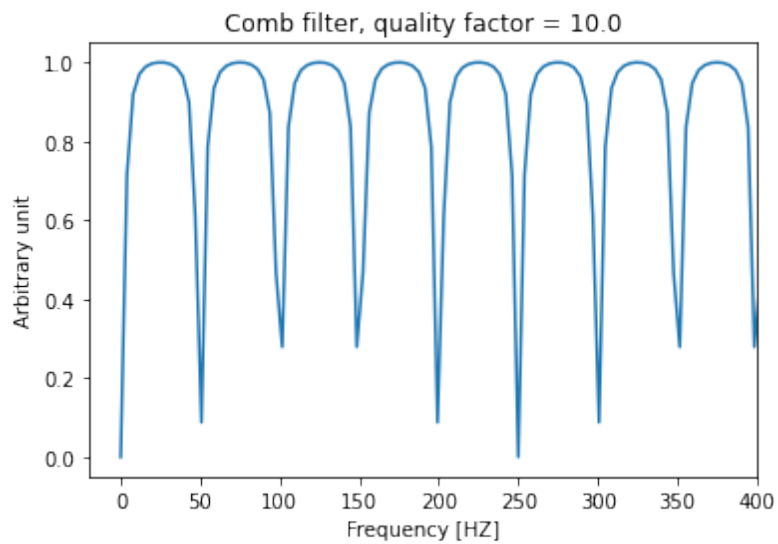


Figure 5.9: Frequency response of a comb filter with notch frequency = 50Hz and quality factor = 10.0.

Chapter 6

Characterization of prototype

6.1 Application note: Intro to ADS1299

The HD-sEMG system prototype – from here on simply referred to as *the prototype* – consists of a dense electrode grid and accompanying data acquisition module suitable for recording sEMG signals from superficial muscles on the ventral side of the forearm.

The sleeve and electrode grid is positioned above the superficial muscles of the forearm that are active during flexion of the wrist – the flexor carpi ulnaris, flexor carpi radialis, palmaris longus and flexor digitorum superficialis. Due to the inclination of the electrode grid on the sleeve, the prototype is not suited for recording other groups of muscle, as electrode pairs must be positioned parallel to the underlying muscle and this cannot be guaranteed for other muscle groups than those specified above.

The data acquisition module consists of an analog front end, specifically the ADS1299, that interfaces to the electrodes. The ADS1299 is placed on an Arduino shield connected to an Arduino Due, and the microcontroller on the Arduino Due communicates with the ADS over SPI. The Arduino Due communicates with a laptop over USB, and the data acquisition module is powered by the same USB connection.

Note:

Under no circumstances should the laptop powering the Arduino Due and shield be connected to the domestic power supply. This is to ensure electrical safety in case of any short-circuits or faulty connections on the PCB.

The ADS1299 consists of an integrated programmable gain amplifier (PGA) and analog-to-digital converter (ADC). A highly-programmable multiplexer allows for many configurable signal-switching options, including EMG-specific functions related to bias derivation and bias drive. A functional block diagram for the ADS1299 is included in Figure 6.1.

In order to communicate with and configure the ADS1299, commands are

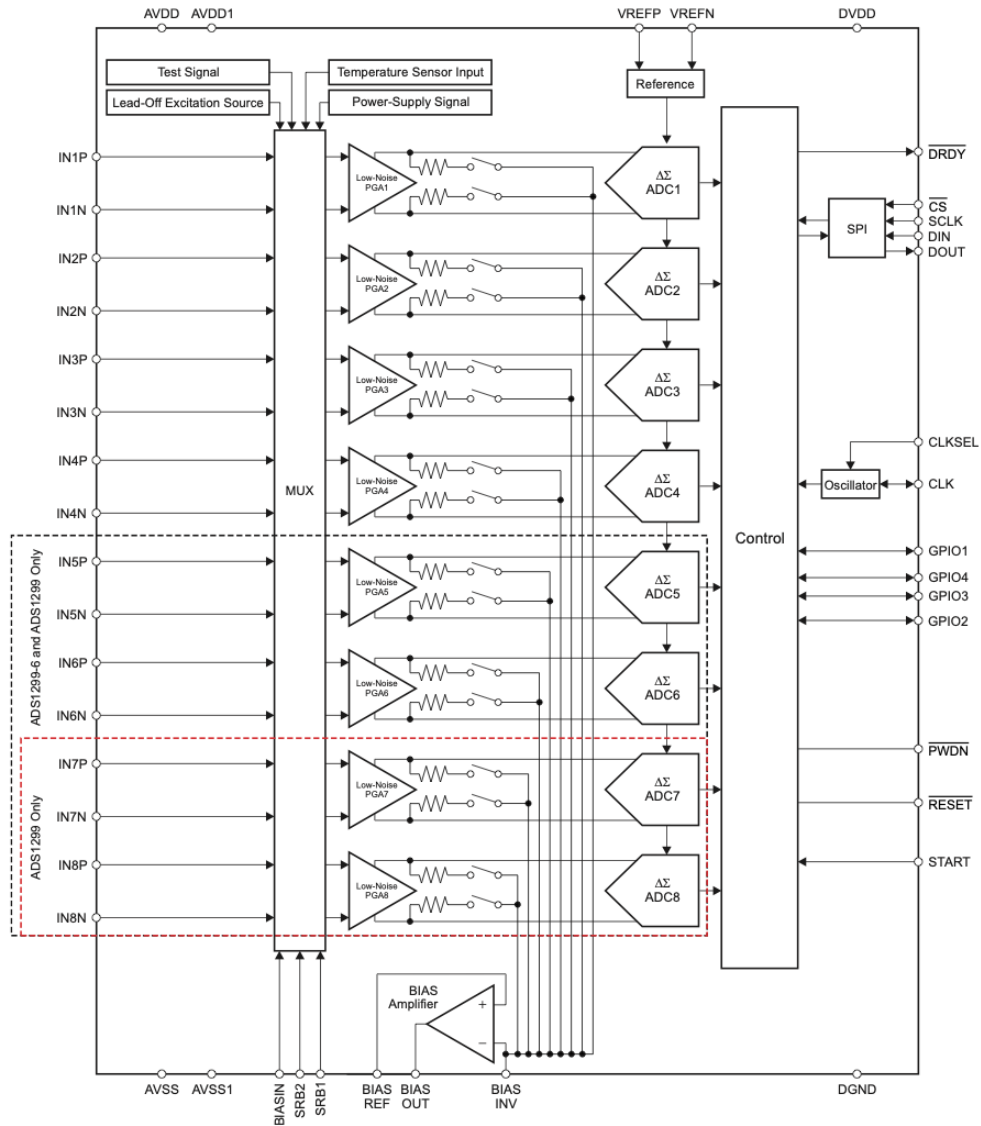


Figure 6.1: Functional block diagram for the ADS1299. From [36].

issued to control and configure device operation. An overview of the commands and their description is given in Table 6.1.

Table 6.1: Overview of ADS1299 command definitions. Adapted from [36].

Commands	Description
System commands	
WAKEUP	Wake-up from standby mode
STANDBY	Enter standby mode
RESET	Reset device
START	Start and restart (synchronize ¹) conversions
STOP	Stop conversion
Data commands	
RDATA	Read data by command
RDATAC	Enable Read Data Continuous mode
SDATAC	Stop Read Data Continuous mode
Register commands	
RREG	Read register
WREG	Write register

Conversions begin when the START command is issued and continues indefinitely until the STOP command is issued. When the STOP command is sent, the conversion in progress is allowed to complete. Conversion data is read by issuing either RDATA or RDATAC and contains the following bits: 24 status bits + 24 data bits × 8 channels = 216 bits. The RDATAC command enables continuous data conversion output without the need to issue subsequent read data (RDATA) commands. The Read Data Continuous mode places the conversion data in the output register and may be shifted out directly. To retrieve data from the device, first issue a START command followed by an RDATAC command. If the device is in RDATAC mode, an SDATAC command must be issued before any other commands can be sent to the device. This also means that the device must be configured for data acquisition before issuing the RDATAC command[36].

Data samples are sent as two's complement 24-bit binary numbers, one for each channel. The least significant bit correspond to a voltage step given by Equation (6.1), which can be used as a scaling factor to convert the samples from bits to voltage.

$$V_{\text{LSB}} = \frac{2 \cdot V_{\text{ref}}}{\text{GAIN} \cdot 2^{24}} = \frac{V_{\text{ref}}}{\text{GAIN} \cdot 2^{23}} = \frac{4.5\text{V}}{\text{GAIN} \cdot 2^{23}} \quad (6.1)$$

The ADS1299 features multiple registers for global settings across channels, as well as registers for channel-specific settings and a few other registers. The most important registers for global settings are the CONFIG1, CONFIG2 and CONFIG3 registers. CONFIG1 configures the sampling rate and contains settings for the clock

¹If multiple devices are daisy-chained

and daisy-chaining, CONFIG2 features configurations for test signal generation, while CONFIG3 is used to set the internal or external reference, as well as configure bias operation. Bias operation is further described in Section 6.1.3. Channel-specific settings are configured in the CH[1:8]SET registers, with one register per channel, as well as the BIAS_SENSP and BIAS_SENSN registers. The CH[1:8]SET registers control the operational mode, gain and other channel-specific settings, and Section 6.1.1 addresses the configurations used for the prototype. The BIAS_SENSP and BIAS_SENSN registers control the selection of using positive and negative electrode inputs as feedback to the bias amplifier. Another important register is the MISC1 register, which controls whether the device should operate in single-ended or differential mode.

It is important to set the voltage reference source of the ADS1299, or else all measurements will be faulty. The voltage reference must be 4.5V, which can be provided either internally or externally and is controlled by setting or clearing the PD_REFBUF bit in the CONFIG3 register.

Note:

The ADS1299 default configuration is to use an external reference voltage, however the required pins are not available on the Arduino shield. Forgetting to enable the internal reference voltage by setting the PD_REFBUF bit in the CONFIG3 register will therefore lead to invalid measurements.

The reference voltage is generated with respect to the negative voltage supply. The ADS1299 supports both unipolar and bipolar voltage supply, however since sEMG signals can have both positive and negative values, bipolar supply is recommended[36]. The supply is configured by adjusting the following jumpers on the Arduino shield: Jumper 4 is set to pins 2-3 to set AVDD to +2.5V and Jumper 5 is set to pins 1-2 to set AVSS to -2.5V.

6.1.1 Channel configurations

As mentioned, the CH[1:8]SET registers control channel-specific settings. This includes the gain settings of the PGA, whether a channel should be powered down or operate normally, as well as configuring the channel inputs. The channel inputs can be set to normal electrode input, which is used for data acquisition, the inputs can be shorted for offset or noise measurements, as well as be used for test signals or bias drive (if not using a separate bias electrode, as explained in Section 6.1.3). The gain of the PGA is set by writing the corresponding value for the GAINn[2:0] bits, while power-down is controlled by the PDn bit. Clearing this bit configures the channel for normal operation, which is the default power mode. Finally, the MUXn[2:0] bits determine the channel input selection, the default being normal electrode input.

6.1.2 Operational mode

The ADS1299 can be configured in differential mode or single-ended mode. When in differential mode, each channel represents a differential voltage between two adjacent electrodes, as illustrated in the schematic in Figure 6.2. Up to 16 electrodes can then be connected to the analog input of the PGA, forming a total of 8 channels. Each channel consists of one positive and one negative electrode input, denoted IN_{xP} and IN_{xN} , respectively.

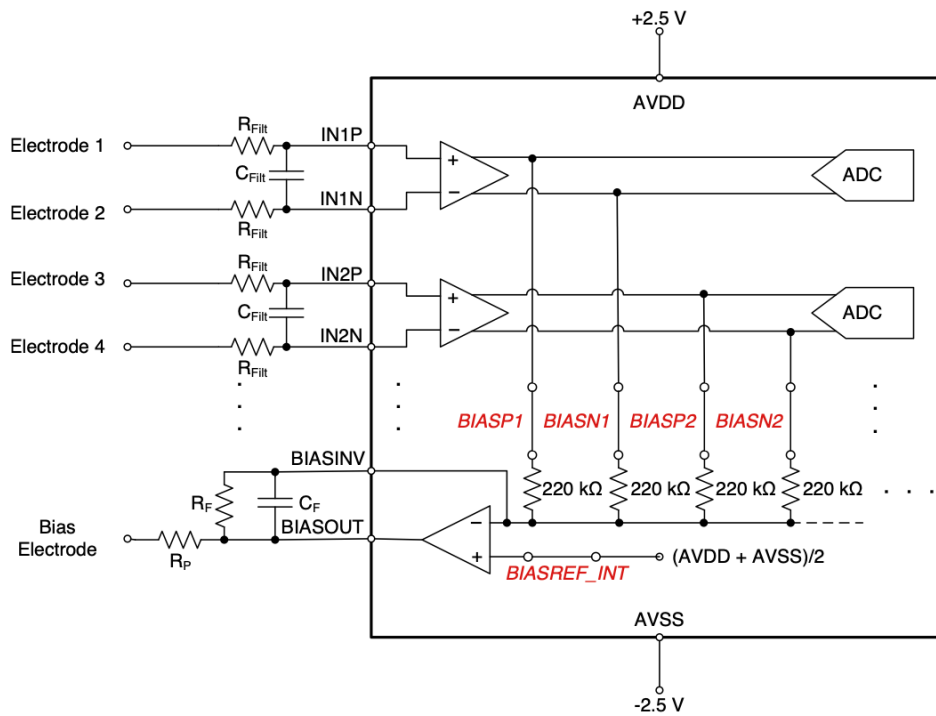


Figure 6.2: Schematic of the ADS1299 and connected electrodes configured in differential mode. From [36].

In single-ended mode, the channels consist of a positive electrode input while a common reference electrode serves as the negative input. The positive electrode inputs are then measured with respect to the reference electrode, as shown in Figure 6.3, meaning only eight (positive) electrodes are needed. The reference electrode is placed on electrically neutral tissue, for instance an area of the skin covering mostly bone.

In both differential mode and single-ended mode, an alternative bias electrode can be used to drive the user's body to a reference voltage to counter the negative effects of common-mode drifts. Additionally, bias can be measured as an average of a set of, or all, the electrode inputs. This is the role of the $BIASP_x$ and $BIASN_x$ switches in Figure 6.2 and Figure 6.3. Configuring bias drive is further explained in Section 6.1.3.

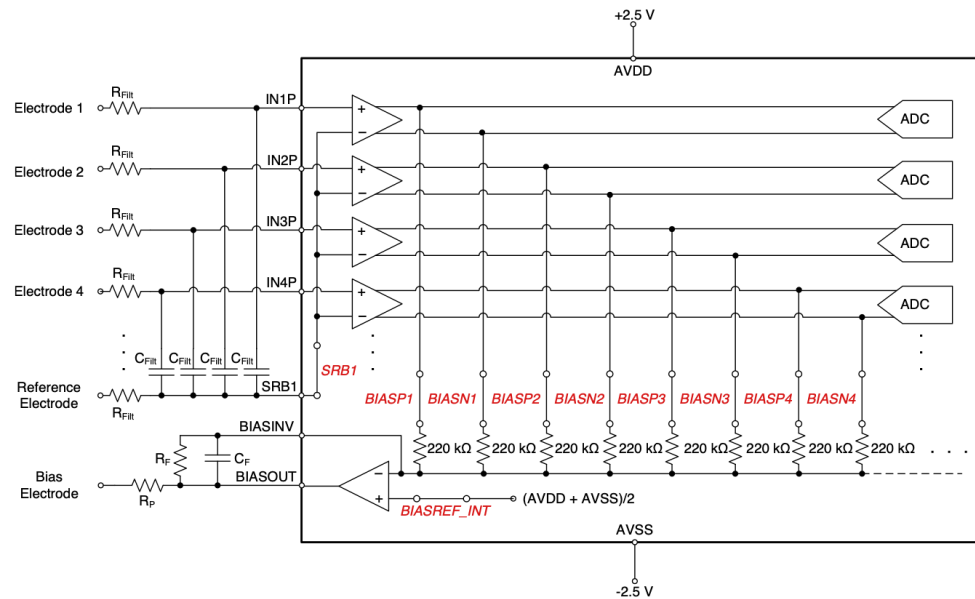


Figure 6.3: Schematic of the ADS1299 and connected electrodes configured in single-ended mode. From [36].

To configure the ADS1299 to operate in differential or single-ended mode, the SRB1 bit is either cleared or set, respectively, in the MISC1 register.

6.1.3 Bias drive

When configured in differential mode, the ADS1299 measures fully differential signals where the common-mode voltage is the midpoint of the positive and negative analog input from the positive and negative electrodes. As explained in Section 2.4.1, noise easily couples onto the human body and can cause the common-mode voltage to drift. If such a drift is too large, it can push the input common-mode voltage out of the measurable range of the ADS1299's ADC. To counter this, the ADS1299 includes an on-chip bias drive amplifier connected to the bias drive electrode output. The goal of this feature is to drive the user's body – assuming a bias drive electrode is attached to the user – in order to maintain the other electrode common-mode voltages within the measurable range of the ADC [36].

The bias drive amplifier is enabled by setting the $\overline{\text{PD_BIAS}}$ bit in the CONFIG3 register². The bias amplifier can be configured to use an internal bias reference, given as the analog midsupply voltage $\frac{\text{AVDD} + \text{AVSS}}{2}$, or an external bias reference voltage, present at the BIASREF pin, by setting or clearing the BIASREF_INT bit in the CONFIG3 register, respectively. The BIASREF pin is not available on the Arduino shield with the ADS1299, and the prototype therefore always uses the internal bias

²Take care not to overwrite the $\overline{\text{PD_REFBUF}}$ bit when writing to the CONFIG3 register, as this will power down the internal voltage reference buffer.

reference to drive the user's body to that voltage. The bias electrode is attached to an arbitrary point on the user's body.

As an additional feature, the ADS1299 provides the option to use the analog electrode inputs as feedback to the bias amplifier in order to more effectively stabilize the output to the amplifier reference voltage. This is done by setting corresponding bits in the BIAS_SENSP and BIAS_SENSN registers to gather feedback from positive and negative electrodes, respectively.

6.1.4 Channel offset

According to the data sheet, the ADS1299 is expected to have a channel offset, typically up to $60\mu\text{V}$ [36]. It is interesting to see whether the observed channel offsets for the prototype coincides with the channel offset reported by the data sheet. Channel offset measurements are performed both with internally shorted electrodes and with electrodes externally shorted to analog ground. This allows for evaluating whether the electrodes introduce an additional offset across channels.

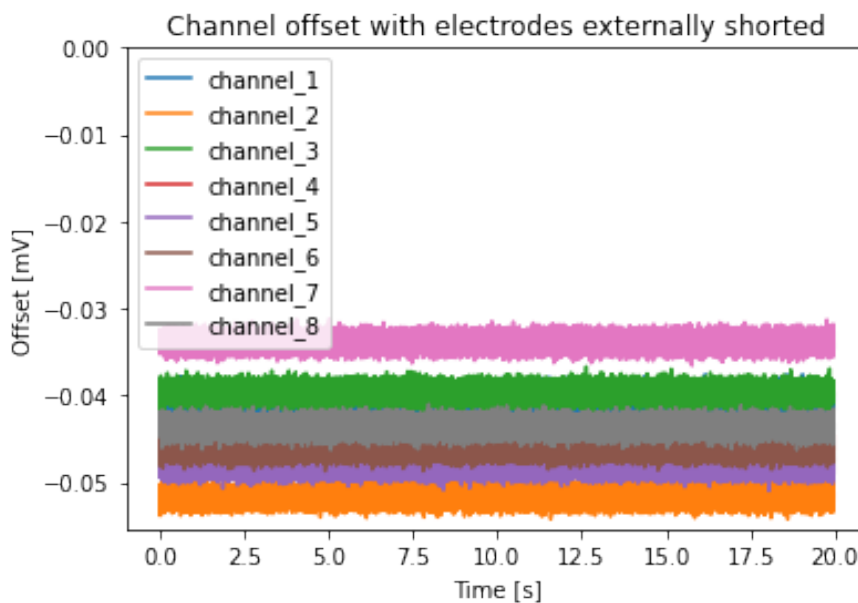


Figure 6.4: Channel offset for electrodes shorted externally to analog ground.

Figure 6.4 shows the observed channel offset for when electrodes are externally shorted to analog ground. The channel offset for internally shorted electrodes is found to be nearly identical. The channel offset is between $30\text{-}60\mu\text{V}$, which is to be expected according to the data sheet of the ADS1299. As a means of calibration, the channel offsets are subtracted from the respective channels before any further processing of the sEMG signals acquired during basic data capture.

6.2 Basic data acquisition

Before any recording, the skin and electrodes are cleansed by applying alcohol to a cotton pad and wiping the surface of the skin and the electrodes. This is done to remove debris that can cause artifacts in the recordings. The sleeve and electrode grid is placed above the muscles of interest, and the sleeve is secured in place by adjusting the velcro straps. The recording setup is shown in Figure 6.5.

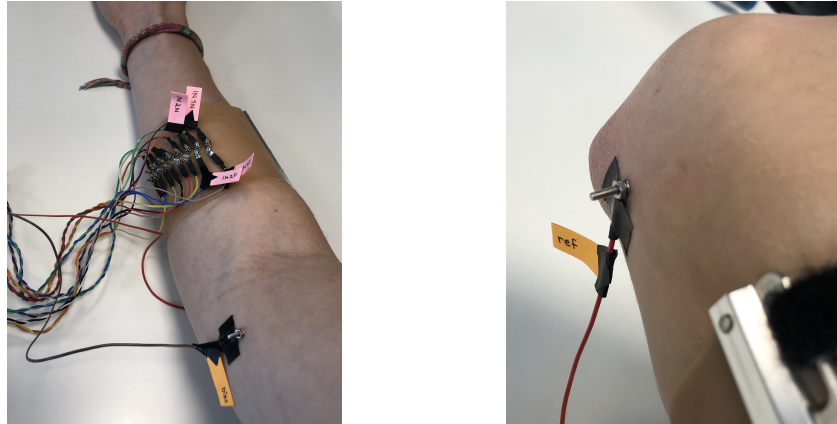


Figure 6.5: Setup of the recording includes placing the electrode grid on the ventral side of the forearm above the muscles responsible for flexing the wrist. The reference electrode is placed on the elbow above an area consisting of mostly bone, while the bias electrode is attached to an arbitrary point on the skin, both using adhesive tape.

The recording flow typically consists of an initial offset measurement, as explained in Section 6.1.4, followed by the recording of sEMG signals. For a normal sEMG recording with default sampling rate and gain, the following configurations are made by writing to the respective registers of the ADS1299.

Sampling rate The sampling rate is set to 4kHz.

Channel configurations The channels are configured as normal electrode input, and the gain is set to 12.

Operational mode The prototype is configured for differential mode, as this is the recommended configuration for sEMG measurements on the human body[36]. However, measurements are recorded in both differential and single-ended mode for comparison.

Bias amplifier The bias amplifier is enabled and using the internal bias reference. Data acquisition is performed both with and without the BIAS_SENS-functionality to compare its effect.

With the above settings, a 20 second recording is made to illustrate the workings of the prototype. The recording consists of three muscle contractions of differ-

ent intensity – one weak, one medium and one strong contraction – involving the muscles responsible for flexing the wrist. The weak contraction is made by barely flexing the wrist, while the strong contraction is a near-maximum flexion of the wrist. To compare differential and single-ended mode, as well as the effects of the BIAS_SENS-functionality, the recording is made four times with the respective configurations. The recordings are performed on one female subject, who happens to be the author herself, and the results are shown in Figure 6.7, Figure 6.8, Figure 6.9 and Figure 6.10. Figure 6.6 gives a closer look of the acquired sEMG signal from channel 3 recorded in differential mode.

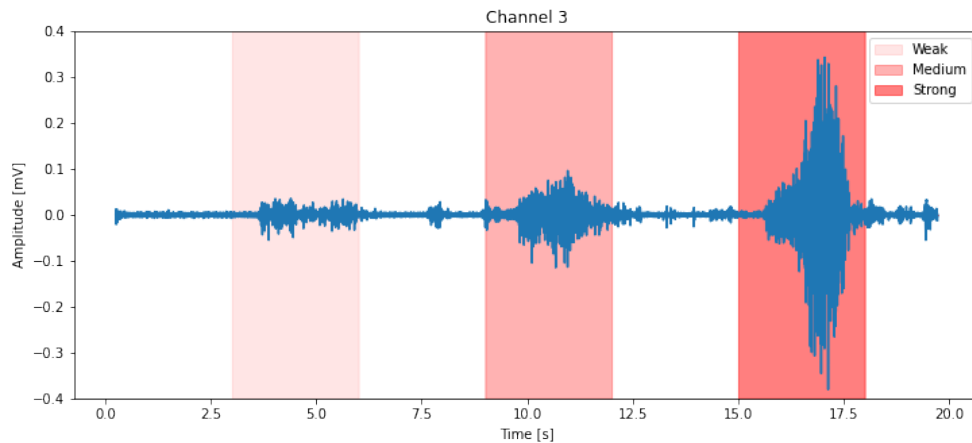


Figure 6.6: Acquired sEMG signal from channel 3 recorded in differential mode. Shaded areas indicate when the subject is told to contract and with what contraction level.

A simple Python script is used to configure the ADS1299, start data conversions and set the ADS1299 in Read Data Continuously mode. The script then samples timestamped data from all channels and tells the subject when to rest and when to perform a muscle contraction, at 3 second intervals. The point of time when the subject is told to perform the weak, medium and strong contractions is indicated by the shaded areas in Figure 6.6.

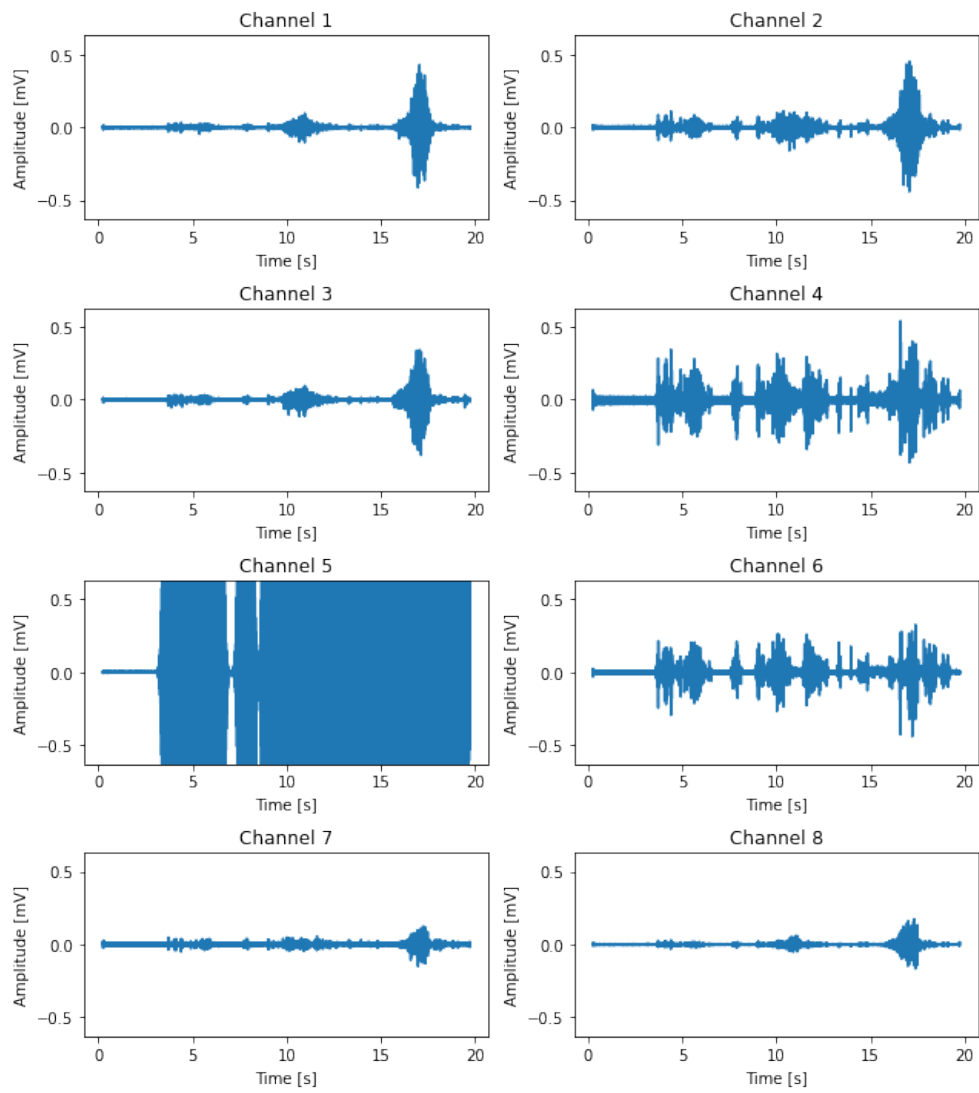


Figure 6.7: Recorded sEMG signals in differential mode.

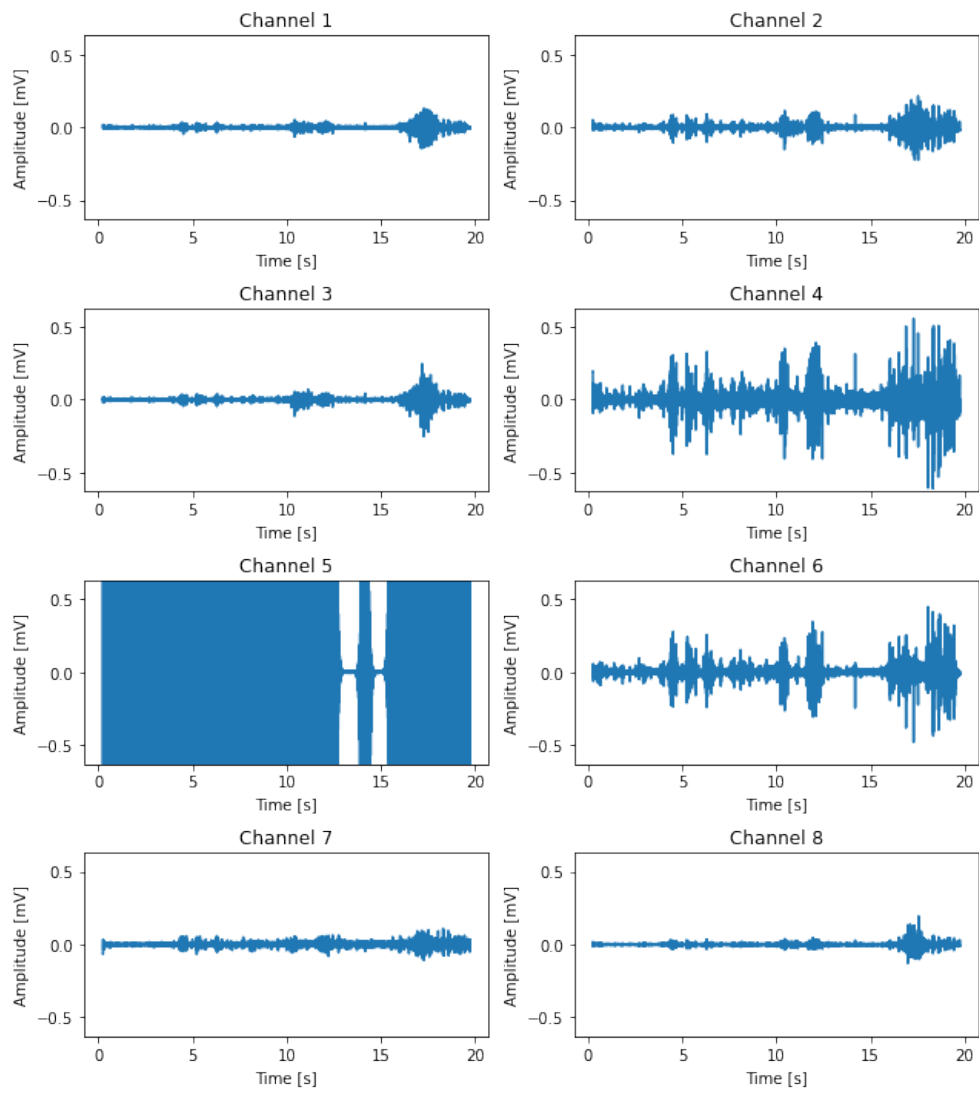


Figure 6.8: Recorded sEMG signals in differential mode with BIAS_SENS enabled.

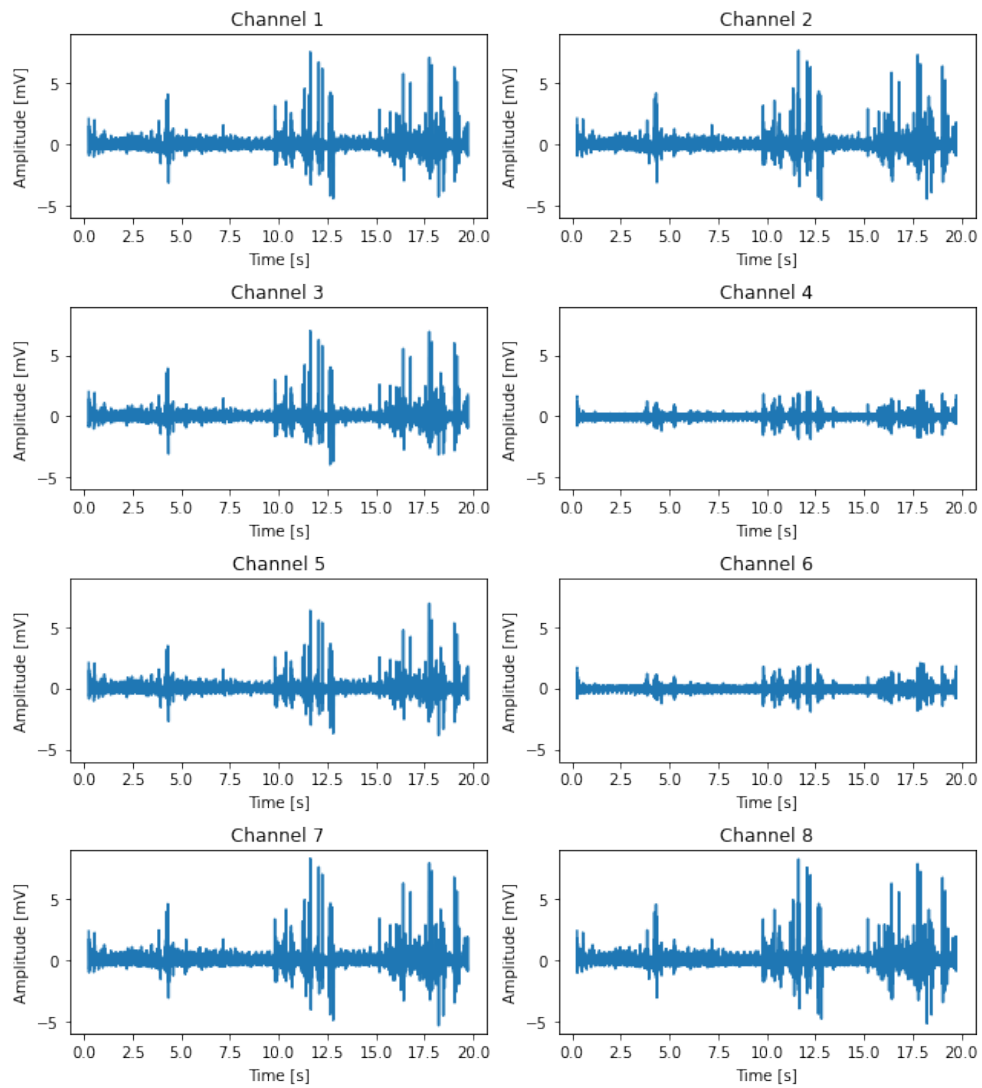


Figure 6.9: Recorded sEMG signals in single-ended mode.

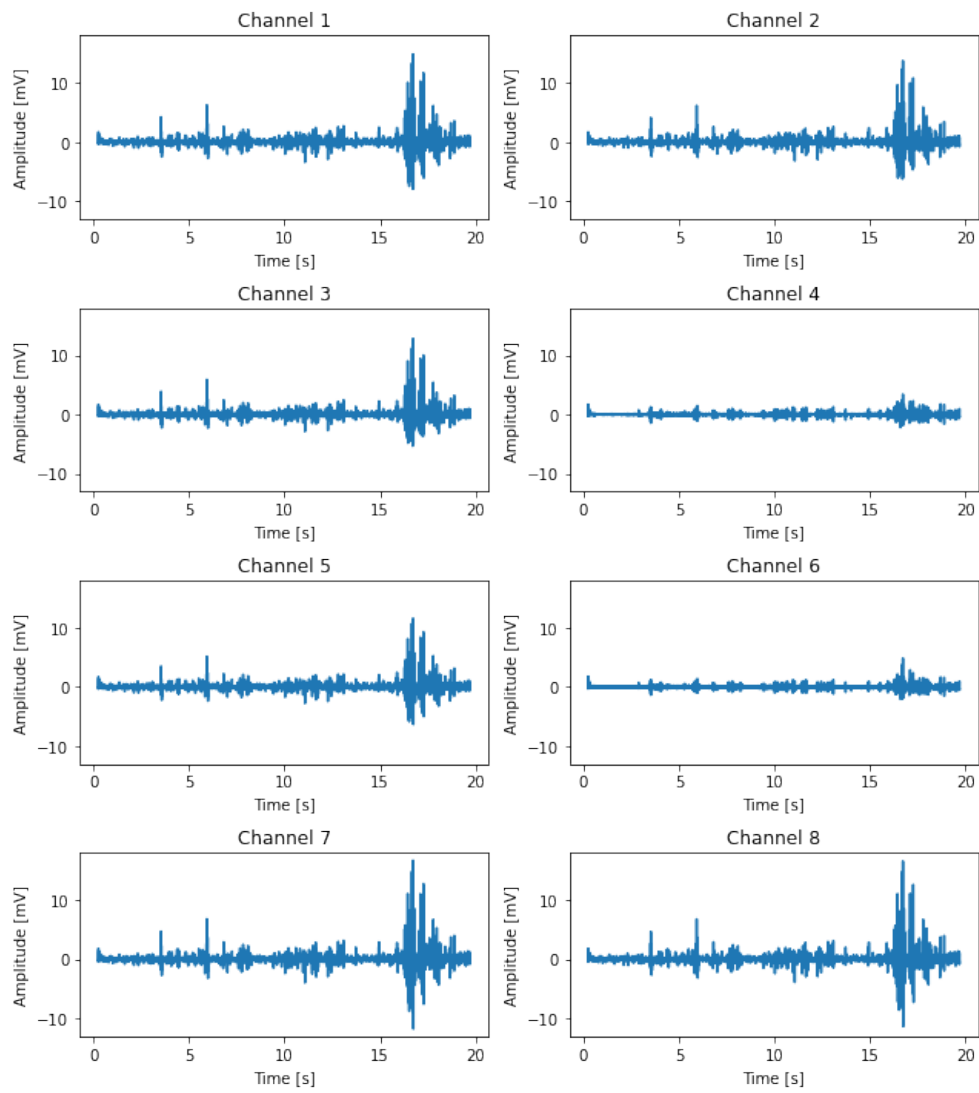


Figure 6.10: Recorded sEMG signals in single-ended mode with BIAS_SENS enabled.

6.3 SNR

The signal-to-noise ratio (SNR) is usually given as a ratio between the power of a discrete time signal and the power of the noise affecting said signal. The power of a given signal $x(n)$ is defined as

$$P(x) = \frac{1}{N} \sum_{n=0}^{N-1} x(n)^2 \quad (6.2)$$

The SNR is given as

$$SNR = \frac{P_{signal}}{P_{noise}} \quad (6.3)$$

where P_{signal} and P_{noise} is the power of the signal and the noise, respectively. However, usually the signal is contaminated by noise, and finding the power of the signal alone is not trivial. Instead, one can measure the constant noise power a device produces without an input and subtract this from the signal power. The SNR then becomes

$$SNR = \frac{P_{signal} - P_{noise}}{P_{noise}} \quad (6.4)$$

where P_{signal} is the power of the signal contaminated by noise and P_{noise} is the power of the noise alone [44, p. 105-106].

It is common to denote SNR values in decibels (dB), and the SNR is then given as [44, p. 106]

$$SNR = 10 \cdot \log_{10} \left(\frac{P_{signal} - P_{noise}}{P_{noise}} \right) \quad (6.5)$$

To find the power of the noise alone requires a measure of the overall noise floor of the prototype. The noise should preferably be measured at the output of the analog amplifier using an oscilloscope, however the circuit that the ADS1299 is embedded in does not reveal the required test points to complete such measurements. Instead, the noise floor is obtained from a portion of the sEMG recording where the arm is at rest. As for the signal power, the portion corresponding to the strongest contraction is used. The obtained signal and noise powers belong to the sEMG signal recorded in differential mode, more specifically from channel 3, as shown in Figure 6.11. As a result, the SNR of the HD-sEMG prototype system is found to be 29.7dB.

6.4 Technical specification

This section includes a technical specification of the prototype and accompanying data acquisition module, including a list of components, physical dimensions and materials, as well as an overview of the different connectors used between the modules.

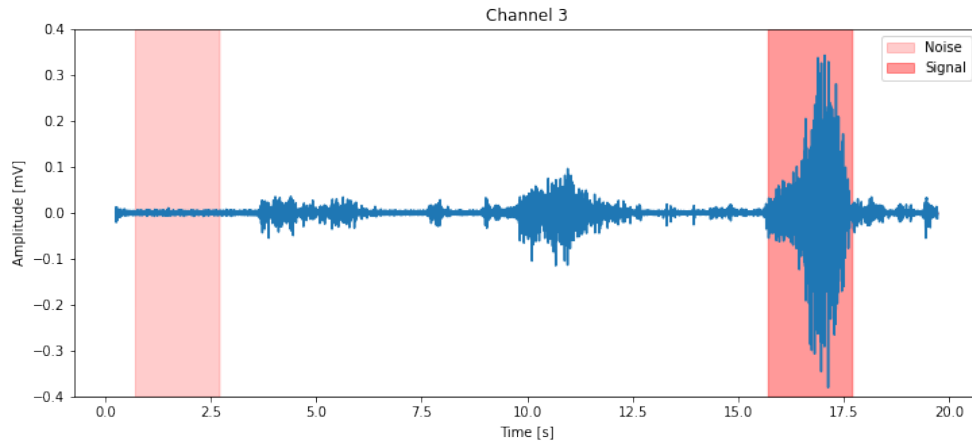


Figure 6.11: Noise and signal power obtained from the respective shaded areas of the sEMG signal from channel 3 recorded in differential mode.

6.4.1 Data acquisition module

The most essential characteristics of the data acquisition module are given in Table 6.2. Most of the characteristics are obtained from the data sheet for the ADS1299-x family[36], with the exception of the prototype channel offset, prototype SNR and throughput. For further characteristics related to the ADS1299 itself, the reader is encouraged to check the data sheet for the ADS1299-x family.

6.4.2 Physical

Components

An overview of the physical components that make up the hardware of the prototype for the HD-sEMG system is given in Table 6.3.

Dimensions

Table 6.4 lists the dimensions of the physical components and modules of the HD-sEMG prototype system.

Materials

Table 6.5 gives an overview of the materials that the different physical components consist of.

Connectors

The different kinds of connectors used between the modules are listed in Table 6.6.

³Calculated from (sample size x channels + headers) x sampling rate, which at default sampling rate gives (3 bytes x 8 channels + 3 bytes) x 4kHz \approx 0.864Mbps.

Table 6.2: Characteristics of the data acquisition module of the HD-sEMG prototype system.

Data Acquisition Module	
Control unit	Arduino Due (Atmel SAM3X8E CPU)
Processing unit	Texas Instruments ADS1299
Channels	8 channels
Mode	Differential or single-ended mode
Analog operating voltage	$\pm 2.5V$
Internal reference voltage	4.5V
Programmable gain	1, 2, 4, 8, 12, 24 (default: 12x gain)
Sampling rate	250Hz – 16kHz (default: 4kHz)
ADC resolution	24-bits per channel
Nominal bandwidth	55kHz (at 12x gain)
Input impedance	Min. 1000M Ω
Input-referred noise	ADS1299: 1 μV_{pp}
Channel offset	ADS1299: $\leq 60 \mu V$ Prototype: 30-60 μV
SNR	ADS1299: 121dB Prototype: 29.7dB
Throughput	0.864Mbps ³ (at default sampling rate)

Table 6.3: Overview of the physical components of the HD-sEMG prototype system.

	Quantity
Electrodes	
Electrode	16
Threaded nut	34
Washer	20
Mounting	
Sleeve	1
Brace	2
Strap	2
Cables	
20-pin flat ribbon cable	1
Twisted-pair electrode cable	8
Single electrode cable	2
USB 2.0 (USB-A to USB-B-micro)	1

Table 6.4: Dimensions of the physical components and modules of the HD-sEMG prototype system. All dimensions are given in millimeters.

	Width [mm]	Height [mm]	Length [mm]	Diameter [mm]
Electrodes	-	-	8.48	3.76
Threaded nut	4.44	1.56	-	-
Rectangular washer	2.87	0.77	12.04	-
Electrode grid	44.49	-	9.94	-
Sleeve	80.04	-	156.26	-
Data acquisition module	53.34	29.74	107.53	-

Table 6.5: Materials of the physical components of the HD-sEMG prototype system.

	Material
Electrodes	
Electrodes	316 stainless steel
Threaded nut	18-8 stainless steel
Washer	18-8 stainless steel
Mounting	
Sleeve	Rubber
Braces	Aluminium
Straps	Velcro

Table 6.6: Connectors between the modules of the HD-sEMG prototype system.

	Connector type
Electrode grid	20-pin male-female connector 20-pin color-coded ribbon cable, separated and twisted in pairs
Data acquisition module	24-pin male header 24-pin mating female connector 24-pin flat ribbon cable USB 2.0 (USB-A to USB-B-micro)

Chapter 7

Discussion

This chapter contains an evaluation of the requirements from the functional specification that addresses whether the prototype fulfills the requirements. The results obtained from the sEMG recordings with the HD-sEMG prototype system are discussed, and further improvements of the prototype are considered in light of the requirements evaluation and the results.

7.1 Requirements evaluation

Table 7.1 is a repetition of the functional specification from Table 4.1 with the cross-references replaced by a status to indicate whether a requirement has been fulfilled or not. The status can be either “Fulfilled”, “Partially fulfilled” or “Not fulfilled”. As the design choices are a reflection of the functional specification, this section will not go into why a requirement is labelled “Fulfilled”. Requirements labelled “Partially fulfilled” or “Not fulfilled” are further discussed in the following sections.

R1.1 Ensure electrical safety

Requirement **R1.1** is the only *hard* requirement that is not completely fulfilled. When used correctly, the user is ensured to not be connected to the domestic power supply, and the requirement is assumed to be fulfilled in this scenario. However, the prototype streams data to a client laptop over USB and is powered through the same USB connection. Though the prototype itself is not directly connected to the domestic power supply, there is nothing that prevents the user from connecting the laptop to the domestic power supply, which will create a connection from the user to the domestic power supply. A written warning is included in the documentation as well as in the Python scripts that are used to sample data, however the inclusion of such warnings do not guarantee electrical safety.

A suggestion for future work is to implement wireless transfer of data to allow the ADS1299 and sampling circuitry to be fully battery powered. Alternatively, the Python scripts can run on a battery-powered Raspberry Pi connected to the

Table 7.1: Evaluation of the requirements from the functional specification for the HD-sEMG prototype system.

ID	Requirement	Type	Status
R1	General		
R1.1	Ensure electrical safety	Hard	Partially fulfilled
R1.2	Biocompatible materials	Hard	Fulfilled
R1.3	Adjustable fixation to fit future users	Hard	Fulfilled
R2	Electrode grid		
R2.1	Balanced contact impedances	Soft	Partially fulfilled
R2.2	Dry electrodes	Hard	Fulfilled
R2.3	Inter-electrode distance $\leq 5\text{mm}$	Soft	Not fulfilled
R2.4	Extendable grid	Soft	Fulfilled
R3	Data acquisition module		
R3.1	Input impedance $\geq 100\text{M}\Omega$	Hard	Fulfilled
R3.2	Simultaneous sampling of channels	Hard	Fulfilled
R3.3	At least 8 channels	Soft	Fulfilled
R3.4	Sampling frequency $> 800\text{Hz}$	Hard	Fulfilled
R3.5	At least 16-bit resolution	Soft	Fulfilled
R3.6	Programmable gain	Soft	Fulfilled
R3.7	CMRR $\geq 90\text{dB}$	Hard	Fulfilled
R3.8	High SNR	Soft	Not fulfilled
R3.9	Low input-referred noise	Soft	Fulfilled

Arduino Due and shield over USB, while the Raspberry Pi either stores the data or transmits it wirelessly to a laptop for further processing.

R2.1 Balanced contact impedances

Through the choice of electrodes and manufacturing considerations, the electrodes are made as identical as possible to ensure balanced contact impedances. However, requirement **R2.1** has been labelled “Partially fulfilled” as there are no means to evaluate whether it has been fulfilled or not¹. Additionally, the high-level noise floor, low SNR and the 50Hz interference from the domestic power line give reason to believe that the contact impedances are not perfectly balanced.

¹The electrode-skin impedance is a non-linear function of current, and at the detection set-up, the electrode current is virtually zero[14, p. 110].

R2.3 Inter-electrode distance \leq 5mm

The inter-electrode distance of the electrode grid had to be increased to 5.5mm in order to avoid short-circuiting the electrodes, and requirement **R2.3** is consequently not fulfilled. As a result, there is a risk of introducing aliasing in space. With an inter-electrode distance of 5.5mm, and using the same calculations as in Section 4.2.3 in a backwards-manner, the theoretical maximum temporal frequency that can be measured is 364Hz. This means that having an inter-electrode distance of 5.5mm can introduce aliasing in the upper frequencies of the sEMG signals. That being said, most of the frequency content of sEMG signals are found in the frequency range 20-150Hz[45]. Additionally, the inter-electrode distance in requirement **R2.3** is based on an average action potential conduction velocity. By simulating motor unit action potentials, Afsharipour *et al.* (2014) found that the largest inter-electrode distance that avoids spatial aliasing is 10mm, but that for experimental and clinical applications the inter-electrode distance is recommended to be below this value. To summarize, an increase of 0.5mm in inter-electrode distance is not likely to affect the prototype's acquisition of sEMG signals to a large extent.

To reduce the inter-electrode distance and avoid aliasing completely, a suggestion is to use threaded nuts that are made of a non-conductive material, assuming threaded electrodes are still used.

R3.8 High SNR

Requirement **R3.8** has been labelled "Not fulfilled", as the SNR of the prototype system is found to be 29.7dB, which is generally low. However, the requirement does not specify what is considered "high" SNR. The prototype SNR is considerably lower than the SNR of the ADS1299. Based on what can be gathered from the literature, there is no consensus on what is considered "good" or "bad" SNR, as SNR is a relative term and it depends on the signal that is analyzed. Low-power signals will consequently have lower SNR, and it is already established that the electrode-skin interface is noisy.

As an example, Freed *et al.* (2012) observed a mean SNR of around 40dB for their WEAR system consisting of an electrode grid of eight dry electrodes. However, the grid is positioned on the calf and used for gait analysis, and it is therefore unclear whether the WEAR system's SNR is comparable to the SNR of the HD-sEMG system prototype, which is placed on the forearm. Ruvalcaba *et al.* (2020) compared the use of dry brass electrodes and a commercial system with gelled electrodes when performing wrist flexions. The SNR was measured to be 49dB and 60dB, for the dry brass electrodes and the commercial electrodes, respectively[47]. An SNR of 29.7dB can in some cases be considered acceptable, however this value is obtained from one of the few good sEMG recordings from the prototype and is not a reliable value.

7.2 Locating the noise source

The observed low SNR of the prototype is believed to be caused by a relatively large amount of noise in the system. In order to locate the noise source, the power spectrum is evaluated for three different parts of the system: **1)** the ADS1299, **2)** the cables and **3)** the electrode-skin interface. This is achieved by sampling data with the following configurations: **1)** electrodes are internally shorted, **2)** electrodes are externally shorted to the bias electrode, and **3)** electrodes are configured as normal electrode inputs and data is sampled while keeping the arm completely at rest. The respective power spectres are shown in Figure 7.1.

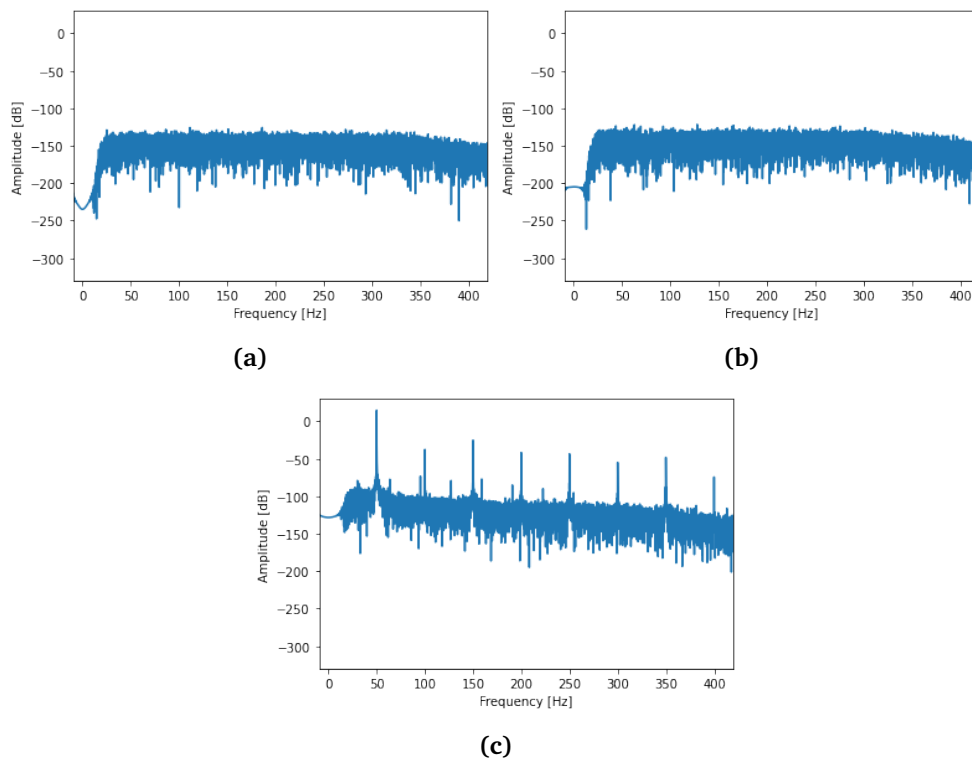


Figure 7.1: Power spectrum obtained when **(a)** electrodes are internally shorted, **(b)** electrodes are externally shorted to the bias electrode, and **(c)** electrodes are configured as normal electrode inputs and arm is at rest.

Comparing Figure 7.1a, Figure 7.1b and Figure 7.1c, it is clear that the source of noise can be located to the electrode-skin interface, as the power spectres related to the ADS1299 and the cables are near identical. The power spectrum related to the electrode-skin interface is contaminated by power line harmonics. According to Merletti and Farina, p. 73-75, power line interference is often associated with fluctuations in electrode-skin impedance, and as already discussed in the requirements evaluation, there is reason to believe that the contact impedances are imbalanced. Though the comb filter effectively suppresses the power line

harmonics, it cannot remove all of the interfering frequencies without degrading the sEMG signal itself.

Evidently, there is little to gain from making electrodes from scratch, as the electrodes have some unknown characteristics that are challenging or impractical to account for. An immediate thought is that the electrodes are flat instead of dome-shaped, though dome-shaped electrodes were originally preferred. Both Coapt and Steeper², which are manufacturers of surface electrodes and prosthetic devices, recommend using dome-shaped electrodes for sEMG applications. According to Coapt, dome-shaped electrodes provide more accurate sEMG recordings[34], presumably due to the low-pass filtering effect that occurs for larger electrode surface areas, thus reducing high-frequency noise. Though the issue here is not high-frequency noise, there is likely much to gain from using commercial electrodes.

As the problem has been isolated to the electrodes, future effort can be put into a more careful design of electrodes or alternatively consider commercial electrodes, though at a higher cost, to ensure quality and reduce the likelihood of electrode-skin impedance imbalance.

7.3 HD-sEMG recordings with the prototype

This section analyzes the sEMG recordings from Figure 6.6 to Figure 6.10. Already at first sight, it is clear that some unfortunate phenomenon greatly affects channel 5 and partly channel 4 and 6. When comparing the sEMG recordings, the signals from channel 4, 5 and 6 are therefore excluded, but instead analyzed separately in Section 7.3.1. The comparison of the sEMG signals recorded in the different operational modes and with bias feedback enabled or disabled is based on signal amplitude and noise levels, with emphasis on the ability to discern contraction times and distinguish between the different contraction levels.

7.3.1 Electrode-skin contact

The recordings from channel 5 in Figure 6.7 and Figure 6.8 illustrates the challenge of finding a suitable electrode placement and ensuring good electrode-skin contact. At a first glance, channel 5 appears to be almost completely saturated when recording in differential mode, both with and without bias sensing. According to Merletti and Farina, the properties of the electrode-skin interfaces are different for different electrodes and will also change in time during an sEMG recording. Common disturbances include[3, p. 73-75]:

- Motion artifacts caused by variations in or momentary loss of electrode-skin contact

²Similar to Coapt, Steeper offers remote metal dome electrodes. These are further described in Appendix A.3.

- Movement of cables, resulting in variation of parasitic capacitances between cables
- Fluctuations in contact quality, which results in change in noise levels
- Variation in charge distribution between the skin and the electrode

Channel 5 shows varying degrees of saturation throughout the recording. For instance, during the differential recording in Figure 6.7, the saturation does not occur until the weak contraction is performed at around 3 seconds into the recording. The electrode pair belonging to channel 5 is presumably placed on a region of the forearm with poor electrode-skin contact, possibly on a region prone to movements and shape-changes as the muscles contract. Since the channels are densely spaced, surrounding channels should be affected by the same phenomenon. Figure 7.2 compares channels 4-6 more closely.

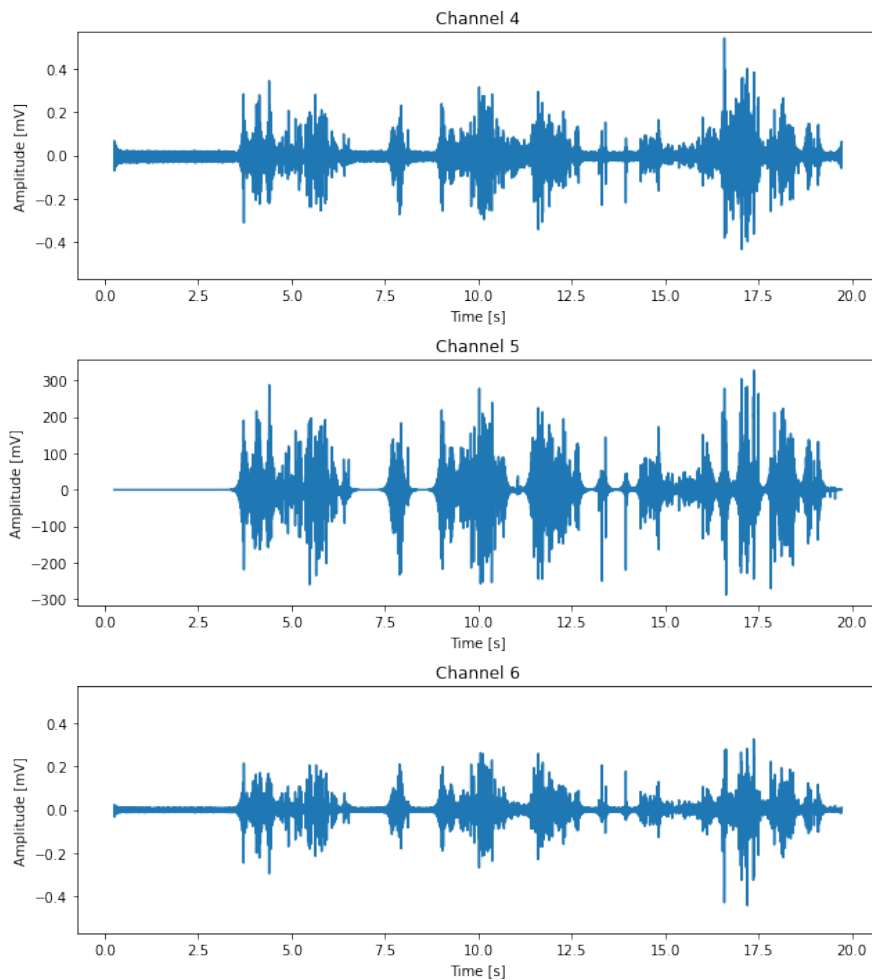


Figure 7.2: Recorded sEMG signals from channel 4, 5 and 6 in differential mode.

Channel 4 and 6, which are the channels on either side of channel 5 in the

dense electrode grid, have a similar appearance to that of channel 5. Additionally, channel 4 and 6 appear more noisy compared to the other channels. By inspecting the difference in amplitude scaling of Figure 7.2 it is also clear that channel 5 is not in fact saturated, but that the measured noise levels are considerably higher for channel 5 than for the other channels. These observations support the assumption that channel 5 is prone to changes in electrode-skin contact, likely due to incorrect placement of the electrode pair.

7.3.2 Differential mode

As already discussed, it is obvious that the electrodes are a limiting factor. Consequently, the acquired signals are of relatively poor quality overall. Additionally, the signals recorded across different channels are inconsistent, which reduces the overall redundancy of the acquired signals. Regardless, with respect to channels 1-3, the sEMG signals recorded in differential mode without bias feedback appear rather satisfactory in terms of discernability of the contraction times and levels.

When bias feedback is enabled, the sEMG signals recorded in differential mode appear more noise compared to when bias feedback is not enabled. Why this is the case remains unclear, as one would believe that including feedback about the bias should reduce noise rather than increase it. Nevertheless, bias feedback seems to have a positive effect on the signals recorded in single-ended mode.

7.3.3 Single-ended mode

At first sight, the signals recorded in single-ended mode appears noisy and indiscernible. Though the amplitude of the signals are larger compared to the signals recorded in differential mode, so are the noise levels. The high noise levels make the sEMG signals difficult to interpret as the weak contractions are hardly discerned from the noise. While enabling the `BIAS_SENS`-functionality significantly suppresses the noise and further improves the signal amplitude of the sEMG signals, the weak contractions become even harder to discern.

As a result, differential mode without bias feedback is the preferred configuration for recording sEMG signals with the HD-sEMG prototype system developed during this work, as the sEMG signals recorded in differential mode demonstrate superiority in terms of overall noise level, as well as being able to discern the point of contraction and the different contraction levels. That being said, the recorded signals are of overall poor quality, as the output can only be as good as the input. More work has to be put into ensuring good electrode-skin contact and impedance balance before the prototype can acquire signals of better quality than those observed in this work.

7.4 Prototype improvements

With more time available, it would be advantageous to design a custom printed circuit board (PCB) for the data acquisition module. Though the HackEEG project could be used as a starting point, as schematics and drivers are readily available, designing a custom PCB would allow the addition of more than 8 channels through daisy-chaining multiple ADS1299s. As already discussed, not all channels are guaranteed to have good electrode-skin contact, which highlights the need for an even higher number of channels to increase redundancy of the signals. Additionally, using a custom PCB would significantly reduce the overall costs since the ADS1299 itself comes at a price point that is approximately seven times lower than the Arduino shield with the ADS1299.

Further, seeing as the electrodes are the bottlenecks of the prototype, the ADS1299 is not utilized at its full potential. Having an analog front end with such high SNR and low input-referred noise does not come to use when being limited by the electrodes. One could also argue that the ADS1299 is a bit “overkill” for the current application. Having 24-bit resolution and up to 16kHz sampling rate is not really necessary in this situation – 16-bit resolution and 4kHz sampling is enough for prosthesis control[30].

Taking this into consideration, the ADS1299’s “little brother”, the ADS1198, would be a suitable alternative analog front end for this prototype. The ADS1198 has support for simultaneous sampling of 8 channels and like the ADS1299 it can be daisy-chained. Additionally, the ADS1198 satisfies the requirements related to input impedance, CMRR, SNR and input-referred noise, and it is three and a half times cheaper than the ADS1299. However, one note should be made about the resolution of the ADC. Seeing as the sEMG signals are heavily processed in order to suppress noise and power line harmonics, a lower-resolution ADC is not guaranteed to provide the same results without making the suggested improvements to the electrodes. With 24-bit resolution, each bit represents a smaller range of signal values compared to an ADC with 16-bit resolution, as an ADC with higher resolution will have larger dynamic range. Dynamic range is the ratio between the smallest and largest value that a system can represent[44]. This means that both small signal components and large noise components can be represented in a higher-resolution signal without saturating the ADC. Due to the large headroom, the noise can be removed through digital signal processing, while the small signal components are still intact with sufficient resolution.

Finally, with the current setup, the acquired sEMG signals from the prototype are only suitable for analysis in post. As a next step towards using the prototype in a prosthesis control-related setting, real-time offset measurement, as well as real-time signal processing, should be implemented in the future.

To summarize, the prototype has a potential for future high-density sEMG recordings, and with the addition of more channels and improved electrodes, the redundancy of the acquired signals, as well as the overall signal quality, can be significantly increased.

Chapter 8

Concluding remarks

8.1 Conclusion

A working prototype for recording high-density surface EMG signals from the ventral side of the forearm is implemented. The overall signal quality is poor and the acquired signals are not redundant across all channels, mostly due to an imbalance in electrode-skin interface impedance and the challenge of finding an accurate electrode placement. Regardless, the prototype allows for distinguishing between weak, medium and strong muscle contractions when utilizing a differential electrode configuration and when the electrode channels are placed correctly above the muscles of interest. Future efforts should be put into a more deliberate electrode design, or alternatively consider commercial electrodes, in order to ensure good signal quality across all channels, as well as extend the data acquisition module to include even more electrode channels to increase redundancy and robustness of the prototype.

8.2 Future work

Suggestions for future work, as discussed in Chapter 7, are summarized below.

- Implement wireless transmission of data to ensure electrical safety.
- Design new electrodes with focus on balancing the skin contact impedance, or alternatively consider commercial electrodes, to ensure signal quality and reduce noise related to impedance imbalance.
- Design a custom PCB with daisy-chained analog front ends in order to extend the number of channels and possibly overcome the challenges related to electrode placement.
- Implement real-time offset measurement and signal processing as a next step towards prosthesis control.

Bibliography

- [1] J. Kilby, K. Prasad and G. Mawston, 'Multi-channel surface electromyography electrodes: A review,' *IEEE Sensors Journal*, vol. 16, no. 14, pp. 5510–5519, 2016. DOI: 10.1109/JSEN.2016.2569072.
- [2] D. F. Lovely, *Powered Upper Limb Prostheses: Control, Implementation and Clinical Application*, A. Muzumdar, Ed. Springer Berlin Heidelberg, 2004, ISBN: 978-3-642-18812-1. DOI: 10.1007/978-3-642-18812-1.
- [3] R. Merletti and D. Farina, *Surface Electromyography: Physiology, Engineering, and Applications*. Wiley-IEEE Press, 2016, ISBN: 9781118987025. DOI: 10.1002/9781119082934.
- [4] O. Aszmann and D. Farina, *Bionic Limb Reconstruction*. Springer International Publishing, Jan. 2021, ISBN: 978-3-030-60745-6.
- [5] S. Tam, M. Boukadoum, A. Campeau-Lecours and B. Gosselin, 'A fully embedded adaptive real-time hand gesture classifier leveraging hd-semg and deep learning,' *IEEE transactions on biomedical circuits and systems*, vol. 14, no. 2, pp. 232–243, 2020, ISSN: 1932-4545. DOI: 10.1109/tbcas.2019.2955641.
- [6] K. Stray, 'Two-channel user-feedback for hand prosthetic,' Term Project, Norwegian University of Science and Technology, Trondheim, Norway, 2021.
- [7] J. D. Enderle, S. M. Blanchard and J. D. Bronzino, *Introduction to Biomedical Engineering*, Second Edition. Academic Press, 2005, ISBN: 978-0-12-238662-6.
- [8] O. Stavdahl, 'Optimal wrist prosthesis kinematics: Threedimensional rotation statistics and parameter estimation,' Ph.D. dissertation, Norwegian University of Science and Technology, Trondheim, Norway, 2002, ISBN: 82-471-5526-5.
- [9] J. Hall and A. Guyton, *Textbook of Medical Physiology*, Twelfth Edition. Saunders/Elsevier, 2011, ISBN: 9781416045748.
- [10] D. Purves, G. Augustine, D. Fitzpatrick, W. Hall, A. LaMantia, R. Mooney, L. White and M. Platt, *Neuroscience*, International Sixth Edition. Oxford University Press, Incorporated, 2018, ISBN: 9781605358413.

- [11] R. Merletti, A. Holobar and D. Farina, 'Mathematical techniques for non-invasive muscle signal analysis and interpretation,' in *Encyclopedia of Biomedical Engineering*, R. Narayan, Ed., vol. 3, Elsevier, 2019, pp. 95–111, ISBN: 978-0-12-805144-3. DOI: <https://doi.org/10.1016/B978-0-12-801238-3.99987-2>.
- [12] H. A. Dahl and E. Rinvik, *Menneskets funksjonelle anatomi*. Cappelen Damm Akademisk, 2010, ISBN: 9788202316327.
- [13] C. Antfolk, M. D'Alonzo, B. Rosén, G. Lundborg, F. Sebelius and C. Cipriani, 'Sensory feedback in upper limb prosthetics,' *Expert Review of Medical Devices*, vol. 10, no. 1, pp. 45–54, 2013, PMID: 23278223. DOI: 10.1586/erd.12.68.
- [14] R. Merletti and P. Parker, *Electromyography: Physiology, Engineering, and Non-Invasive Applications*. Wiley-IEEE Press, 2004, ISBN: 9780471678380. DOI: 10.1002/0471678384.ch18.
- [15] A. D. Roche, H. Rehbaum, D. Farina and O. C. Aszmann, 'Prosthetic myoelectric control strategies: A clinical perspective,' *Current Surgery Reports*, vol. 2, no. 44, 2014. DOI: 10.1007/s40137-013-0044-8.
- [16] D. Farina, T. Lorrain, F. Negro and N. Jiang, 'High-density emg e-textile systems for the control of active prostheses,' in *2010 Annual International Conference of the IEEE Engineering in Medicine and Biology*, 2010, pp. 3591–3593. DOI: 10.1109/IEMBS.2010.5627455.
- [17] P. Zhou, M. Lowery, J. Dewald and T. Kuiken, 'Towards improved myoelectric prosthesis control: High density surface emg recording after targeted muscle reinnervation,' in *2005 IEEE Engineering in Medicine and Biology 27th Annual Conference*, 2005, pp. 4064–4067. DOI: 10.1109/IEMBS.2005.1615355.
- [18] W. Geng, Y. Du, W. Jin, W. Wei, Y. Hu and J. Li, 'Gesture recognition by instantaneous surface emg images,' *Scientific Reports*, vol. 6, no. 1, 2016. DOI: 10.1038/srep36571.
- [19] A. Freed, A. D. C. Chan, E. D. Lemaire and A. Parush, 'Wearable emg analysis for rehabilitation (wear) - surface electromyography in clinical gait analysis,' in *2011 IEEE International Symposium on Medical Measurements and Applications*, 2011, pp. 601–604. DOI: 10.1109/MeMeA.2011.5966728.
- [20] A. Freed, A. D. C. Chan, E. D. Lemaire, A. Parush and E. Richard, 'Pilot test of the prototype wearable emg analysis for rehabilitation (wear) system,' *CMBES Proceedings*, vol. 35, 2012.
- [21] B. Afsharipour, S. Soedirdjo and R. Merletti, 'Two-dimensional surface emg: The effects of electrode size, interelectrode distance and image truncation,' *Biomedical Signal Processing and Control*, vol. 49, pp. 298–307, 2019, ISSN: 1746-8094. DOI: <https://doi.org/10.1016/j.bspc.2018.12.001>.

- [22] A. Boschmann and M. Platzner, 'Reducing classification accuracy degradation of pattern recognition based myoelectric control caused by electrode shift using a high density electrode array,' in *2012 Annual International Conference of the IEEE Engineering in Medicine and Biology Society*, 2012, pp. 4324–4327. DOI: 10.1109/EMBC.2012.6346923.
- [23] A. Boschmann and M. Platzner, 'Reducing the limb position effect in pattern recognition based myoelectric control using a high density electrode array,' in *2013 ISSNIP Biosignals and Biorobotics Conference: Biosignals and Robotics for Better and Safer Living (BRC)*, 2013, pp. 1–5. DOI: 10.1109/BRC.2013.6487548.
- [24] J. van Vugt and J. van Dijk, 'A convenient method to reduce crosstalk in surface emg,' *Clinical Neurophysiology*, vol. 112, no. 4, pp. 583–592, 2001, ISSN: 1388-2457. DOI: [https://doi.org/10.1016/S1388-2457\(01\)00482-5](https://doi.org/10.1016/S1388-2457(01)00482-5).
- [25] R. Howard, 'The application of data analysis methods for surface electromyography in shot putting and sprinting,' Ph.D. dissertation, University of Limerick, Limerick, Ireland, 2017. DOI: 10.13140/RG.2.2.15907.04640.
- [26] H. J. Hermens, B. Freriks, C. Disselhorst-Klug and G. Rau, 'Development of recommendations for sEMG sensors and sensor placement procedures,' *Journal of Electromyography and Kinesiology*, vol. 10, no. 5, pp. 361–374, 2000, ISSN: 1050-6411. DOI: [https://doi.org/10.1016/S1050-6411\(00\)00027-4](https://doi.org/10.1016/S1050-6411(00)00027-4).
- [27] M. Z. Jamal, 'Signal acquisition using surface emg and circuit design considerations for robotic prosthesis,' in *Computational Intelligence in Electromyography Analysis*, G. R. Naik, Ed., IntechOpen, 2012, ch. 18. DOI: 10.5772/52556. [Online]. Available: <https://doi.org/10.5772/52556>.
- [28] A. I. Martin, C. Toledo, J. A. Mercado, A. Vera, L. Leija and J. Gutierrez, 'Evaluation of dry electrodes for semg recording,' in *2018 Global Medical Engineering Physics Exchanges/Pan American Health Care Exchanges (GMEPE/PAHCE)*, 2018, pp. 1–5. DOI: 10.1109/GMEPE-PAHCE.2018.8400758.
- [29] R. Merletti, 'The electrode–skin interface and optimal detection of bioelectric signals,' *Physiological Measurement*, vol. 31, no. 10, 2010. DOI: 10.1088/0967-3334/31/10/e01.
- [30] B. Rodríguez-Tapia, I. Soto, D. M. Martínez and N. C. Arballo, 'Myoelectric interfaces and related applications: Current state of emg signal processing—a systematic review,' *IEEE Access*, vol. 8, pp. 7792–7805, 2020. DOI: 10.1109/ACCESS.2019.2963881.
- [31] K. Englehart, B. Hudgins and P. Parker, 'Multifunction control of prostheses using the myoelectric signal,' 2001, pp. 153–208, ISBN: 978-0-8493-0140-7. DOI: 10.1201/9781420042122.ch5.

- [32] S. Day. 'Important factors in surface emg measurement,' Bortec Biomedical Ltd. (2002), [Online]. Available: <http://bortec.ca/Images/pdf/EMG%5C%20measurement%5C%20and%5C%20recording.pdf>.
- [33] J. G. Webster, *Medical Instrumentation Application and Design*, Fourth Edition. John Wiley & Sons, 2009, ISBN: 9781118312858.
- [34] *Handbook: Dome electrodes*, Version 9.2, Coapt LLC., Chicago, IL, USA, 2021. [Online]. Available: <https://coaptengineering.com/wp-content/uploads/2021/09/Coapt-Dome-Electrode-Handbook-v9.2.pdf>.
- [35] E. Distrilec. 'Bossard m2 pan head machine screw.' (2022).
- [36] *Low-noise, 8-channel, 24-bit analog-to-digital converter for biopotential measurements*, ADS1299, Rev. C, Texas Instruments Incorporated, Jan. 2017.
- [37] *Rha2000 series amplifier arrays*, RHA2000 series, Intan Technologies, Jul. 2012.
- [38] M. Pires, J. Junior and S. Stevan Jr, 'Development of an 8 channel semg wireless device based on ads1299 with virtual instrumentation,' *Journal of Applied Intrumentation and Control*, vol. 6, no. 1, pp. 9–18, 2018, ISSN: 2318-4531.
- [39] M. Valderrama, E. González and F. García, 'Development of a low-cost surface emg acquisition system device for wearable applications,' in *2021 IEEE 2nd International Congress of Biomedical Engineering and Bioengineering (CI-IB BI)*, 2021, pp. 1–4. DOI: 10.1109/CI-IBBI54220.2021.9626100.
- [40] L. Zhang, Y. Shi, W. Wang, Y. Chu and X. Yuan, 'Real-time and user-independent feature classification of forearm using emg signals,' *Journal of the Society for Information Display*, vol. 27, no. 2, pp. 101–107, 2019. DOI: <https://doi.org/10.1002/jsid.749>.
- [41] S. LLC. 'Hackeeg shield for arduino due.' (2022), [Online]. Available: <https://www.starcat.io/products/hackeeg-shield/> (visited on 12/03/2022).
- [42] *Arduino due*, Arduino, 2022. [Online]. Available: <https://docs.arduino.cc/hardware/due>.
- [43] J. G. Proakis and D. G. Manolakis, *Digital Signal Processing*, Fourth Edition. Pearson Education, 2007, ISBN: 0-13-187374-1.
- [44] M. Hayes, *Digital Signal Processing*, 2nd Edition. McGraw-Hill Education, 2011, ISBN: 9780071635097.
- [45] R. Merletti, 'Standards for reporting emg data,' *International Society of Electrophysiology and Kinesiology*, vol. 9, no. 1, 1999.
- [46] B. Afsharipour, K. Ullah and R. Merletti, 'Spatial aliasing and emg amplitude in time and space: Simulated action potential maps,' in *XIII Mediterranean Conference on Medical and Biological Engineering and Computing 2013*, L. M. Roa Romero, Ed., Springer International Publishing, 2014, pp. 293–296, ISBN: 978-3-319-00846-2.

- [47] J. A. Ruvalcaba, M. I. Gutiérrez, A. Vera and L. Leija, 'Wearable active electrode for semg monitoring using two-channel brass dry electrodes with reduced electronics,' *Journal of Healthcare Engineering*, vol. 2020, 2020. DOI: 10.1155/2020/5950218.
- [48] *Handbook: Complete control system gen2*, Version 5.2, Coapt LLC., Chicago, IL, USA, 2021. [Online]. Available: <https://coaptengineering.com/wp-content/uploads/2021/09/Coapt-Gen2-Handbook-v5.2.pdf>.
- [49] *Technical instructions: Trusignal ac electrodes*, STPPR187 Issue 1, Steeper Group, San Antonio, TX, USA, 2020. [Online]. Available: <https://www.steepergroup.com/SteeperGroup/media/SteeperGroupMedia/Prosthetics/Upper%5C%20Limb%5C%20Prosthetics/Espire%5C%20Elbow/Downloads%5C%20and%5C%20Resources/Steeper-TruSignal-AC-Electrodes-Technical-Instructions.pdf>.
- [50] TMSi. 'Hd-emg electrodes.' (2022), [Online]. Available: <https://www.tmsi.com/products/hd-emg-electrodes/> (visited on 04/03/2022).

Appendix A

Commercially available electrodes and prosthetic systems

A.1 Coapt Complete Control System Gen2

This section is an excerpt of the handbook (V 5.2) for Coapt's second generation Complete Control System, [48].

Being an advanced control solution for upper limb prostheses, the Complete Control System Gen2 uses pattern recognition of myoelectric signals to match the user's intention to make an arm or hand movement. The Complete Control System allows for control of multiple prosthetic movements and eliminates the need for control switching¹. The use of pattern recognition also allows for more flexible electrode placement, as isolated signals or precise electrode placement is no longer a requirement. This simplifies electrode location dependence and reduces the need for spending a lot of time on adjusting system settings and configurations.

The device itself is a packaged electronic control system and is to be used in conjunction with an upper-limb prosthetic device. The device features an EMG interface for myoelectric signal inputs from muscles, as well as a prosthesis interface for control outputs. A calibration button functions as a user-interface for quick on-board calibration and reduces the need for taking the prosthetic device off when making adjustments. The Complete Control System Gen2 comes in a kit, as depicted in Figure A.1, and contains the following components:

1. Complete Controller main processor
2. EMG Interface Cable (clinician-specified termination type)

¹Usually the user has to perform distinct actions, like co-contractions, pulses or fast and slow gestures, when going from one control mode – for instance hand rotation – to another – for instance opening/closing of hand. This can be cumbersome and limits seamless control of the prosthetic device



Figure A.1: Contents of the Complete Control System Gen2 kit. From [48].

3. Device Interface Cable (clinician-specified termination type)
4. Complete Calibrate button
5. Socket cut-out template for the Complete Calibrate button
6. Fabrication Aid (disposable mock-up of Complete Controller)
7. Complete Communicator USB Bluetooth Dongle

The handbook also includes a clinician guide for planning EMG electrode sites. This includes a thorough whole-handed palpation to determine where in the residual limb muscle tissue is located, followed by positioning of electrode contacts.

A.2 Coapt Dome Electrodes

This section presents a small excerpt from Coapt’s Dome Electrode Handbook (V 9.2)[34]. The Coapt Dome Electrode is designed for conducting passive measurements of biopotential signals non-invasively, and its suggested usage is for measuring sEMG signals. The electrode is made of stainless steel for safety and longevity, and no conductive gel is required. The electrode has a dome shape, which simplifies placement and allows for more accurate recordings of sEMG signals. As shown in Figure A.3, the dome of the electrode is 9.525mm in diameter, and Coapt recommends an inter-electrode spacing of 30 – 60mm. It is also recommended to place the electrodes in a socket, cuff enclosure or similar, as shown in Figure A.2b, to “limit movement of the Dome Electrode away from the intended skin placement site” – in other words, to limit unwanted effects from electrode shifts. The electrodes should be placed so that the dome side is in contact with the skin and the stud can be connected to a mating thread for conduction of the biopotential measurements. The assembly is secured in place using a flat washer, split lock washer and tightening nut. This is illustrated in Figure A.2a.

The Dome Electrode comes in a kit that contains the following components:

- 316L Stainless Steel Dome Electrode
- Stainless Steel Size 4-40 Nut
- Stainless Steel Flat Washer
- Stainless Steel Split Lock Washer

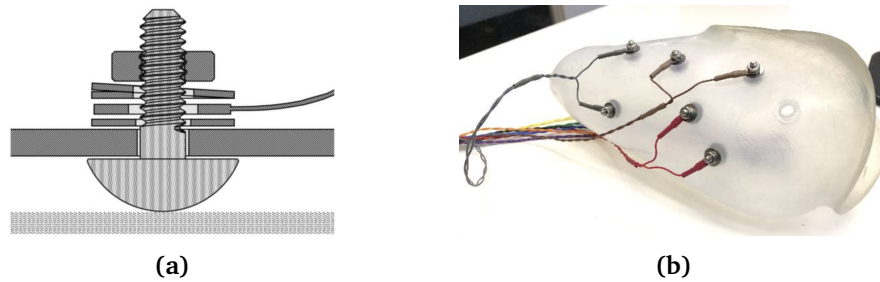


Figure A.2: (a) Cross section of electrode connection and assembly in prosthetic socket, and (b) Coapt Dome Electrodes mounted in socket for prosthetic device. From [34].

A more detailed description of the Stainless Steel Dome Electrode is shown in the specification in Figure A.3.

A.3 Steeper TruSignal AC Electrodes

Although providing a different attachment mechanism, the Steeper Group offers remote metal dome electrodes similar to that of Coapt. The Steeper TruSignal AC Electrodes[49] come in a kit, shown in Figure A.4, consisting of wire harnesses attached to circuit boards that snap onto the remote metal dome electrodes. The on-electrode boards filter the myoelectric signals and pass them to the prosthetic device. The wires are shielded in order to protect the signals from electronic noise. Steeper recommends placing the electrodes along the longitudinal axis of the muscle with an inter-electrode distance of 10mm. The kit also includes a pair of reference electrodes that should be placed “off-axis” to avoid interference with muscle signals. Three choices of dome size is offered – large, medium and paediatric – but their respective dome diameters is unavailable from the Steeper TruSignal AC Electrodes Instruction Manual[49].

A.4 TMSi HD-EMG electrode grids

TMSi is a rather small – and maybe less known – company that designs and develops measurement solutions for electrophysiological research, including amplifiers, electroencephalography (EEG)² electrodes and headcaps, as well as high-density sEMG arrays. TMSi offers two different-sized arrays, shown in Figure A.5, both being an 8x8 grid with 64 channels. The smallest array has an inter-electrode distance of 4mm, while the distance between the electrodes in the larger one is 8.5mm. The diameter of the electrodes, as well as the total size of the arrays, are unavailable at the time of writing. Though not explicitly stated, the grids being

²EEG is the measurement of electrical activity in the brain[9, p. 723].


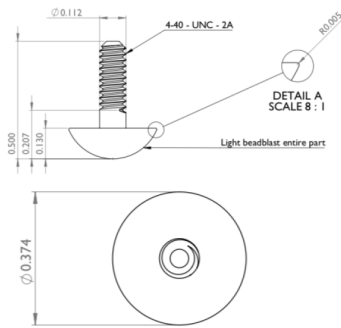
316L STAINLESS STEEL DOME ELECTRODES	
DOME ELECTRODE	
QUANTITY IN PACKAGE	18
	Diameter: 0.375 in (9.525 mm) Height: 0.130 in (3.302 mm)
DIMENSIONS OF DOME	
DIMENSION OF THREAD	Diameter: 0.112 in (2.845 mm) Height: 0.37 in (9.398 mm)
TOTAL DOME SURFACE AREA	0.43 in ² (2.80 cm ²)
CONNECTION	4-40 thread
MATERIAL	316L Stainless Steel
RECORDING FREQUENCY BAND	0-1000Hz

Figure A.3: Component specification for the Coapt Stainless Steel Dome Electrode. From [34].

8x8 and offering 64 channels indicates that monopolar electrodes are used. The arrays are to be used with adhesive gel, as the electrodes consist of Ag/AgCl[50].

TMSi offers a third option for conducting sEMG measurements. Multiple micro-electrodes can be placed in a custom topology and connected to a shielded multi-cable with 32 channels. Though not technically a high-density array in itself, the micro-electrodes can be arranged to form a 32 channel high-density sEMG array[50].



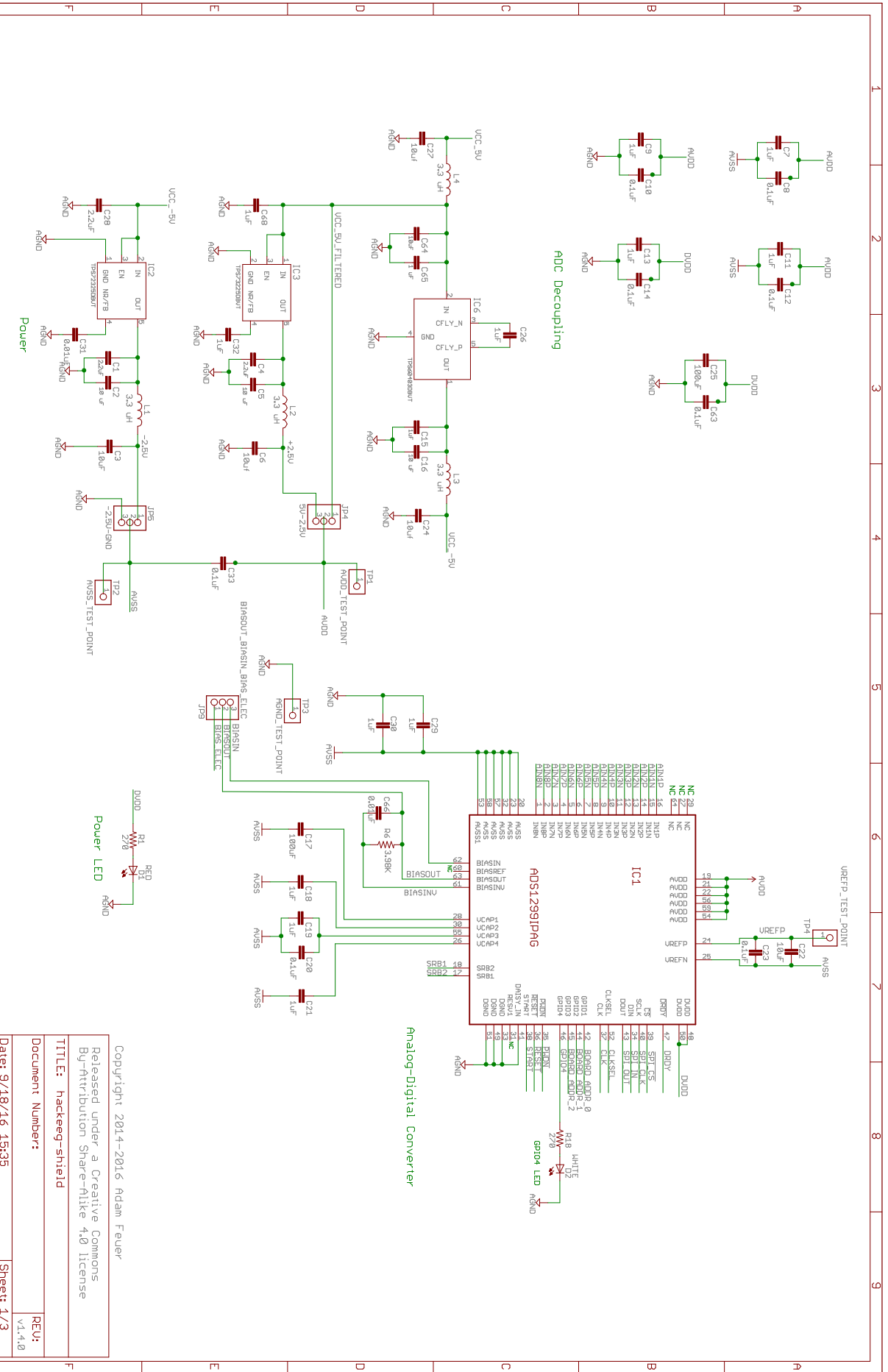
Figure A.4: Steeper TruSignal AC Electrodes. From [49].



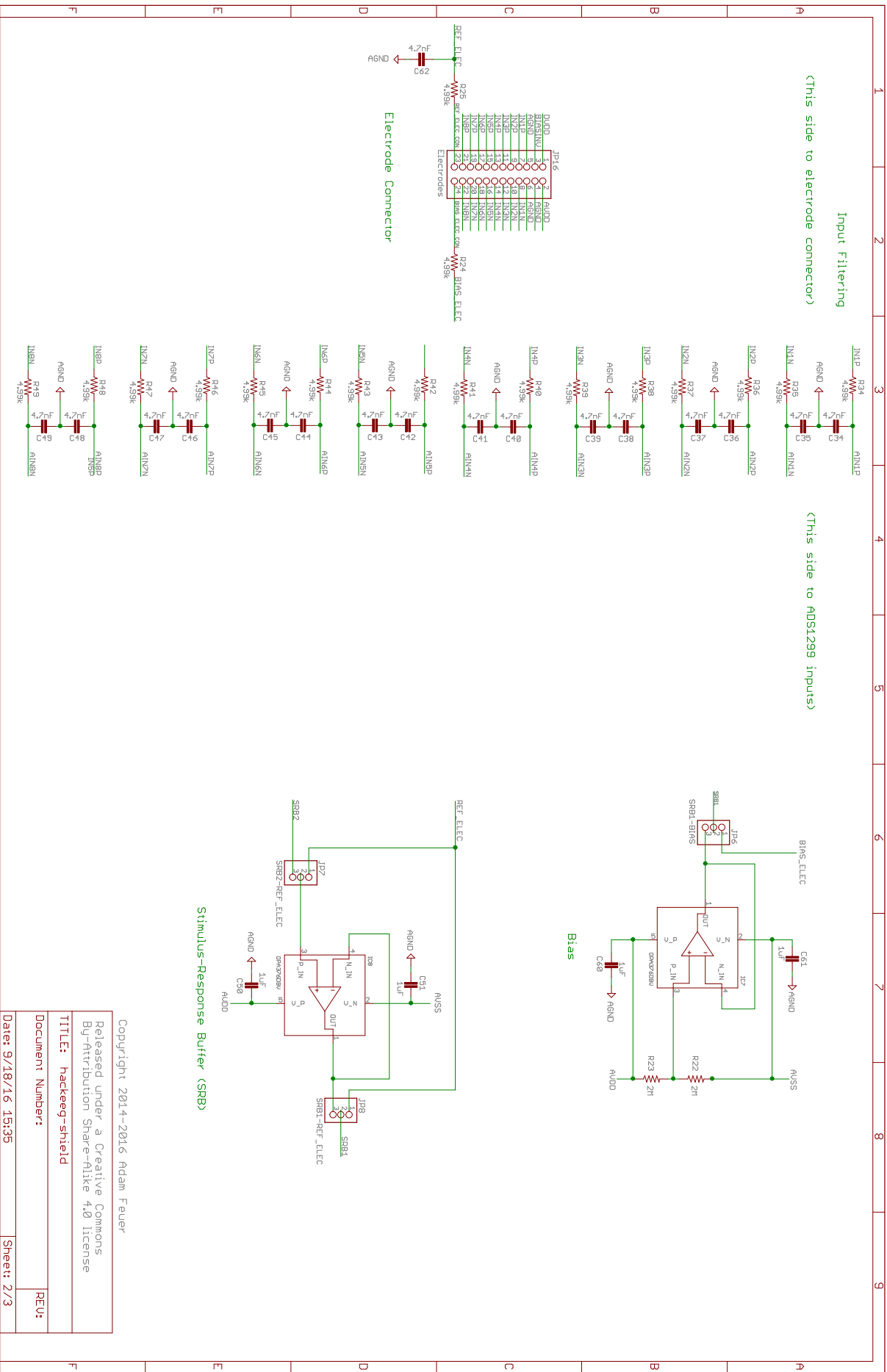
Figure A.5: TMSi HD-EMG electrode grids. From [50].

Appendix B

Schematics for HackEEG Arduino shield



Copyright 2014-2016 Adam Feuer
 Released under a Creative Commons
 By-Attribution Share-Alike 4.0 license
TITLE: hackeeg-shield
 Document Number:
 REV: v1.1.0
 Date: 9/18/16 15:35 Sheet: 1/3



Copyright 2014-2016 Adam Feuer
 Released under a Creative Commons
 Attribution-ShareAlike 4.0 license
TITLE: hackeeg-shield
Document Number:
REV:
Date: 9/18/16 15:35 **Sheet:** 2/3

